TALREN 4 – v 1.x

C. Technical manual

LIST OF FIGURES

LIST OF TABLES

1 INTRODUCTION

This section is aimed at expliciting the mechanical principles which are the basis of the "TALREN" program for the stability analysis of geotechnical structures. It presents the essential equations which describe these principles, taking into account weighting factors for actions and partial safety factors applied to the material resistance (refer to chapter 6).

The details of the data and calculation results are exposed in chapter B of this manual.

Examples of TALREN calculations are given in chapter D of this manual.

2 CALCULATION METHODS FOR SLOPE STABILITY, WITHOUT REINFORCEMENT - BASIC EQUATIONS

CONVENTIONS

The conventions used in the program are summarised on Figure 1.

Capital letters designate forces.

Lower-case letters designate stresses.

A letter designated with a <'> corresponds to an effective force or stress.

The slope is defined with the uphill portion at the left of the drawing to maintain the standard orientation for Cartesian coordinates.

Contrary to the normal convention, the angle *a* between the failure surface and the horizontal, is taken to be positive clockwise, as shown on Fig. 1, in order to conserve the sign convention generally used by the various slope stability programs.

In the equations, the symbol $\int$ represents the definite integral evaluated between the two boundary abscissa values, corresponding to the intersection points between the failure surface and the slope.

$$\int = \int_{x_0}^{x_1}$$

2.1. FUNDAMENTAL EQUATIONS

The fundamental equation for the Ultimate Limit State analysis is:

$$\Gamma_{s3}.\tau.(\Gamma_{s1}.G, \Gamma_Q.Q, G_W) \leq \tau_{\max}.\left(\frac{\tan\phi}{\Gamma_\phi}, \frac{c}{\Gamma_c}\right) \qquad (0)$$

An additional factor Γ is included to establish the equality. This factor should be greater than or equal to 1 to ensure equilibrium.

$$\Gamma.\Gamma_{s3}.\tau = \tau_{\max} \qquad (0a)$$

where:

Γ_{s3} : weighting factor for the uncertainty in the calculation method shear

τ : stress along the failure surface

Γ_{s1} : weighting factor for the soil unit weights

G : permanent loads (weight of soils)

Γ_Q : weighting factor for the loads

Q : variable loads (loads)

G_w : water load

τ_{max} : maximum shear stress mobilised along the failure surface

ϕ : soil internal friction angle

Γ_ϕ : partial safety factor for ϕ

c : soil cohesion

Γ_c : partial safety factor for c

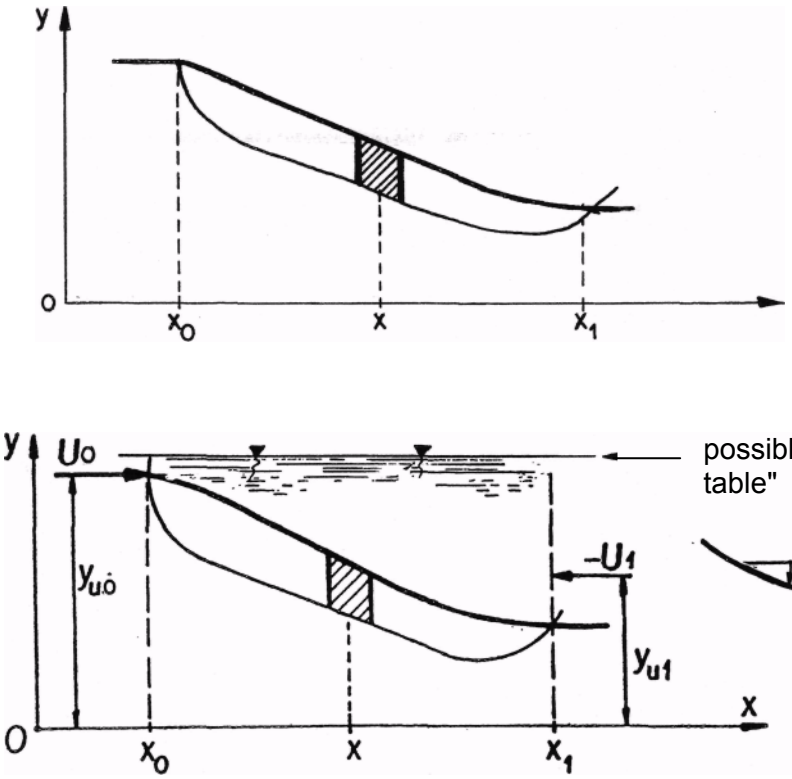

Figure 1: Schematic diagram of the slope - Conventions

The form of the failure surface is assumed a priori to be arbitrary. The equilibrium equations for a slice having thickness dx can be written:

- Projection on OX (horizontal):

$$- dE' - dU + \sigma.\tan\alpha.dx - \tau.dx = 0 \quad (1)$$

- Projection on OY (vertical):

$$dT - \Gamma_{s1}.\gamma.h.dx + \sigma.dx + \tau.\tan\alpha.dx = 0 \quad (2)$$

- Moment with respect to point 0:

$$\int \left(\left[\sigma + \tau.\tan\alpha - \Gamma_{s1}.\gamma.h \right] x - \left[\sigma.\tan\alpha - \tau \right] y \right) dx + \Sigma M_{ext} = 0 \quad (3)$$

with:

$$\Sigma M_{ext} = T_1.x_1 - T_0.x_0 + E'_1.y_{e1} - E'_0.y_{e0} + U_1.y_{u1} - U_0.y_{u0} + \Sigma M_{add} \quad (3a)$$

where:

ΣM_{ext} : represents the moment resulting from the forces located outside the soil mass (surface loads, external water tables, etc.)

dE' : variation in the horizontal component of the effective interslice forces

dT : variation in the vertical component of the interslice forces

σ : normal stress along the failure surface

E'_0, E'_1 : values of E' at the extremities of the failure surface

T_0, T_1 : values of T at the extremities of the failure surface

U_0, U_1 : values of the horizontal forces at the extremities resulting from the water located outside the slope

dU : variation in the horizontal water pressure between slices (including water located outside the slope)

γh : weight per unit width of the "soil/water" column

M_{add} : additional moment

At point M, Coulomb's law considering the classical safety factor can be expressed by:

$$\tau = \frac{c}{F_{soil}} + (\sigma - u).\frac{\tan\phi}{F_{soil}} \text{ with } F_{soil} \geq 1 \quad (4)$$

where:

τ : shear stress

σ : normal stress

u : pore pressure

c : cohesion

ϕ : soil internal friction angle

F_{soil} : safety factor for the soil (generally denoted as F when there is no possible confusion)

Applying the principle of the Ultimate Limit State, and combining equations (0a) and (4) one obtains:

$$\Gamma.\Gamma_{s3}.\tau = \frac{c}{\Gamma_c} + (\sigma - u).\frac{\tan\phi}{\Gamma_\phi} = \tau_{\max} \tag{4a}$$

or:

$$\tau = \frac{c}{\Gamma.\Gamma_{s3}.\Gamma_c} + (\sigma - u).\frac{\tan\phi}{\Gamma.\Gamma_{s3}.\Gamma_\phi} \tag{4b}$$

Considering eq. (4b) and taking into account the equality conditions, the expression for a and t shown in eq. (1), (2) and (3) can be written:

$$\sigma.\tan\alpha - \tau = \sigma.\left(\tan\alpha - \frac{\tan\phi}{\Gamma.\Gamma_{s3}.\Gamma_\phi}\right) - \frac{c}{\Gamma.\Gamma_{s3}.\Gamma_c} + \frac{u.\tan\phi}{\Gamma.\Gamma_{s3}.\Gamma_\phi} \tag{5}$$

$$\sigma + \tau.\tan\alpha = \sigma.\left(1 + \frac{\tan\alpha.\tan\phi}{\Gamma.\Gamma_{s3}.\Gamma_\phi}\right) + \left(\frac{c}{\Gamma.\Gamma_{s3}.\Gamma_c} - \frac{u.\tan\phi}{\Gamma.\Gamma_{s3}.\Gamma_\phi}\right).\tan\alpha \tag{6}$$

Considering only these two equations no solution to the problem is possible. It is therefore necessary to impose an additional relationship between the parameters. (refer to RAULIN).

The various calculation methods differ by the nature of this arbitrary assumption.

2.2. FELLENIUS METHOD

The Fellenius method was originally applied to circular failure surfaces. The origin of the axes (Point O) is therefore taken successively at the centre of each circle studied. Considering the sign convention used in TALREN, this leads to the expression:

$$\begin{aligned} x &= -R.\sin\alpha \\ y &= -R.\cos\alpha \end{aligned} \tag{7}$$

The method assumes that the dE' and dT forces are parallel to the slice base, giving:

$$dT = dE'.\tan\alpha \tag{8}$$

This set of assumptions is redundant. The set of equations (1) to (4b) cannot therefore be solved simultaneously.

The adopted solution (although false) consists of eliminating τ from eq. (1) and (2), which results in:

$$\sigma_{Fel} = \Gamma_{s1}.\gamma.h.\cos^2\alpha + \frac{dU}{dx}\sin\alpha.\cos\alpha \tag{9}$$

Substituting σ from eq. (9) and τ from eq. (4b) into eq. (3), and considering eq. (7), leads to the following expression:

$$\Gamma.\Gamma_{s3} = \frac{\int\left(\frac{c}{\Gamma_c} + \left(\Gamma_{s1}.\gamma.h.\cos^2\alpha - u + \frac{dU}{dx}.\sin\alpha.\cos\alpha\right).\frac{\tan\phi}{\Gamma_\phi}\right).\frac{dx}{\cos\alpha}}{\int\Gamma_{s1}.\gamma.h.\sin\alpha.dx + \sum\frac{M_{ext}}{R}} \tag{10}$$

where ΣM_{ext} is given by eq. (3a).

Remarks

a) Originally, this method did not consider separately the effect of water on the interslice interactions (dU / dx = 0 in eq. 10) and did not consider the external ($\Sigma M_{ext} = 0$).

Expressed in the classical form of a summation of the various slices, having width b_i, eq. (10) becomes:

$$\Gamma_{Fel} = \frac{\sum_{i=1}^{n}\left(\frac{c_i}{\Gamma_{ci}} + \left[\Gamma_{s1}.\gamma_i.h_i.\cos^2\alpha_i - u_i + \frac{dU_i}{b_i}.\sin\alpha_i.\cos\alpha_i\right].\frac{\tan\phi_i}{\Gamma_{\phi i}}\right).\frac{b_i}{\cos\alpha_i}}{\Gamma_{s3}.\left(\sum_{i=1}^{n}\left[\Gamma_{s1}.\gamma_i.h_i.b_i.\sin\alpha_i\right] + \sum\frac{M_{ext}}{R}\right)} \qquad (11)$$

Equation (4b) can then be written:

$$\sigma_{Fel} = \frac{\tau_{\max}}{\Gamma_{s3}.\tau} = \frac{\sum\tau_{\max}.R}{\Gamma_{s3}.\sum\tau.R} \qquad (12)$$

Γ_{Fel} therefore has the form:

$$\Gamma_{Fel} = \frac{\text{Re}\,sisting\ moment}{\Gamma_{s3}.Overturning\ moment} \qquad (12a)$$

This expression (although incorrect) is generally retained as the definition of the safety factor and applies only to the case of circular failure surfaces.

In its original form, this method cannot be applied to the case of a submerged slope and only by introducing the effect of water located within the slope (dU/dx * 0) can one generalise the method.

b) One can directly determine the safety factor $\Gamma_{(M)}$, different for each point along the failure surface, by eliminating σ and τ from eq. (1), (2) and (4b). In practice, the value Γ_{Fel} given by eq. (10) represents the average of $\Gamma_{(M)}$ factored by $\Gamma_{S1}.\gamma.h.b.\sin\alpha(M)$.

c) As a result of this factoring, the eq. (1) and (2) cannot be satisfied by the value r determined from eq. (3). This results in the remark given below eq. (8) concerning the redundancy of the assumptions.

2.3. SIMPLIFIED BISHOP METHOD

The simplified Bishop method assumes:

$$dT = 0 \tag{13}$$

It is applied to circular failure surfaces.

The solution of the system of equations is obtained by eliminating σ in eq. (2) and (4b) and substituting the expression for τ calculated in eq. (3). One should note that in the Fellenius method, the moment resulting from σ is 0 with respect to the circle centre.

The expression therefore becomes:

$$\Gamma_{Bish} = \frac{\int \left(\frac{\frac{c}{\Gamma_c} + \left(\Gamma_{s1}.\gamma.h - u\right).\frac{\tan\phi}{\Gamma_\phi}}{1 + \frac{\tan\alpha.\tan\phi}{\Gamma_{Bish}.\Gamma_{s3}.\Gamma_\phi}} \right).\frac{dx}{\cos\alpha}}{\Gamma_{s3}.\left(\int \Gamma_{s1}.\gamma.h.\sin\alpha.dx + \sum \frac{M_{ext}}{R} \right)} \tag{14}$$

where ΣM_{ext} is the moment resulting from the external forces, given by eq. (3a).

To simplify the expression, let's consider

$$m(\alpha) = 1 + \frac{\tan\alpha.\tan\phi}{\Gamma_{Bish}.\Gamma_{s3}.\Gamma_\phi} \tag{15}$$

Eliminating τ from eq. (2) and (4b) leads to the expression for the effective normal stress and the tangential stress,

$$\sigma'_{Bish} = \frac{\Gamma_{s1}.\gamma.h - u - \frac{c.\tan\alpha}{\Gamma_{Bish}.\Gamma_{s3}.\Gamma_c}}{m(\alpha)}$$

$$\tau_{Bish} = \frac{\frac{c}{\Gamma_c} + \left(\Gamma_{s1}.\gamma.h - u\right).\frac{\tan\phi}{\Gamma_\phi}}{\Gamma_{Bish}.\Gamma_{s3} + \frac{\tan\alpha.\tan\phi}{\Gamma_\phi}} \tag{16}$$

Remarks on the simplified Bishop method

a) This method pertains to the analysis of circular failure surfaces and similarly to the Fellenius method, the safety factor can be expressed as:

$$\Gamma_{Bish} = \frac{\text{Re}\,sisting\ moment}{\Gamma_{s3}.Overturning\ moment}$$

b) Equation (14) is implicit in Γ_{Bish} and can be solved by the discretisation of wedges having a finite thickness. Without external forces, as originally presented, the Bishop formula can be written:

$$\Gamma_{Bish} = \frac{\sum_{i=1}^{n}\left(\frac{c_i}{\Gamma_{ci}} + \left[\Gamma_{s1}.\gamma_i.h_i - u_i\right].\frac{\tan\phi_i}{\Gamma_{\phi i}}\right).\frac{b_i}{\cos\alpha_i}}{\Gamma_{s3}.\left(\sum_{i=1}^{n}\left[\Gamma_{s1}.\gamma_i.h_i.b_i.\sin\alpha_i\right] + \sum\frac{M_{ext}}{R}\right)} \qquad (17)$$

The resolution of the problem can lead to several distinct solutions depending on the value of Γ_{Bish} chosen to initialise the iterative process.

c) Equation (1) is not used in determining Γ_{Bish} and this condition is not therefore verified. This results in the redundancy of the assumptions made in the simplified Bishop method.

d) The presence of m(α), which can be equal to 0 for certain negative values of a, in the denominator of the expressions for σ' and Γ_{Bish}, can induce a high degree of distortion in the convergence of the iterative calculation of Γ_{Bish}.

This inconvenience, shown by various authors, leads to the introduction of a convergence test in TALREN, which will be explained in section 3.4.6.

2.4. PERTURBATION METHOD

The "Perturbation" method, developed by Raulin, Rouques and Toubol (1974), is a calculation method for non-circular failures, along an arbitrarily shaped surface.

An additional assumption characterising this method relates to the value of the effective normal stress. It can be expressed as a function of the effective normal stress derived from the Fellenius method by the following relationship:

$$\sigma'_{pert} = \sigma_{pert} - u = (\sigma_{Fel} - u).(\lambda + \mu.\tan^n \alpha) \tag{18}$$

where σ_{Fel} is derived from eq. (9)

λ and μ are 2 dimensionless parameters calculated by the program simultaneously with Γ. n = 1 or 2 (chosen by the operator)

The expression (λ + μ.tan$^n\alpha$) is the "perturbation" factor of the Fellenius stress, taken in this case as a reference, since it can be directly calculated.

The development of the equations leads to the following relationships.

Combining eq. (1), (5) and (18) yields eq. (19):

$$\int \left(\left[\sigma'_{Fel}.(\lambda + \mu.\tan^n \alpha) + u \right] \left(\tan\alpha - \frac{\tan\phi}{\Gamma\phi^*} \right) - \left(\frac{c}{\Gamma_c^*} + \frac{u.\tan\phi}{\Gamma_\phi^*} \right) \right).dx - (E'_1 - E'_0) - (U_1 - U_0) = 0 \tag{19}$$

with: $\Gamma_\phi^* = \Gamma.\Gamma_{s3}.\Gamma_\phi$ and $\Gamma_c^* = \Gamma.\Gamma_{s3}.\Gamma_c$

Combining eq. (2), (6) and (18) yields eq. (20):

$$\int \left(\left[\sigma'_{Fel}.(\lambda + \mu.\tan^n \alpha) + u \right] \left(1 + \frac{\tan\alpha.\tan\phi}{\Gamma\phi^*} \right) + \left(\frac{c}{\Gamma_c^*} - \frac{u.\tan\phi}{\Gamma_\phi^*} \right).\tan\alpha \right).dx - \int \Gamma_{s1}.\gamma.h.dx + (T_1 - T_0) = 0 \tag{20}$$

Combining eq. (3), (5), (6) and (18) yields eq. (21):

$$\begin{aligned} &\int \left(\left[\sigma'_{Fel}.(\lambda + \mu.\tan^n \alpha) + u \right] \left(1 + \frac{\tan\alpha.\tan\phi}{\Gamma\phi^*} \right) + \left(\frac{c}{\Gamma_c^*} - \frac{u.\tan\phi}{\Gamma_\phi^*} \right).\tan\alpha - \Gamma_{s1}.\gamma.h \right).x.dx \\ &- \int \left(\left[\sigma'_{Fel}.(\lambda + \mu.\tan^n \alpha) + u \right] \left(\tan\alpha - \frac{\tan\phi}{\Gamma\phi^*} \right) - \left(\frac{c}{\Gamma_c^*} + \frac{u.\tan\phi}{\Gamma_\phi^*} \right) \right).y.dx \\ &+ T_1.x_1 - T_0.x_0 + E'_1.y_{e1} - E'_0.y_{e0} + U_1.y_{u1} - U_0.y_{u0} + \sum M_{add} = 0 \end{aligned} \tag{21}$$

These three expressions can be rewritten in the simplified form:

(19) → (22) $\lambda.(H_1 + H_2/\Gamma) + \mu.(H_3 + H_4/\Gamma) + H_5 + H_6/\Gamma = 0$

(20) → (23) $\lambda.(V_1 + V_2/\Gamma) + \mu.(V_3 + V_4/\Gamma) + V_5 + V_6/\Gamma = 0$

(21) → (24) $\lambda.(O_1 + O_2/\Gamma) + \mu.(O_3 + O_4/\Gamma) + O_5 + O_6/\Gamma = 0$

Where the variables have the significations given in eq. (25):

$$
\begin{aligned}
H_1 &= \int \sigma'_{Fel}.\tan\alpha.dx \\
H_2 &= \int -\sigma'_{Fel}.\tan\phi^*.dx \\
H_3 &= \int \sigma'_{Fel}.\tan^{(n+1)}\alpha.dx \\
H_4 &= \int -\sigma'_{Fel}.\tan^n\alpha.\tan\phi^*.dx \\
H_5 &= \int u.\tan\alpha.dx - (E'_1 - E'_0) - (U_1 - U_0) \\
H_6 &= \int -c^*.dx \\
O_1 &= \int \sigma'_{Fel}.(x - y.\tan\alpha).dx \\
O_2 &= \int \sigma'_{Fel}.(x.\tan\alpha + y).\tan\phi^*.dx \\
O_3 &= \int \sigma'_{Fel}.(x - y.\tan\alpha).\tan^n\alpha.dx \\
O_4 &= \int \sigma'_{Fel}.(x.\tan\alpha + y).\tan^n\alpha.\tan\phi^*.dx \\
O_5 &= \int \left[u.(x - y.\tan\alpha) - \gamma.h^*.x\right]dx + T_1.x_1 - T_0.x_0 + E'_1.y_{e1} - E'_0.y_{e0} + U_1.y_{u1} - U_0.y_{u0} + \sum M_{add} \\
O_6 &= \int c^*.(x.\tan\alpha + y).dx \\
V_1 &= \int \sigma'_{Fel}.dx \\
V_2 &= \int \sigma'_{Fel}\tan\alpha.\tan\phi^*.dx \\
V_3 &= \int \sigma'_{Fel}\tan^n\alpha.dx \\
V_4 &= \int \sigma'_{Fel}\tan^{n+1}\alpha.\tan\phi^*.dx \\
V_5 &= \int (u - \gamma.h^*).dx + T_1 - T_0 \\
V_6 &= \int c^*.\tan\alpha.dx
\end{aligned}
\qquad (25)
$$

with: $\tan\phi^* = \tan\phi/\Gamma_\phi^*$

$c^* = c/\Gamma_c^*$

$\gamma.h^* = \Gamma_{s1}.\gamma.h$

The system of equations (22), (23) and (24) is linear in λ and μ and only produces a non-trivial solution when the determinant is 0.

$$\begin{vmatrix} H_1 + H_2/\Gamma & H_3 + H_4/\Gamma & H_5 + H_6/\Gamma \\ V_1 + V_2/\Gamma & V_3 + V_4/\Gamma & V_5 + V_6/\Gamma \\ O_1 + O_2/\Gamma & O_3 + O_4/\Gamma & O_5 + O_6/\Gamma \end{vmatrix} = 0 \qquad (26)$$

The determinant leads to a third degree equation for Γ:

$$a_0.\Gamma^3 + a_1.\Gamma^2 + a_2.\Gamma + a_3 = 0 \qquad (27)$$

in which the largest root is taken as the value of Γ_{pert}.

Remarks on the Perturbation method

a) This method, which has been used for many years, gives results very close to those obtained from the Bishop method, for circular failure surfaces.

b) It does not raise the difficulty relating to the convergence. It is not therefore necessary to introduce a convergence test to limit the stresses, as is required in the Bishop method.

c) The method is not applicable to the case of planar failure (or failure by a sliding wedge) because the system of equations (22), (23) and (24) is simplified and the two unknowns' λ and μ are reduced to only one condition.

2.5. CALCULATION WITH YIELD DESIGN METHOD

Chapter under construction.

The calculation with yield design method is being validated and is therefore not yet available in TALREN 4.

3 APPLICATION OF THE BASIC METHODS IN TALREN

3.1. SLOPE PROFILE

For numerical reasons, the slope profile cannot include an overhang (Fig. 2), but can incorporate vertical segments.

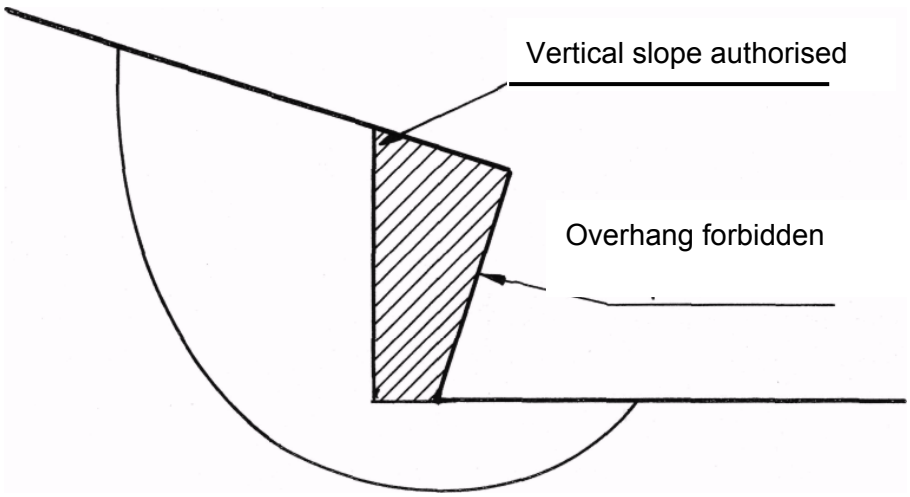

Figure 2: Overhang forbidden for the slope profile

3.2. FAILURE SURFACES

3.2.1. Circular failure surfaces

3.2.1.1. Treatment of circular failure surfaces in "manual search" mode

Investigation of the circular failure surfaces is made automatically in a classical manner, with the aid of a quadrilateral mesh of circle centres (the mesh can be inclined). For each centre, the radius can be increased or decreased by an increment DR, specified by the operator (Fig. 3).

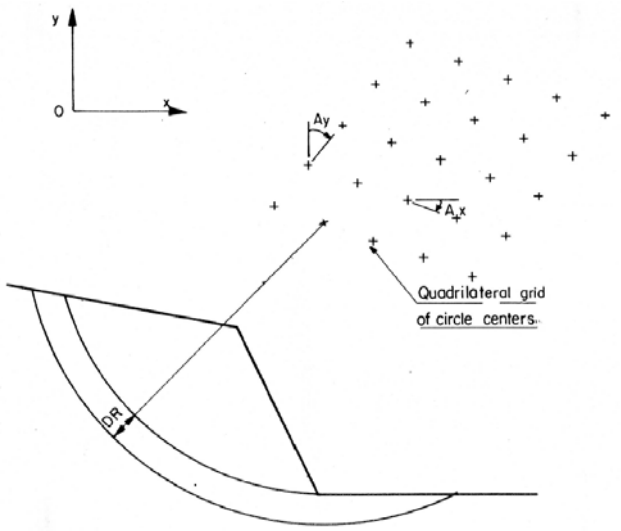

Figure 3: Manual research of failure circles

3.2.1.2. Treatment of circular failure surfaces in "automatic search" mode

The advantage of automatic search is to automatically scan the entire possible space for the centres of the circles, with more or less accuracy (parameter provided by the user). With this automatic search the user doesn't have to define the parameters requested in the case of a manual search.

However, after an automatic search, it is recommended to perform a 2nd calculation (with a 2nd situation for example) using a manual search to refine the search around the critical circle detected by the automatic search.

The principle of automatic search is illustrated in the 2 following figures:

- A first automatic scan detects a critical circle (corresponding to the absolute minimum of the safety factor obtained on all calculated circles).
- Talren 4 then systematically carries out a second automatic scan in the zone around the critical circle detected during the 1st scan.
- The safety factor displayed is the minimum obtained after both scans.

The data requested for an automatic search are detailed in the user manual. The main parameter is the “number of intervals”: it determines the density of the automatic mesh: it corresponds to the number of directions, the number of distances and to the number of radii calculated for each scan. For example, with a number of intervals equal to 10, the total number of circles calculated after 2 scans will be equal to 2 x 10 x 10 x 10 = 2000.

The positioning of the centres at different distances for a same direction is done like this:

- Let L be the length of the segment connecting the passage point imposed for the 1st circle to the other intersection point with the slope (Figure 4);
- The closest centre to the slope is situated at a distance L/2 from this segment;
- The second centre is at a distance L/2 from the first;
- For the next ones, the spacing between the 2 centres on the same direction is equal to L;
- The number of centres along a direction is equal to the "number of intervals".

Note: It is advised to be careful in the analysis of the results of an automatic search. The first scan may for example detect 2 minima for the safety factor which are almost equal and which are located in different zones. The 2nd scan will then refine only the zone corresponding to the first strict minimum, while a second scan in the other zone could have given a smaller safety factor (which will not be identified in this case). Displaying isovalues of the safety factor enables to quickly check whether the minimum safety factor is located in one single zone, or is approached in several different zones.

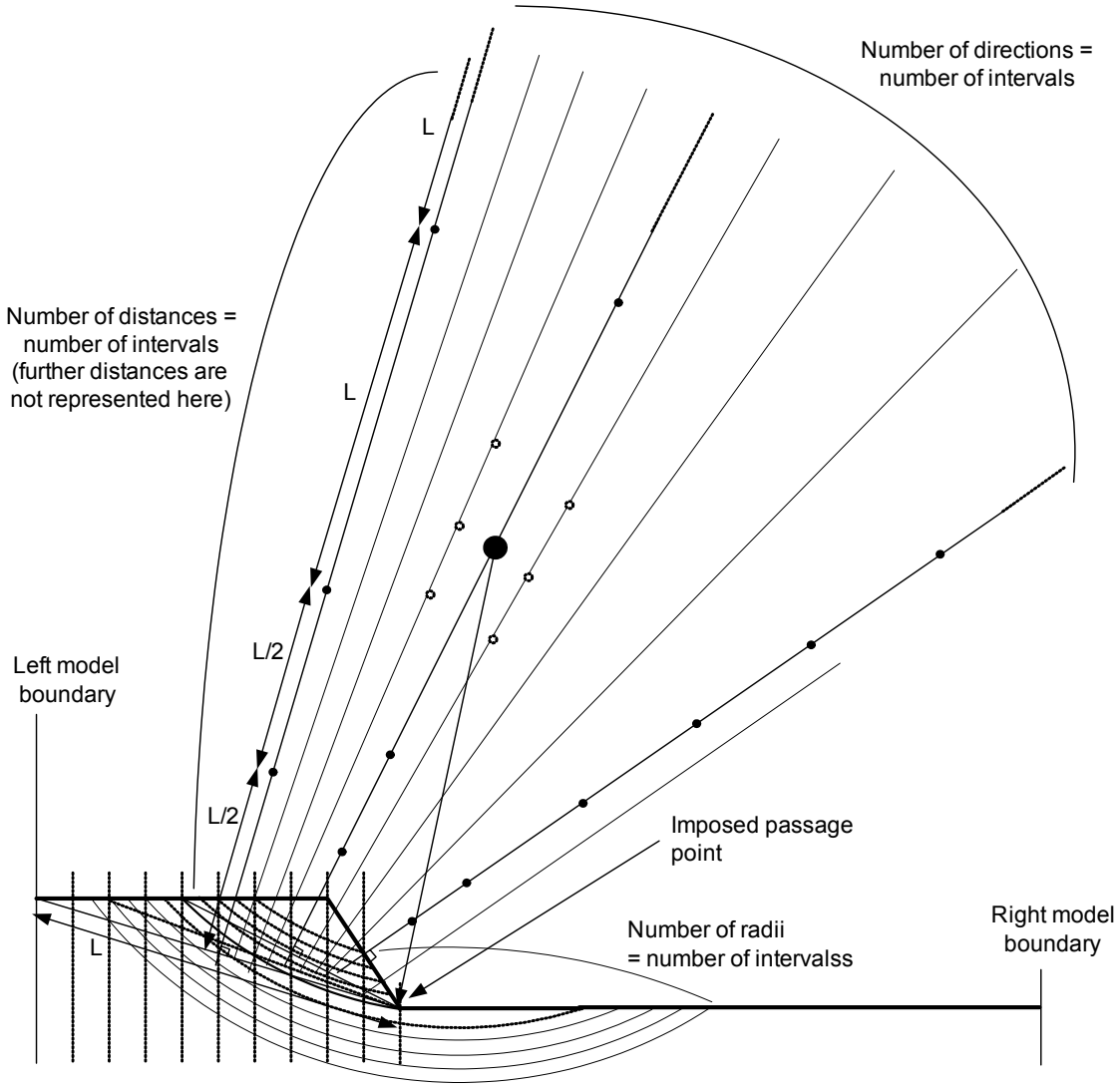

Figure 4: Principle of scan for the automatic search of the critical circle, with imposed passage point for the first circle: First scan

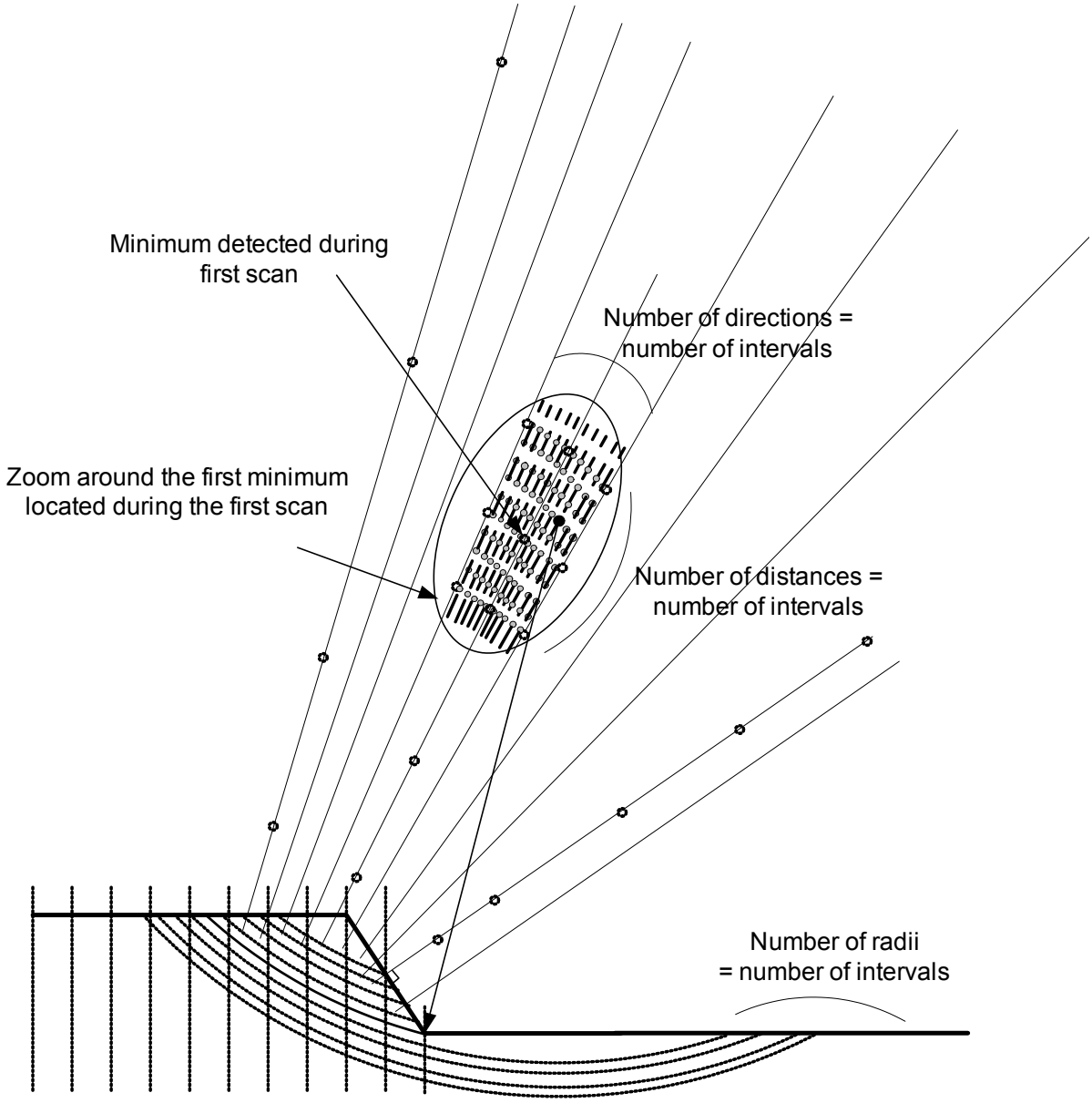

Figure 5: Principle of scan for the automatic search of the critical circle, with imposed passage point for the first circle: Second scan ("zoom")

3.2.1.3. Elimination of an overhang. Composite failure surfaces

Contrary to that obtained from numerical calculations, experience has shown that in certain cases, a failure surface including an overhang ($\alpha > \pi/2$) at the upper portion of the curve (Figure 6) is neither critical nor realistic. The overhanging portion of the failure surface is therefore replaced with a vertical plane for all elevations above the level of the circle centre. The failure surface is therefore refered to as "mixed" or composite.

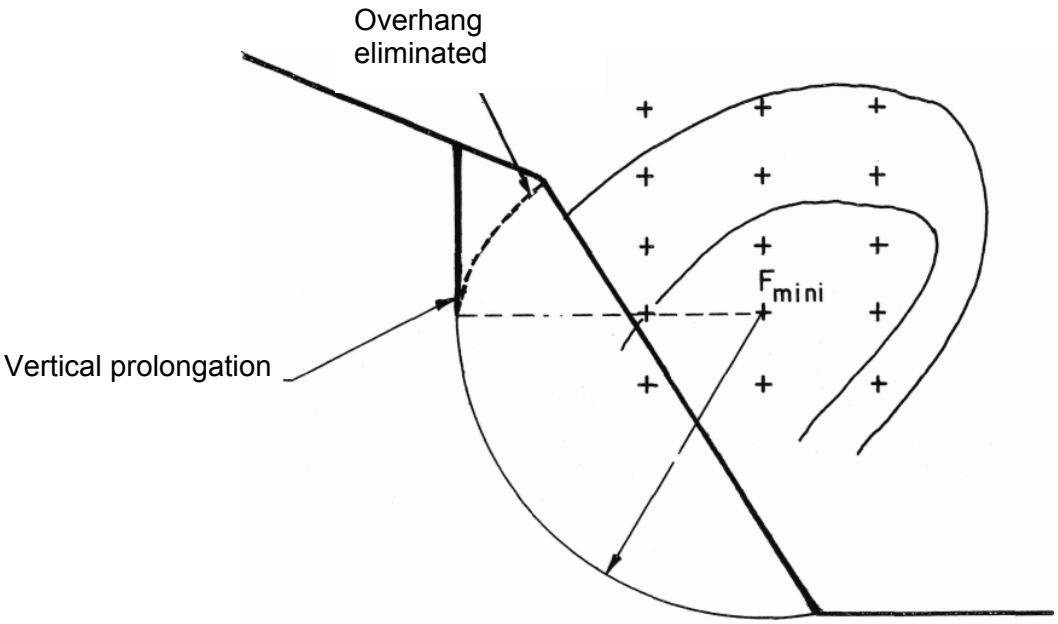

Figure 6: Composite failure surfaces

The Fellenius and Bishop methods are applicable for this type of composite failure by conserving the formulas (10) or (11) and (14) or (17) respectively, and by adopting the following expressions for $\alpha = \pi/2$ (vertical portion):

- For the Fellenius method: $\sigma' = 0$
- For the Bishop method: $\sigma' = \sigma'_{min}$

With: If $\phi \neq 0 \rightarrow \sigma'_{min} = -\frac{c}{\tan\phi}.\frac{\Gamma_\phi}{\Gamma_c} \rightarrow \tau_{max} = 0$

If $\phi = 0 \rightarrow \sigma'_{min} = -\infty \rightarrow \tau_{max} = \frac{c}{\Gamma_\phi}$

There is no theoretical justification in these methods for the vertical extension of the failure surface. However, these methods are already approximate with regards to the actual mechanical behavior. It is obvious that the conditions $\sigma' = 0$ for the Fellenius method and $\sigma' = \sigma'_{min}$ for the Bishop method are very conservative.

Similarly, non-circular failure surfaces introduced in the perturbation method cannot include an overhang. Any overhang is therefore treated in an analogous manner by replacing the upper overhanging portion by a vertical plane.

The cases incorporating artificially created composite surface are to be considered with the utmost caution (refer to section 3.4.).

3.2.1.4. Discretisation of the failure surface

A circular failure surface is discretised into segments of equal length until the vertical portion of the surface, if one exists, is encountered (Figure 7a).

A non-circular failure surface is divided into subsegments of equal length for each primary segment defining the surface (Figure 7b).

All parameters relating to a vertical slice (geometrical parameters, column weight, pore pressure, etc.) are calculated at point M located at the base of the slice (Figure 1).

3.2.2. Polygonal failure surfaces

3.2.2.1. Case of a planar failure or sliding wedge failure

The Fellenius and Bishop methods are directly applicable to the case of a planar failure surface since the radius does not intervene in the equations. For this same reason, these methods are not suitable when line loads and additional moments exist or when seismic parameters are integrated, since these loadings generate moments that cannot be taken into account.

The perturbation method is not directly applicable to this type of surface (Figure 7). However, it is only necessary to divide the failure surface into two segments with slightly different slopes for the perturbation method to be applicable. Furthermore, the limitations presented by the other two methods are eliminated.

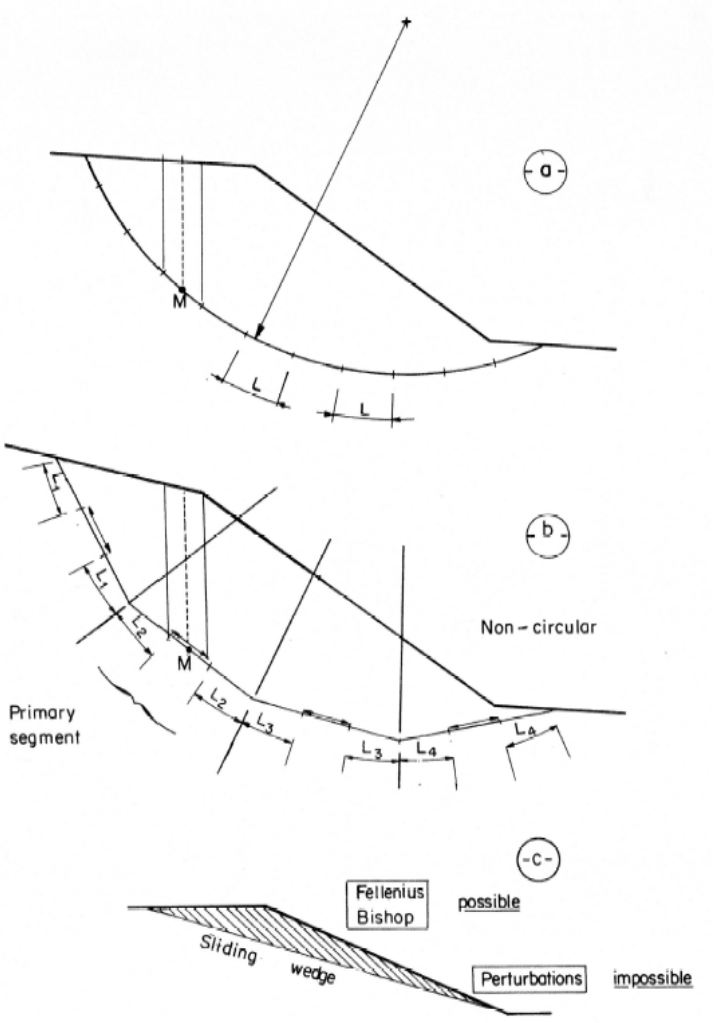

Figure 7: Discretisation of the failure surface

3.2.3. Spiral failure surfaces

Chapter under construciton.

The logarithmic spiral failure surfaces are associated with the yield design calculation method, which is in the process of being validated and is therefore not yet available in TALREN 4.

3.3. PORE PRESSURES

3.3.1. Determining the pore water pressures

Four methods are available to the user for the introduction of pore water pressures.

3.3.1.1. Water table and equipotential lines

The water table is defined by its upper (free surface) and lower (base of the water table) boundaries. The equipotential lines (i.e. lines where all points have a constant head) are assumed to be rectilinear with a variable orientation (defined by the user) depending on the point considered along the free surface (Figure 8). The pore pressure at point M is defined by:

$$u_M = \gamma_w . h_w \tag{28}$$

Below the level of the water table base, the program considers: $u_M = 0$

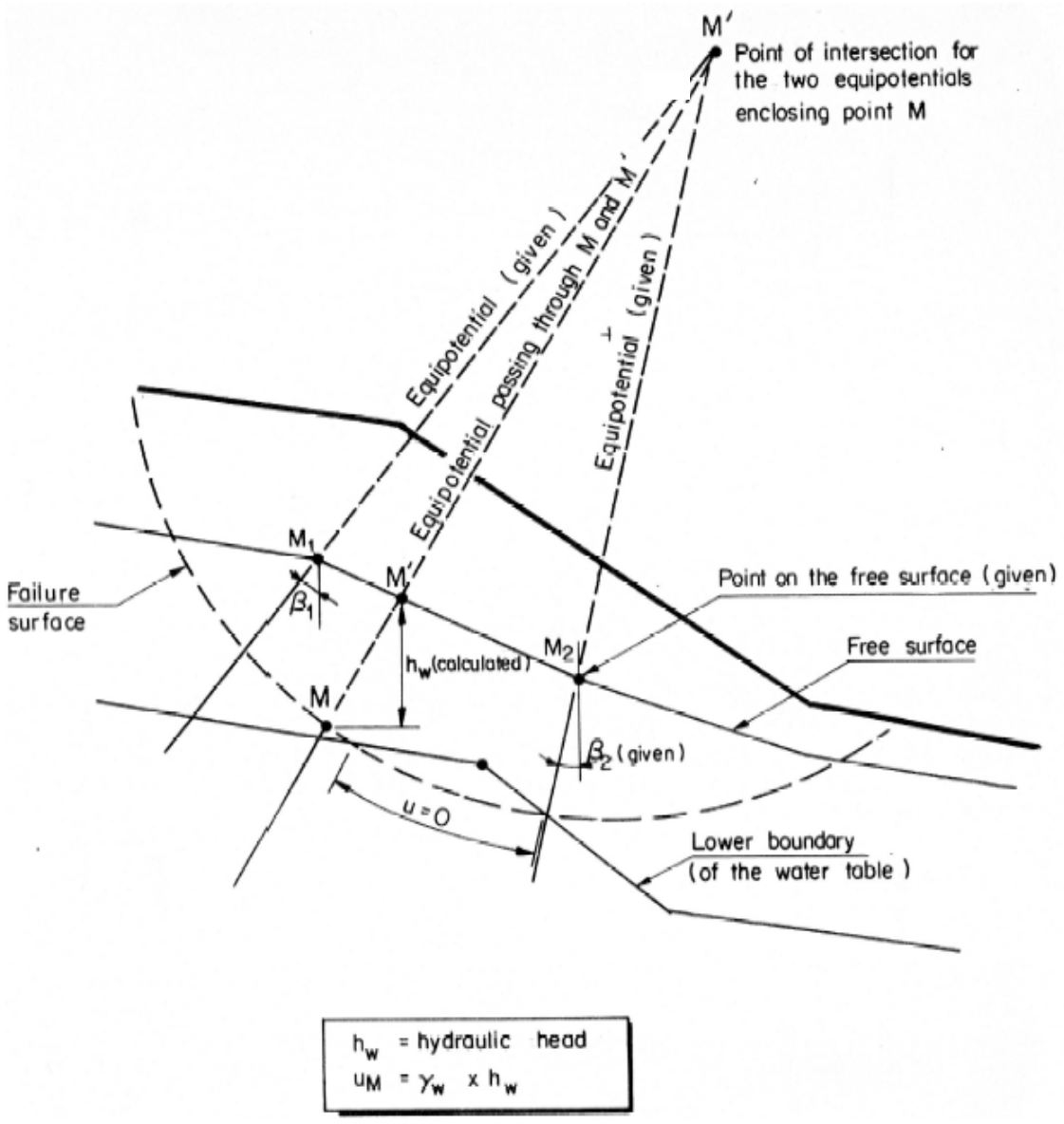

Figure 8: Determination of the pore pressure from the water table data and the equipotential lines

3.3.1.2. Pore pressures given at the points defining a non-circular failure surface

For each point located on a distinct segment, the pore pressure is calculated by linear interpolation between the values at the two adjacent endpoints characterising the segment (Figure 9).

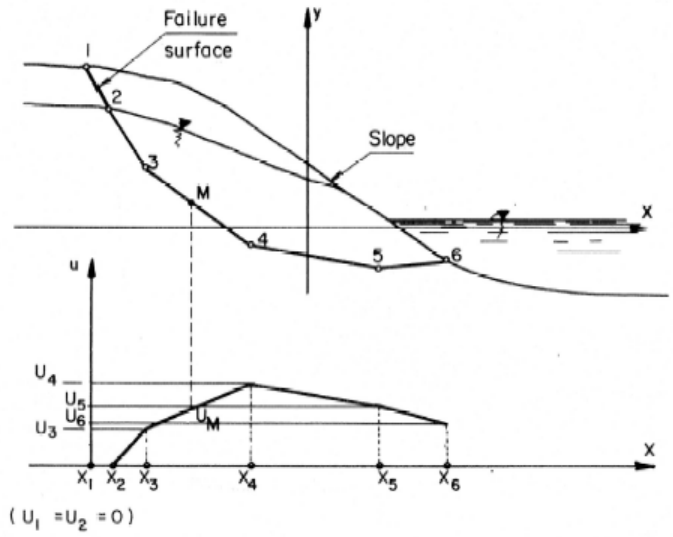

Figure 9: Pore pressure given at the points defining a non-circular failure surface

3.3.1.3. Triangular mesh

The pore water pressure can be defined at the nodes of a triangular mesh (for example: values obtained from a finite element calculation).

After determining the triangle in which the point M on the failure surface is located, the program performs a linear interpolation between the u values at the nodes of the corresponding triangle (Figure 10).

Note 1: To accelerate the search to locate the triangle including the point, the "zoning" option allows the user to define vertical intervals corresponding to given abscissas. Within these intervals, the program performs a preclassification of the mesh triangles (Figure 11). In the presented example, the preclassification assigns to zone IV the triangles 27, 29, 30, 31, 32, 33, 34, 35, 38 since they have at least one node within this zone. For all abscissas within this zone, the search is limited to the corresponding triangles.

Note 2: importation of hydraulic meshes from Plaxis v8

When importing hydraulic meshes from Plaxis v8 (also refer to user manual, part B of the present manual), Talren 4 imports the triangles of the Plaxis mesh (same number of triangles), as well as the 3 exrteme nodes of each triangle (with the pore pressures associated to these nodes). The number of imported nodes is therefore inferior to the number of nodes defined in the Plaxis mesh, because in a Plaxis mesh, each triangle has 6 or 15 nodes depending on the chosen option.

3.3.1.4. u function of the vertical stress

For a given soil, it is possible to define the r_u coefficient so that:

$$u = r_u . \gamma . h \qquad (28b)$$

Note: the value of u calculated in equation 28b does not take into account loads, but takes into account vertical seismic acceleration if defined.

3.3.2. External water tables

When the top of the water table is located outside the slope surface, it is necessary to

introduce one or more external water tables (Figure 12). The forces U_0 and U_1 in the general equation (3) are defined as the horizontal resultants of the thrust at the upper and lower sides of the slope.

For circular failure surfaces and as a result of the modification of the Fellenius method (refer to remark (a) in section 2.2), the introduction of an external water table can be treated by this method. The same applies to the Bishop and Perturbation methods.

For non-circular failures, the presence of an external water table can only be treated by the Perturbation method.

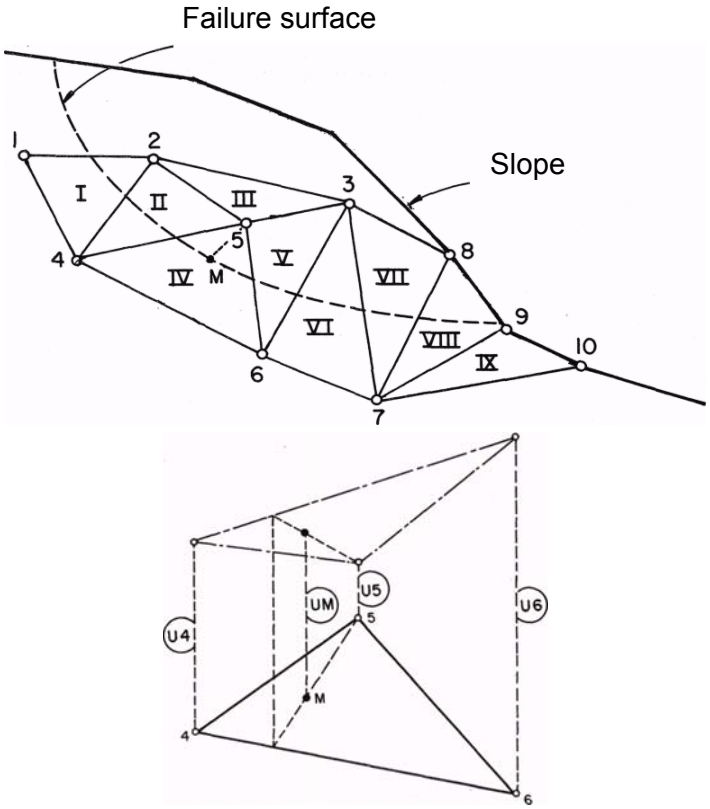

Figure 10: Pore pressures given at the nodes of a triangular mesh

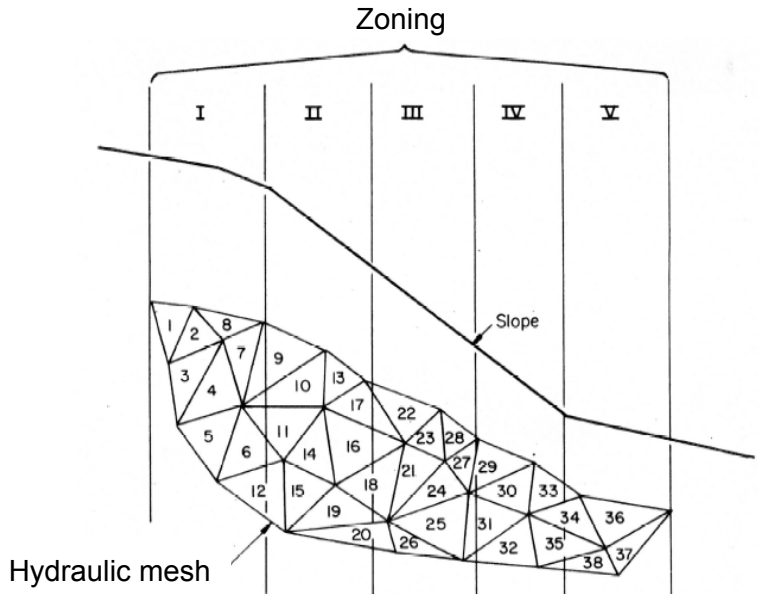

Figure 11: Preclassification zoning of the hydraulic mesh triangles

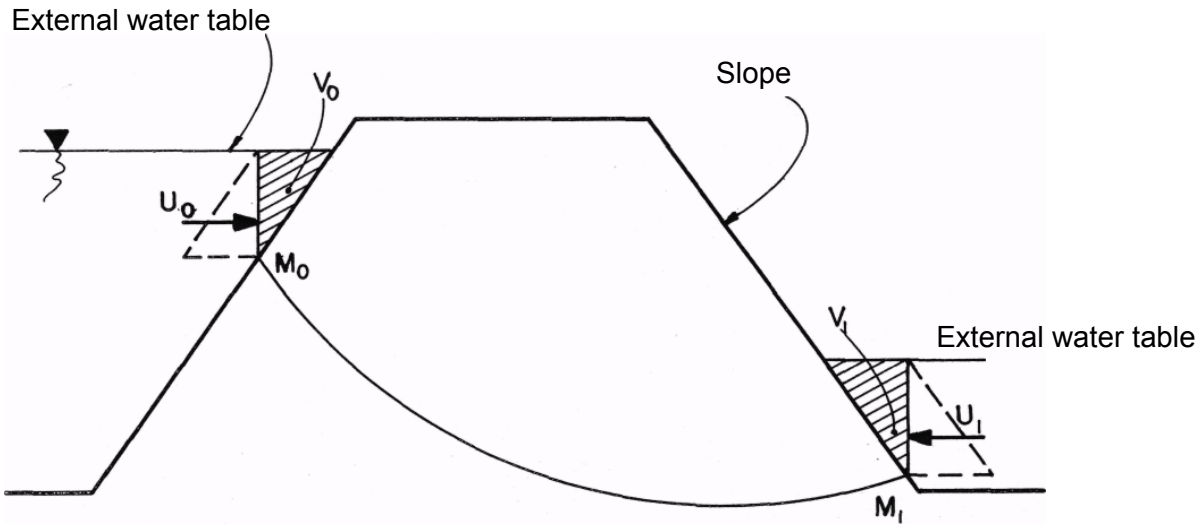

M_0 and M_1: intersections of the failure surface with the slope

V_0 and V_1: water volumes considered as attached to the volume of soil subject to sliding

U_0 and U_1: external forces applied to the volume of soil by the external water

Figure 12: Taking into account an external water table

3.3.3. Case involving the failure of the portion of a slope entirely submerged

For the case where the failure occurs in the portion of a slope entirely submerged and where the soil unit weights are not factored (Figure 13), the fundamental equilibrium equations, can be written as:

$$div[\sigma] = \vec{\gamma} \tag{29}$$

In terms of effective stresses:

$$div([\sigma'] + [u]) = \vec{\gamma} \tag{29a}$$

where:

$$[u] = (\gamma_w . h_w + \Delta u).[1] \tag{30}$$

with Δu: excess pore water pressure with respect to the hydrostatic regime or:

$$div[\sigma'] = \vec{\gamma}' - div\Delta u.[1] + \left(\overrightarrow{\gamma_w} - div(\gamma_w . h_w).[1]\right) \qquad \text{with } \vec{\gamma} = \vec{\gamma}' + \vec{\gamma}_w$$

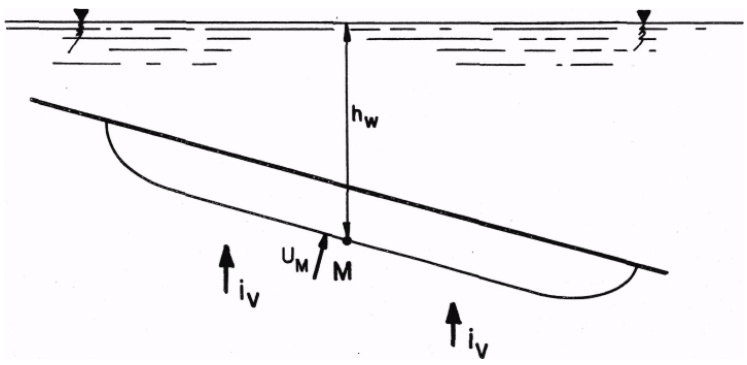

$u_M = \gamma_w . h_w + \Delta u$

Figure 13: Case of a totally submerged slope

The expression between parentheses is equal to 0 and the above equation becomes:

$$div([\sigma'] + \Delta u.[1]) = \vec{\gamma}' \qquad (31)$$

This formula is identical to the total stress equilibrium equation, subjected to the following conditions:

- consideration of the submerged soil weight;
- taking into account the possible generation of excess pore water pressure Δu, evaluated with respect to the hydrostatic pressure $\gamma_w.h_w$.

In the absence of Δu (hydrostatic regime), eq. (31) becomes: $div[\sigma'] = \vec{\gamma}'$

When the unit weights are not factored and the regime is hydrostatic, the safety factor of the submerged slope is identical to that of a slope without a water table and calculated with the submerged unit weights

In the Ultimate Limit State analysis, a weighted coefficient Γ_{s1} is applied to the total unit weight of the soil y, but not to the water unit weight (γ) In the case of a fully submerged slope calculated with submerged unit weights, the weighting factor Γ_{s1}^* applied to γ' is:

$$\Gamma^*_{s1} = \frac{\Gamma_{s1}.\gamma - \gamma_w}{\gamma - \gamma_w} \qquad \text{or} \qquad \Gamma_{s1}.\gamma = \Gamma^*_{s1}.\gamma' + \gamma_w$$

3.4. MECHANICAL PARAMETERS OF THE SOILS. DETERMINATION OF THE STRESSES σ' AND τ

3.4.1. Anisotropic cohesion

TALREN can take in account frictional and frictionless soils with an anisotropic cohesion, whose curve (cohesion as a function of the angle with respect to the horizontal) is defined by the operator as shown on Figure 13b.

The angle of the tangent is known at every point along the failure surface, which allows local determination of mobilised cohesion.

A partial safety factor Γ_ϕ is applied to the internal friction angle and the cohesion values at every discretisation point along the failure surface are factored by Γ_c.

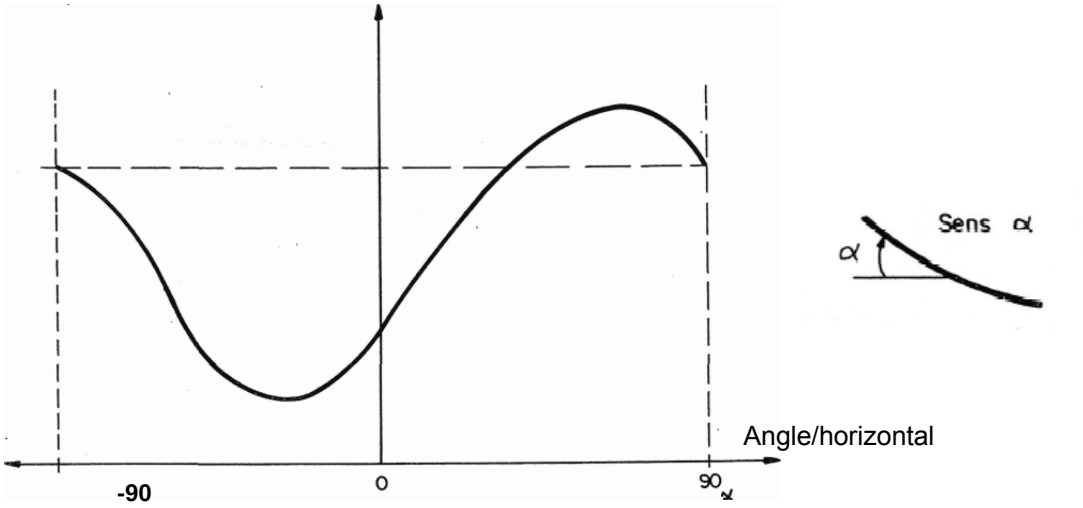

Figure 13b: Definition of anisotropic cohesion

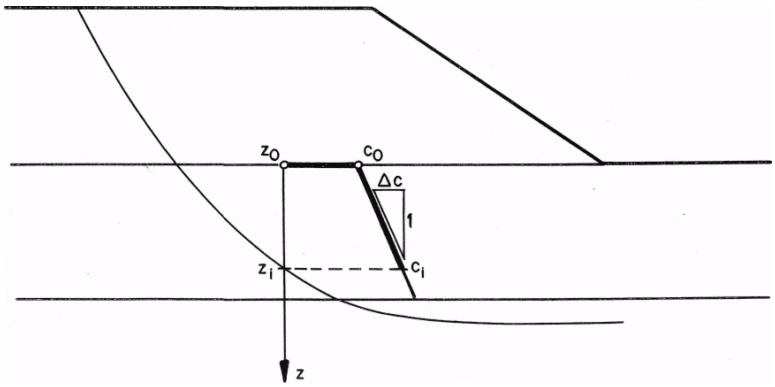

Figure 13c: Cohesion as a function of depth

3.4.2. Variable cohesion with depth

It is possible to define a cohesion which varies with depth for one or more soils. To consider a variable cohesion, one must define the cohesion value at the surface of the layer (c_0) and the variation (Δc) per unit depth in the soil data (Figure 13c). At a specific depth z_i, the cohesion is determined from eq. (31b).

$$c_i = c_0 + \Delta c.(z_0 - z_i) \tag{31b}$$

3.4.3. Shear strength curves

For classical cases, the mechanical strength parameters are defined by Coulomb's law (Figure 14 a and b).

$$\tau = c' + \sigma'.\tan\phi' \text{ (effective stresses) or } \tau = c_u \text{ (total stresses)} \tag{32}$$

In TALREN, it is possible to introduce a nonlinear shear strength curve, for example one corresponding to a dilatant soil (Figure 14c).

The shear strength curve is defined by points, and for each stress level σ', the program determines the corresponding shear strength curve by the procedure presented on Figure 14c. Using this method, the shear stress can be expressed by:

$$\tau = c'^{*} + \sigma'.\tan\phi'^{*} \tag{33}$$

Application of partial safety factors to ϕ' and c', for the case of a nonlinear shear strength curve, is explained on Figure 14d.

3.4.4. Upper zone - Normal stress limit in the Fellenius method

In the upper portion of a failure surface including a vertical extension, $\alpha \to \pi/2$, eq. (9) giving σ_{Fel}, becomes:

$$\sigma_{Fel} \to \frac{dU}{dl} = u \text{ et } \sigma'_{Fel} \to 0 \tag{34}$$

which leads to: $\tau \to \dfrac{c}{\Gamma_c}$

3.4.5. Upper zone - Particular aspects related to the Bishop method

In the Bishop method, it can be seen from eq. (16) that for a failure surface with a vertical extension:

$$\text{when } \alpha \to \pi/2,\ \sigma'_{Bish} \to -\frac{c}{\tan\phi}.\frac{\Gamma_\phi}{\Gamma_c} \ (= \sigma'_{min}) \tag{35}$$

To avoid a numerical problem for values of tgα near $\pi/2$, the program imposes τ_{max} = 0 for $\alpha > \pi/2 - 5.10^{-3}$ radians.

However, an anomaly occurs in this zone as a result of the method used for determining σ'.

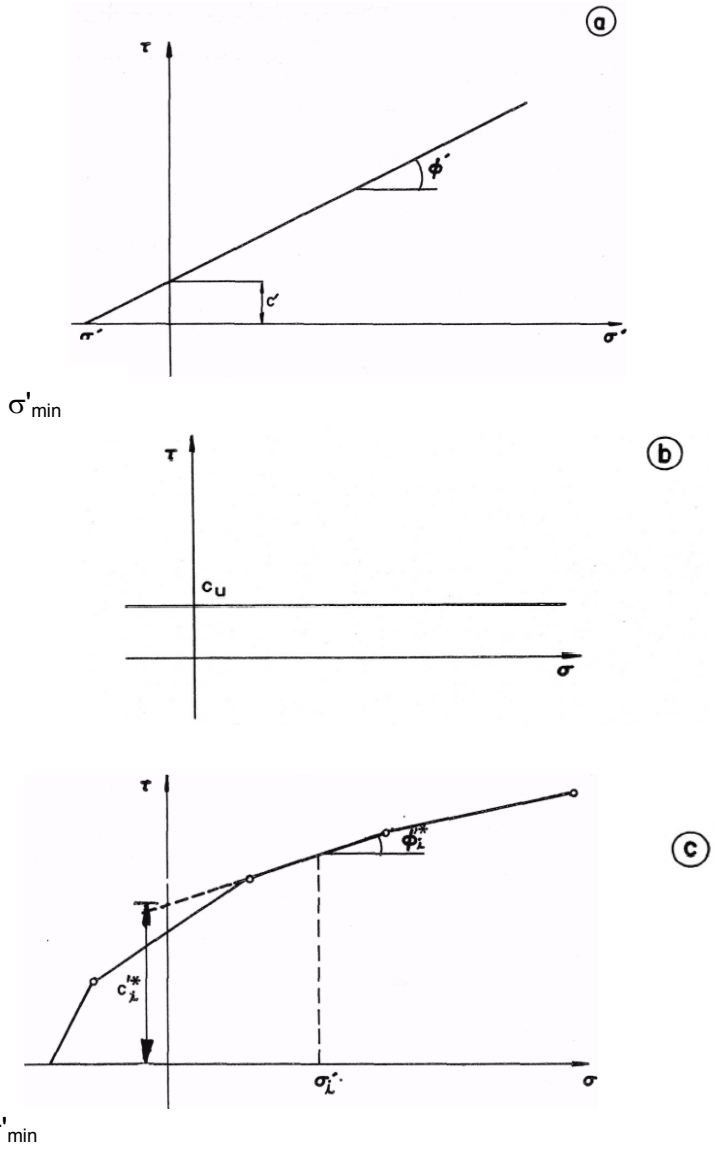

Figure 14a, b and c: Shear strength curves considered by TALREN

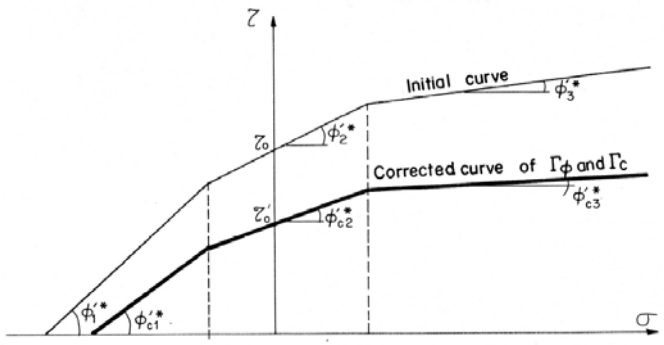

$$\tau_{co} = \frac{\tau_o}{\Gamma_c} \qquad \phi_{ci} = \arctan\left[\frac{\tan\phi_i}{\Gamma_\phi}\right]$$

Figure 14d: Taking into account Γ_c and Γ_ϕ in the case of a nonlinear strength curve

Figure 15 shows the evolution of τ_{max} (given by eq. 16), for $0 < \alpha < \pi/2$. If no friction was mobilised, the value of τ_{max} would be constant and equal to c/Γ_c. Introducing the friction locally decreases the maximum shear (and consequently τ allowable) in the upper wedges, with respect to the case of zero friction (hatched zone on Figure 15).

This reduction is globally compensated by the corresponding increase in Tmax in the other wedges and therefore does not generally create a particular problem.

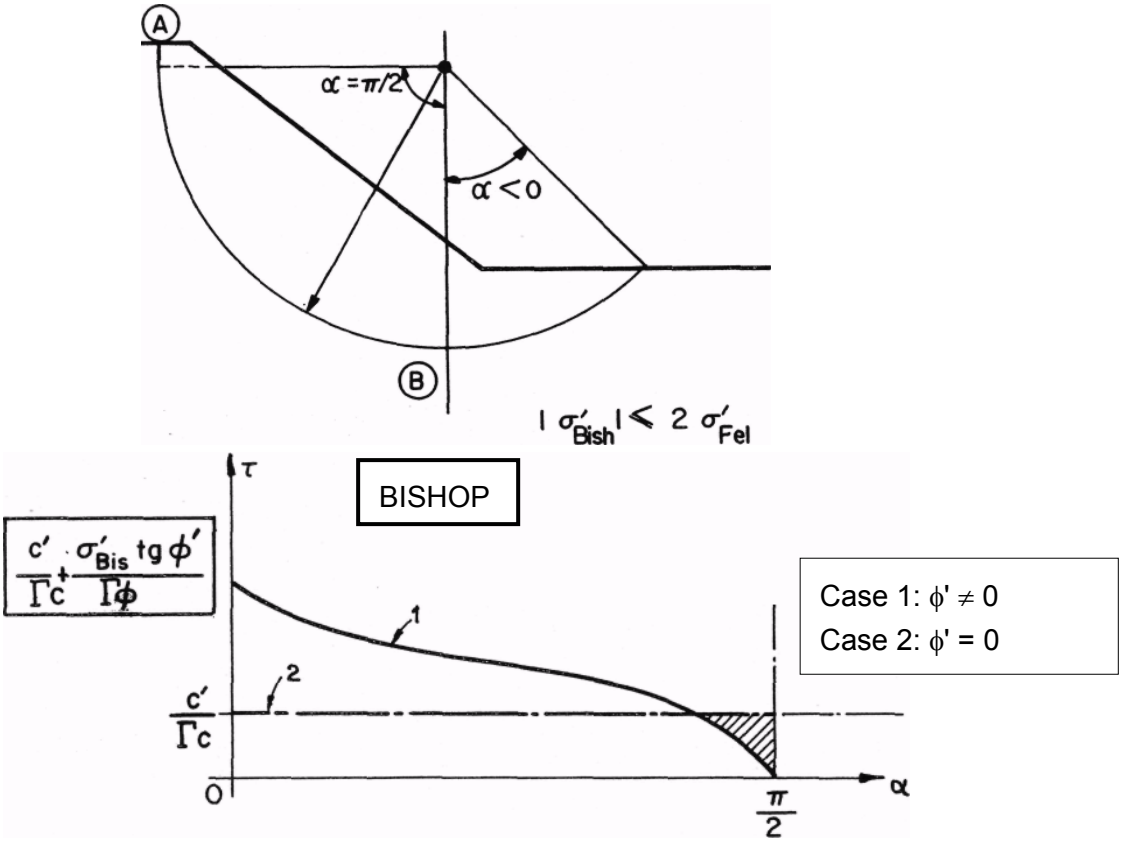

Figure 15: Specific tests to the Bishop method in TALREN

Conversely, for composite surfaces incorporating a large vertical portion (Figure 16a), the suppression of τ for $\alpha \geq \pi/2$ results in two errors:

- Γ is overly pessimistic since one neglects the friction which actually exists along AB;
- Γ is less than if one were to cancel the friction while maintaining the cohesion in the upper wedges (section 3.2.1.2).

Therefore, the proposed extension of the surface must be treated with extreme caution when the position of the minimum safety factor is located below the top of the slope.

a) BISHOP extended

b) Perturbations

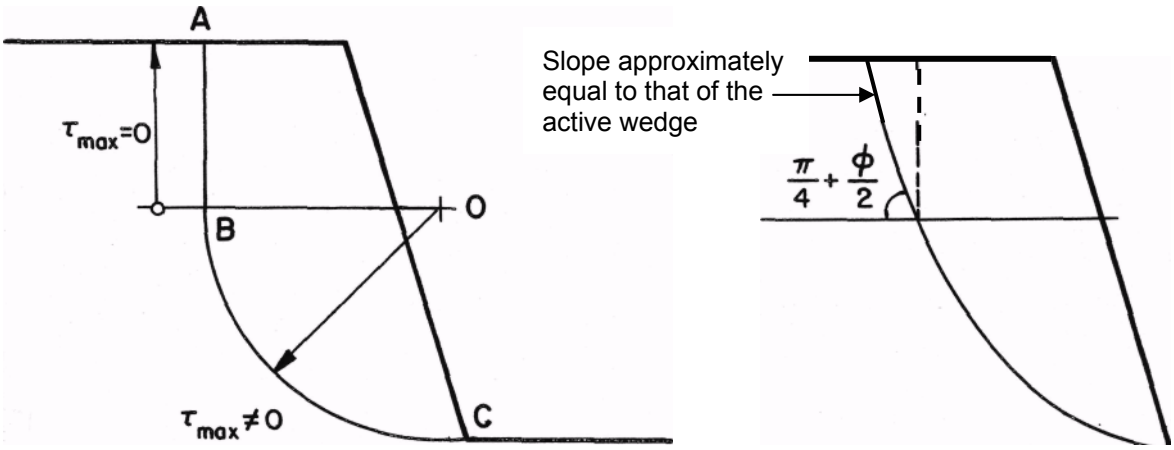

Figure 16: Large distortion cases due to the extension of the Bishop method to the case of composite failure surfaces – Substitution by the Perturbation method advised

3.4.6. Upper zone - Limitation of the normal stress in the Perturbation method

The normal stress given by eq. (18) is defined by:

$$\sigma'_{pert} = \sigma'_{Fel}.\left(\lambda + \mu.\tan^{n}\alpha\right) \qquad (36)$$

For a failure surface with a vertical extension, it was shown that $\sigma'_{Fel} \to 0$ when $\alpha \to \pi/2$

As in the Fellenius method, the term tan ex. in eq. (36) requires an artificial means of calculation to avoid convergence problems for values near $\alpha = \pi/2$.

TALREN imposes:

$$\sigma'_{pert} = 0 \text{ when } \alpha \geq \pi/2 - 1.10^{-5} \text{ radians} \qquad (36a)$$

This rule applies to the vertical upper portion of the failure surface, if one exists.

As with the other methods, this artificially imposed mathematical device does not reflect the actual mechanical behavior and it is therefore preferable to limit the length of the vertical portion to a strict minimum, and to adopt failure surfaces near that of the active wedge for the upper zone (Figure 16b).

3.4.7. Problems relating to the lower part of the failure surface (Bishop method)

At the lower portion of the failure surface, and for the case of an ascending curve ($\alpha < 0$) (Figure 15), the expression $m(\alpha)$ in eq. (15) may be equal to zero. The expression for σ'_{Bishop} (eq. 16) consequently approaches infinity and the iterative convergence process for determining Γ is disrupted.

To avoid this problem, a test is imposed in TALREN. In the lower zone, when $\alpha < 0$, one adopts:

$$\sigma'_{Bish} \leq 2.\sigma'_{Fel} \text{ where } \sigma'_{Fel} \text{ is given by eq. (9).} \qquad (37)$$

This problem does not occur in the other methods.

3.5. LOADS

Taking into account applied loads is a delicate matter for all "at failure" slope stability programs since the effect of a load on the stress distribution along the failure surface depends on the deformation of the soil mass (Figure 17). This distribution is not determined in a precise manner, even for a "non-loaded" soil mass.

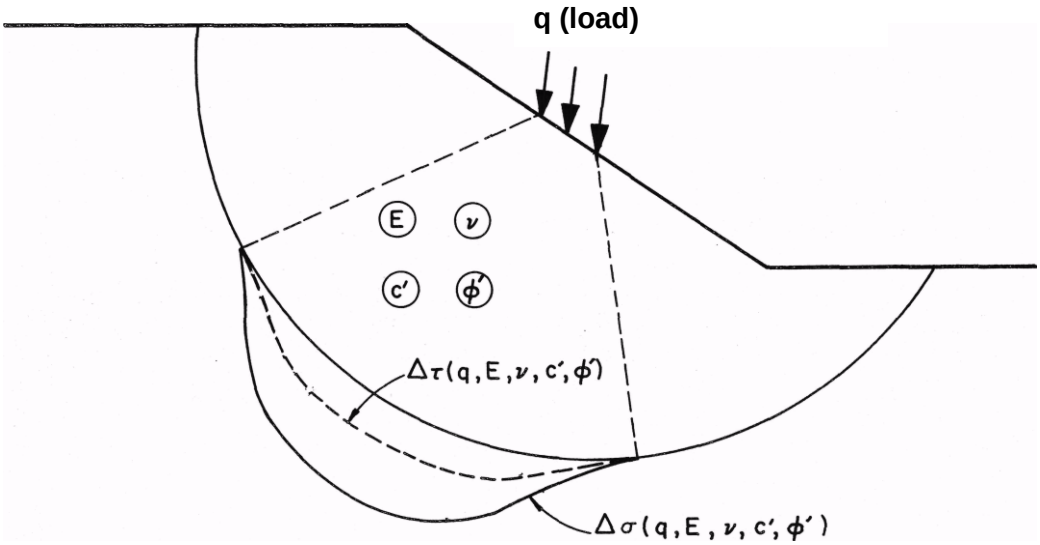

Figure 17: Problem raised by the estimation of the load effect

It is unreasonable to attempt to introduce an estimation of the load effect determined from deformation calculations (ie. Finite Element calculations), since at failure calculations would thereby loose the advantage relating to their simplicity.

Because of the lack of a satisfactory unique solution, two methods are used to simulate the loads:

3.5.1. Vertical distributed loads

It is possible to simulate these loads by a fictitious soil layer having the same stress (Figure 18a). The incidence of the load is consequently localised essentially to the vicinity of its zone of application. However in reality, because of the bias caused by the safety factor and the interslice forces in the particular case of the Bishop method, the load has an effect along the entire failure surface.

3.5.2. Inclined distributed loads

Chapter under construction.

Inclined distributed loads cannot be taken into account, except in the calculation with yield design calculation method (and not in Fellenius, Bishop or perturbations methods).

The yield design calculation method is in the process of being validated and is therefore not yet available TALREN 4.

3.5.3. Inclined (or vertical) linear loads

The need to take into account the horizontal component of the applied loads, in the case of an inclined load, or the desire to more appropriately diffuse their effects, in the case of a vertical load, has led to the procedure of simulating the loads as fictitious ground anchors (Figure 18b). This treatment method will be described in detail in section 5.

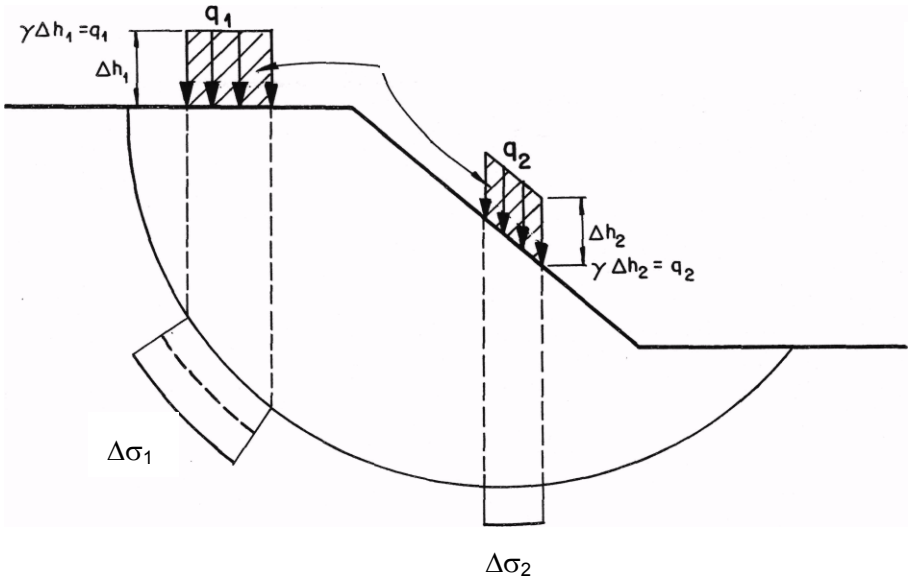

a)

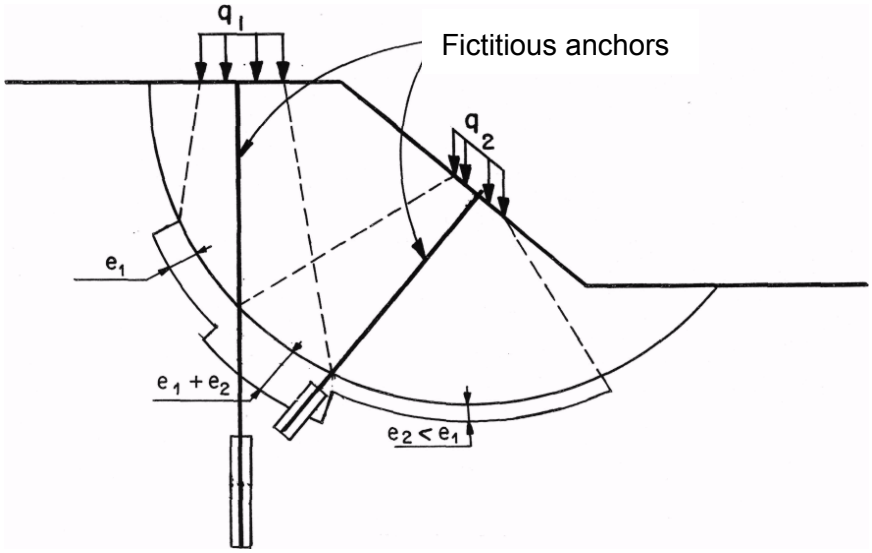

b)

a) simulation by a fictitious soil layer
b) simulation by fictitious anchors

Figure 18: Taking into account loads in TALREN

3.6. SEISMIC EFFECT

The effect of an earthquake is treated by the "pseudo-static" method. The gravity is multiplied by a horizontal (C_{ah}) and vertical ($1 + C_{av}$) acceleration coefficient, in which the values and direction are given by the user (Figure 19).

For polygonal failure surfaces, only the Perturbation method is adapted.

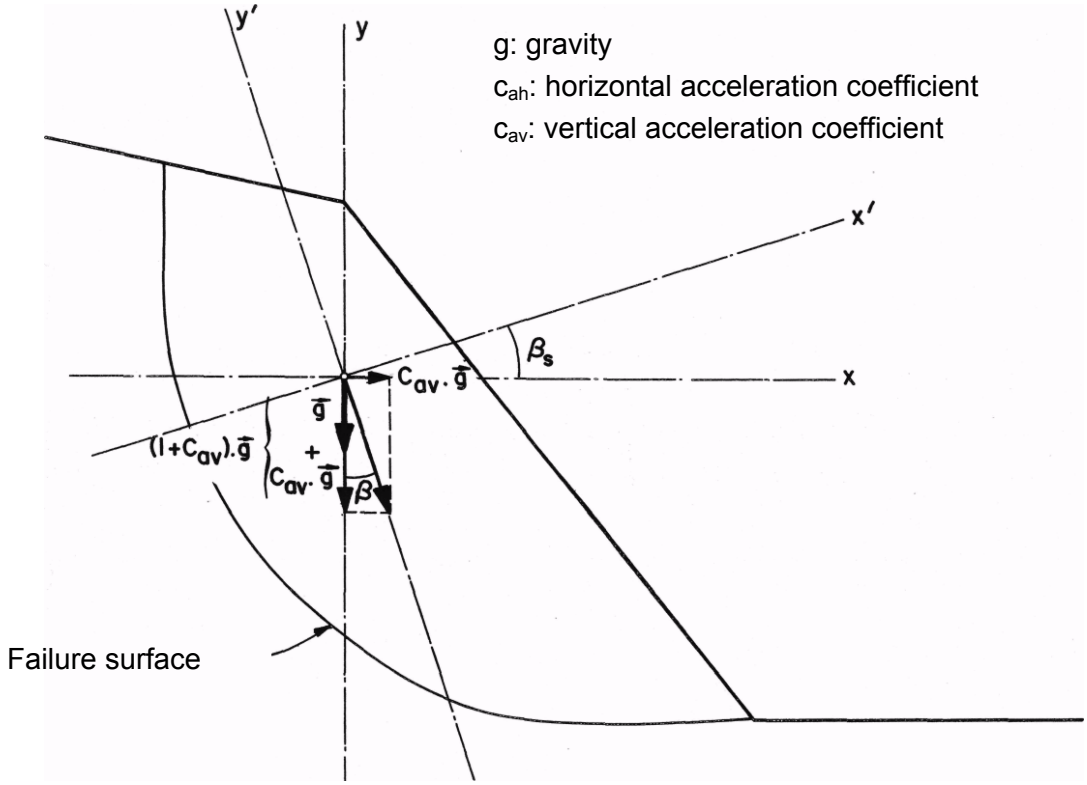

Figure 19: Seismic simulation by the "pseudo-static" method

Remarks:

a) It is important to note that during seismic loading, corresponding to a situation of rapid shearing, the mechanical characteristics and hydraulic conditions to be considered must be carefully chosen (one may need to refer to documents related to this subject).

b) When considering an external water table, it is assumed that the horizontal seismic effect does not apply to the water mass located outside the slope, in order to not induce undesirable shear forces at the slope surface (Figure 21). Although this method is not the recommended procedure, it more accurately models the actual conditions than the rigid application of the "pseudo-static" method.

   Note: In some cases, the hydrodynamic pressures may need to be considered. To estimate these pressures, one should refer to documents pertaining to this topic.

c) Only the vertical acceleration coefficient is applied to the distributed loads.

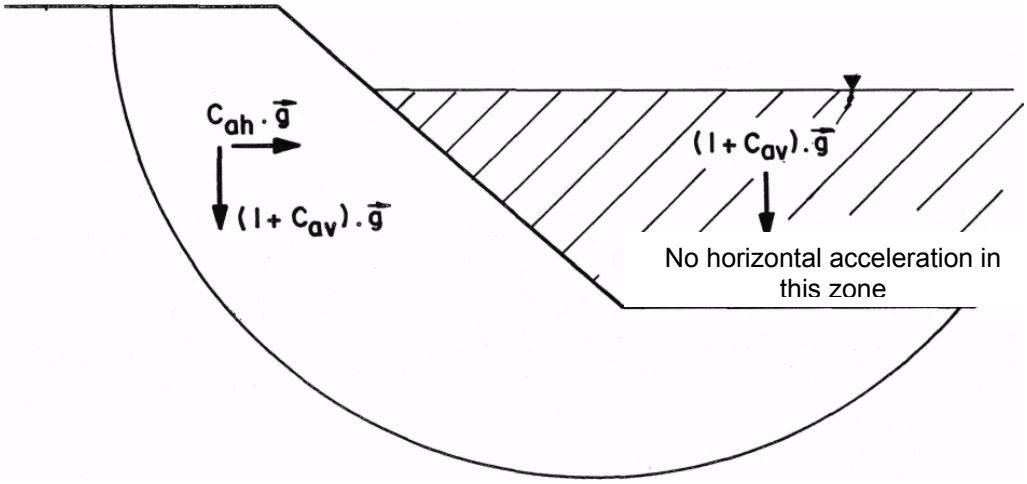

Figure 20: Case of an external water table subjected to an earthquake

4 THEORETICAL STUDY PERTAINING TO THE REINFORCEMENT EFFECT

4.1. REINFORCEMENT TYPES – GENERAL CONSIDERATIONS

TALREN has been specifically conceived to take into account reinforcing elements. The types of reinforcement accepted by the program include all inclusions which can be characterised by one or more of the following parameters:

- tensile strength;
- shear strength;
- bending stiffness.

The following reinforcement types are available (Figure 21):

- prestressed ground anchors;
- soil nails;
- piles and micropiles;
- reinforcing strips;
- retaining structures (sheetpiling, diaphragm walls);
- geotextiles.

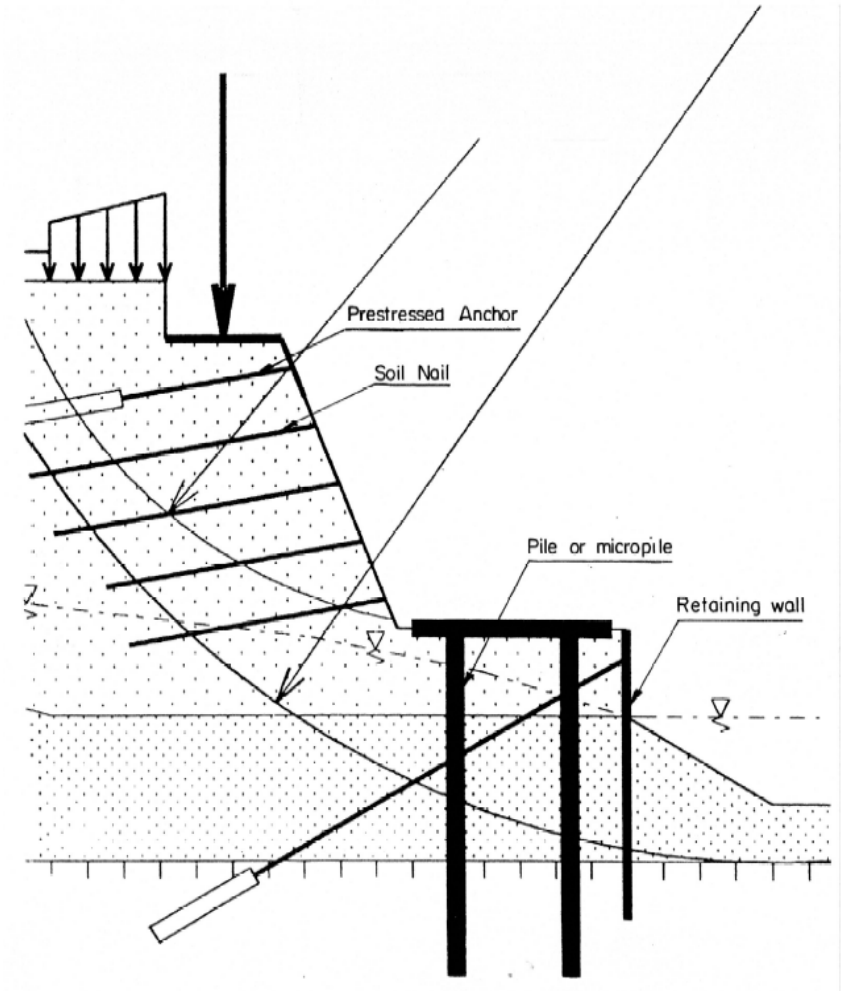

Figure 21: Reinforcements considered by TALREN

The reinforcing elements are taken into account by considering the forces generated at the intersection with the failure surface (Figure 22). These forces are decomposed into:

- an axial force T_n;
- a shear force T_c.

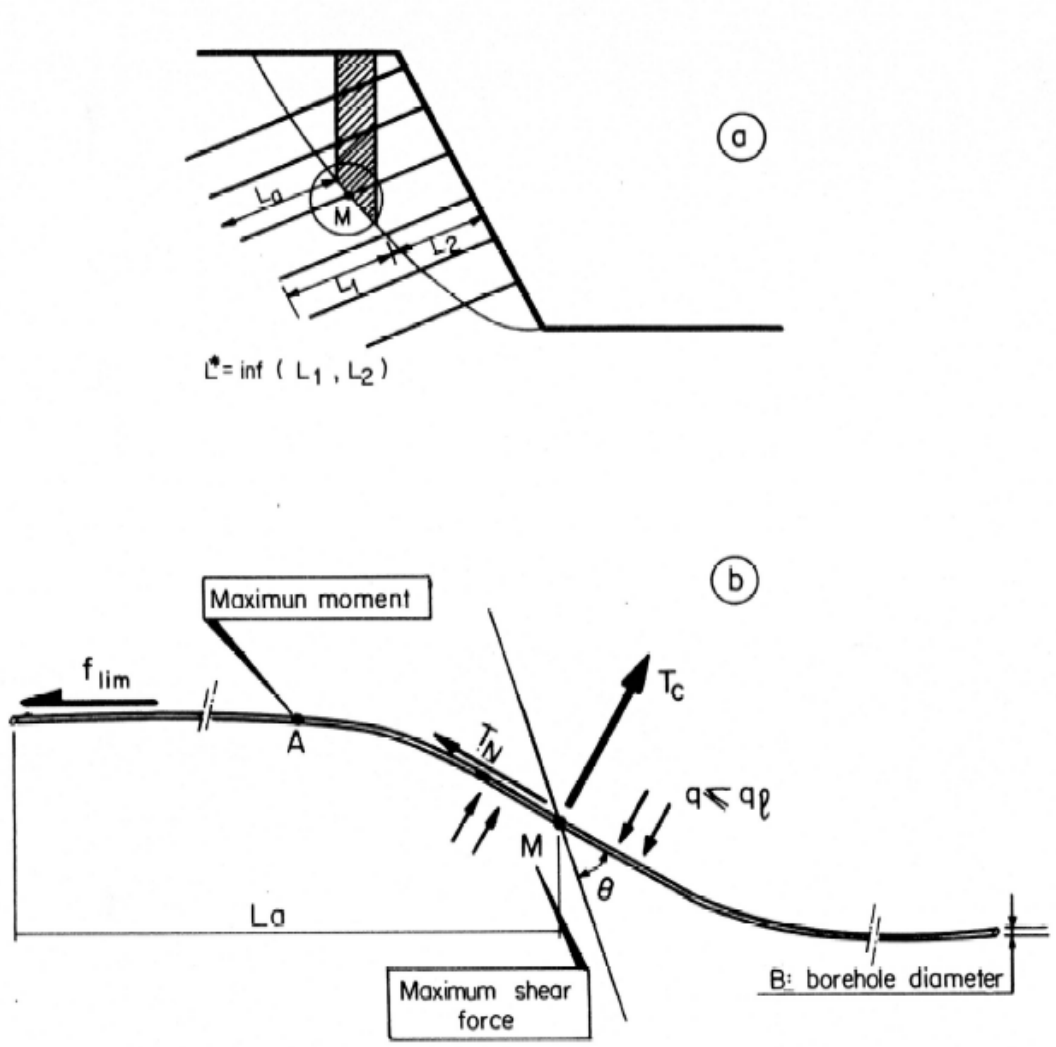

Figure 22: Procedure to take into account the effect a reinforcement

The intersection point (M) between the inclusion and the failure surface is the point of maximum shear force and consequently the bending moment is zero.

Certain rules pertaining to the diffusion of the reinforcement effect within the reinforced soil mass are introduced in TALREN and will be further explained in section 5.4.

Except for the limiting criterion for the soil-inclusion normal force, the deformability of the material is not taken into account. As a result, the calculation does not for example, take into account the stress concentrations observed around stone columns, when preloaded by an embankment. This case must be specially treated (section 5.3.5).

The forces T_n and T_c taken into account in the calculation, are deduced from their "at failure" values, corrected by an appropriate safety factor, as will be discussed in section 5. In the present section, the procedure for determining the "at-failure" forces will be developed.

4.2. "AT-FAILURE" MOBILISATION CRITERIA FOR THE INCLUSIONS

The inclusion forces T_n and T_c in the vicinity of the failure surface are limited by the following criteria:

- inclusion strength properties (tension, shear, bending moment);
- soil-inclusion interaction resistance (normal force and lateral friction).

The problem is hereafter presented in the general form for an inclusion resisting simultaneously tensile forces and bending moments. The limit value for each of these properties is given by the position of the corresponding stability domain boundary on the failure criteria diagram. This diagram wiIl be presented later.

Near the failure surface, the inclusion is assumed to behave like an elastically supported beam (Figure 22), in which the deformation is symmetric with respect to the point of intersection (point M) with the failure surface.

The inclusion's resistance intervenes by a combination of tension and shear at point M and tension/bending at the point of maximum moment (point A).

The soiI-inclusion interaction is limited by the limit normal pressure of the soil at the point of maximum relative displacement (point M) and by the limit adherence f_{lim} along the portion of the inclusion situated outside the failure surface (L_a).

4.2.1. Resistance of the inclusion

4.2.1.1. At point M

The shear force is maximum. The inclusion is assumed to be characterised by its shear resistance, according to the Tresca criterion.

$$\tau_{\max} = k \tag{39}$$

Considering the schematic nature of the problem and in order to simplify its development, it is assumed that the shear stress distribution is uniform along the inclusion's cross section and its pure shear strength can be defined by:R_c = k.S

where S: the cross-sectional area of the material, considered to make up the active portion of the inclusion (Le., the steel for the nails, excluding the grout).

In the same manner, the tensile strength is assumed to be defined by (Tresca):

$$R_n = 2.R_c\,(Tresca)$$

To simplify the expression, the resistance is considered to be positive.

The Mohr's diagram is presented on Figure 23 where σ and τ are the respective normal and shear stresses mobilised in a cross section and r is the radius of the Mohr's circle. This radius must be less than the shear strength k and the expression becomes:

$$r^2 = \tau^2 + \frac{\sigma^2}{2} \le k^2$$

Integrating over the section S gives: $T_c^{\,2} + \frac{T_n^{\,2}}{4} \le R_c^{\,2} \left(= \frac{R_n^{\,2}}{4} \right)$

At the point of zero bending moment (point M), the stability criterion of the bar can be expressed as:

$$\frac{T_n^{\,2}}{R_n^{\,2}} + \frac{T_c^{\,2}}{R_c^{\,2}} \leq 1 \qquad (40)$$

The stability domain of the bar is delimited in the [T_n, T_c] plane by an ellipse with axes R_n and R_c (= R_n/2), at the interior of which the vector T (T_n/ T_c) must be located.

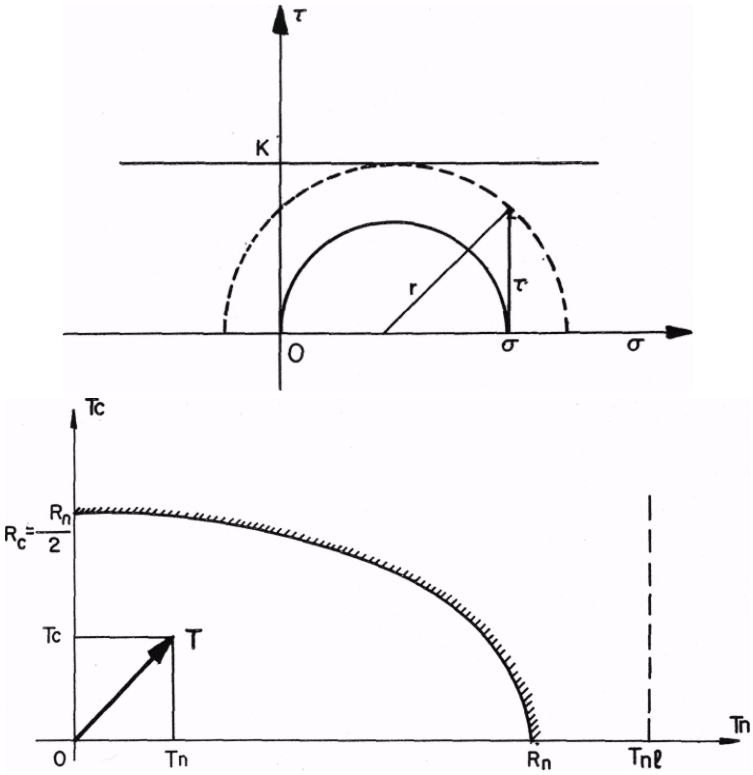

Figure 23: Stability domain of the steel, at the point of zero moment

4.2.1.2. At point A

The moment is maximum. The inclusion works in combined bending. The total plastification of the bar (M_{max}) depends on the tension and the nature of the bar (shape and material).

For example, for a steel bar with a rectangular section h x b (Figure 24), which is completely plastified, the equations become:

$$T_n = 2.k.b.(h_1 - h_2) \text{ and } M_1 = k.b.(h_1^{\,2} + h_2^{\,2})$$

with: $h = h_1 + h_2$

k: shear strength of the steel

$$M_{\max} = M_0 = M_1 - T_n.\left(\frac{h_1 - h_2}{2}\right)$$

or: $$M_{\max} = 2.k.b.h_1.h_2$$

or: $$M_{\max} = \frac{k.b.h^2}{2} - \frac{T_n^{\,2}}{8.k.b}$$

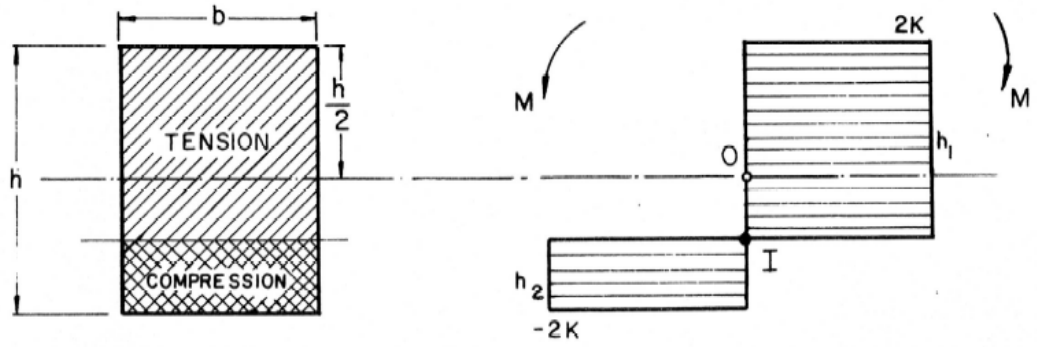

Figure 24: Complete plastification by combined bending

The maximum allowable moment in simple bending $M_{max}(0)$, corresponding to $T_n = 0$, is given by:

$$M_{\max}(0) = \frac{k.b.h^2}{2}$$

which, introducing $R_n = 2.k.b.h$, gives:

$$M_{\max} = M_{\max}(0).\left(1 - \frac{T_n^{\,2}}{R_n^{\,2}}\right) \qquad (41)$$

This criterion is used in conjunction with the soil-bar interaction criterion explained hereafter since the moment in the bar at point A depends on the shear force T_c at point M.

To simplify the development for an inclusion with an arbitrary geometry, it is assumed that the relation $M_{max}(T_n)$ has the same form as eq. (41), where $M_{max}(0)$ is the plastification moment of the inclusion in simple bending. The justification of this assumption is given in Appendix 1.

4.2.2. Soil-inclusion interaction

4.2.2.1. Lateral friction criterion

Pull-out of an inclusion by tension generates a force, in which:

$$T_n \le L_a . f_{\lim} \qquad (42)$$

where: f_{lim}: pull-out resistance of the grout per unit length of the inclusion,
L_a: adherence length beyond the failure surface (Figure 22b)

This criterion corresponds to a vertical line in the $[T_n, T_c]$ diagram (Figure 25).

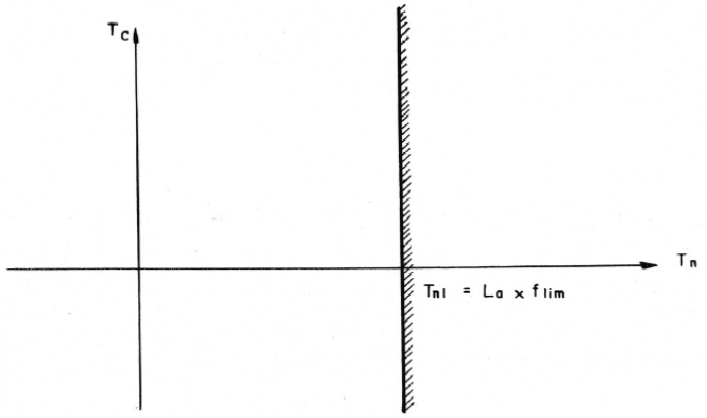

Figure 25: Stability domain for soil-inclusion lateral friction

4.2.2.2. Soil-inclusion normal reaction criterion

During the relative displacement between the stable soil mass and the active zone, the inclusion deforms as indicated on Figure 22. The soil-inclusion normal pressure is maximum at the point of maximum displacement (point M).

One assumes that the normal reaction law is of the elasto-plastic type and can be expressed by the classical notation (Bourges & Frank; 1979) (Figure 26): $p = k_s.y$

$$\text{or } P = p.B = k_s.B.y = E_s.y \tag{43}$$

$$\text{where } p \le p_l \tag{44}$$

B: diameter on which the soil reaction is mobilised

p_l: limit pressure of the soil

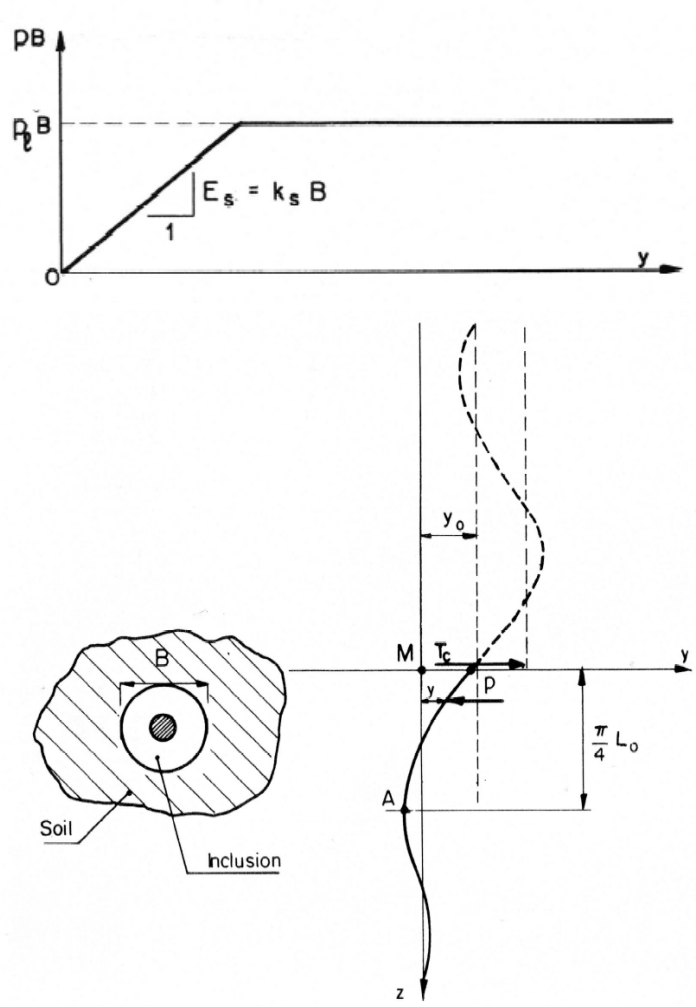

Figure 26: Behaviour law for an inclusion subjected to shear in M

The equilibrium equation for beams on elastic supports leads to:

$$EI.\frac{d^4 y}{dz^4} + E_s.y = 0 \tag{45}$$

where EI is the bending stiffness of the inclusion (annexe 3.4).

The general solution involves the reference (or transfer) length, defined by:

$$L_0 = \left(\frac{4.EI}{E_s} \right)^{1/4}$$

The problem consists of expressing the shear force T_c at point M, as a function of the soil-inclusion normal pressure (p_M) at the same point. The solution depends simultaneously on the inclusion's active length L^* (defined on Figure 22a) and it's bending resistance at point A.

With respect to the adherence length L*, three situations can be theoretically considered:

- $L^* \geq 3.L_0$: The inclusion can therefore be considered as infinitely long. The analytical solution of eq. (45) is therefore simple.
- $L^* \leq L_0$: The inclusion can therefore considered as infinitely rigid. The analytical solution of eq. (45) is also simple.
- $L_0 \leq L^* \leq 3.L_0$: This is the intermediate solution for which the analytical solution is complex to treat.

Considering the theoretical nature of the problem, TALREN assumes that the three situations can be reduced to two cases:

- $L^* < 2.L_0$ (infinitely rigid inclusion)
- $L^* \geq 2.L_0$ (infinitely long inclusion)

Classical nails generally correspond to the category "infinitely long" ($L_0 \leq 1$m), except near the base of the structure where the failure surface is close to the facing.

The solutions for these two cases will be further developed.

It is assumed in TALREN that the shear force T_c at point M is limited by the soil plastification at this point, which can be defined as the limit pressure p_l This parameter relates to the pressuremeter properties and can be expressed as:

$$p_M \leq p_l \qquad (47)$$

Note: This criterion is strict since one can envision that soil plastification resulting from the normal stress can develop along a certain portion of the inclusion, on either side of the failure surface. Since it is not possible to determine along which length the normal stress is limited, the most severe criterion has been chosen and is therefore conservative in terms of safety. Furthermore, this criterion results in a limitation of the relative displacements along the failure surface.

The development mode for T_c and therefore its limit value T_{cl} during soil plastification at point M depends on the order in which the two phenomena occur: soil plastification at point M (criterion T_{cl1}) or plastification of the inclusion at point A (criterion T_{cl2}) (Figure 27)

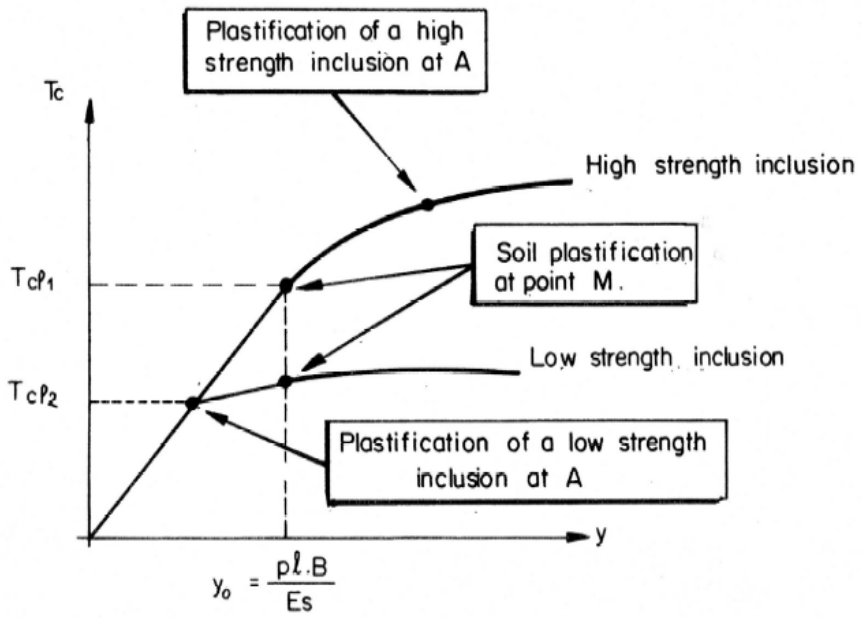

Figure 27: Development of the shear force, Tc (at M) as a function of the lateral displacement y at this point, and the mechanism by which plasticity occurs: soil-inclusion normal pressure at point M and plastification of the inclusion in combined bending at point A

4.2.2.3. Solution of the problem for $L^* \geq 2.L_0$

The solution of equation (46) is:

$$y = \frac{2.T_c}{E_s.L_0}.e^{-x}.\cos x \text{ with } x = \frac{z}{L_0} \tag{48}$$

with z: distance from the point considered to point M

$$M = T_c.L_0.e^{-x}.\sin x \tag{49}$$

The normal pressure is maximum at point $M_{(z=0)}$ and is defined by:

$$p_M = k_s.y(0) = \frac{2.T_c}{B.L_0} \tag{50}$$

The maximum moment occurs at point A, for a distance of $z = (\pi/4).L_0$, with respect to the failure surface and can be defined as:

$$M_A = \frac{\sqrt{2}}{2}.e^{-\pi/4}.T_c.L_0 \approx 0{,}32.T_c.L_0 \tag{51}$$

a) Criterion T_{cl1} ($M_{max} \geq 0{,}16.p_l.B.L_0^2$)

During soil plastification at point M and in the absence of plastification within the bar, the limit shear force of the inclusion at this point can be obtained from eq. (47) and (50):

$$T_{cl1} = p_l . \frac{B.L_0}{2} \tag{52}$$

This criterion is represented by a horizontal line in the (T_n, T_c) (Figure 28).

An increase in the shear force above this value, corresponding to an extension of the plastic zone, is not permitted.

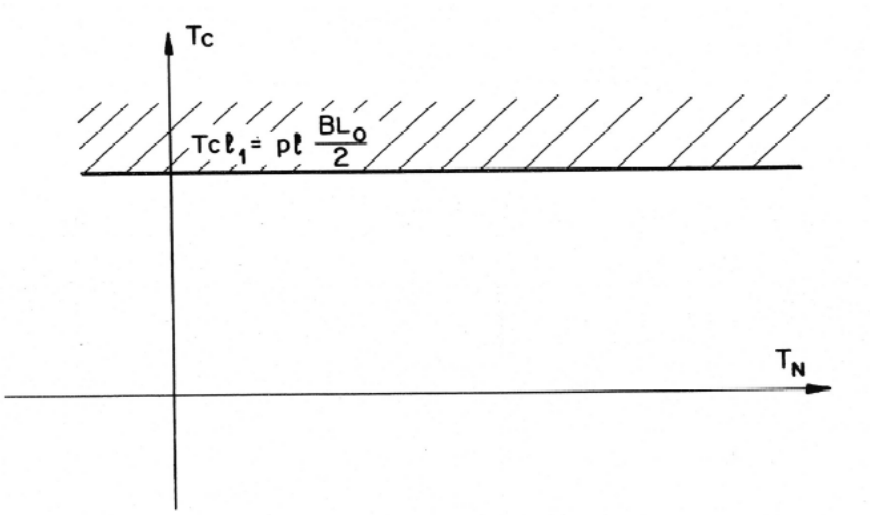

Figure 28: Stability domain resulting from the soil-inclusion normal force interaction at M, without plastification of the inclusion (criterion T_{cl1})

b) Criterion T_{cl2} ($M_{max} < 0{,}16.p_l.B.L_0^2$)

When plastification of the inclusion occurs at point A prior to soil plastification at point M, the shear force at M, derived from eq. (51) becomes:

$$T_{cp} = \sqrt{2}.e^{\pi/4}.\frac{M_{\max}}{L_0} \approx 3{,}1\frac{M_{\max}}{L_0} \tag{53}$$

The corresponding displacement at point M, derived from eq. (47) becomes:

$$y_{Mp} = 2.\sqrt{2}.e^{\pi/4}.\frac{M_{\max}}{E_s.L_0^{\,2}} \approx 6{,}2\frac{M_{\max}}{E_s.L_0^{\,2}} \tag{54}$$

The comparison between T_{cp} (eq. 53) and T_{cl1} (eq. 52) indicates the behavioral mode of the inclusion and leads to a comparison between M_{max} and $0{,}16.p_l.B.L_0^2$.

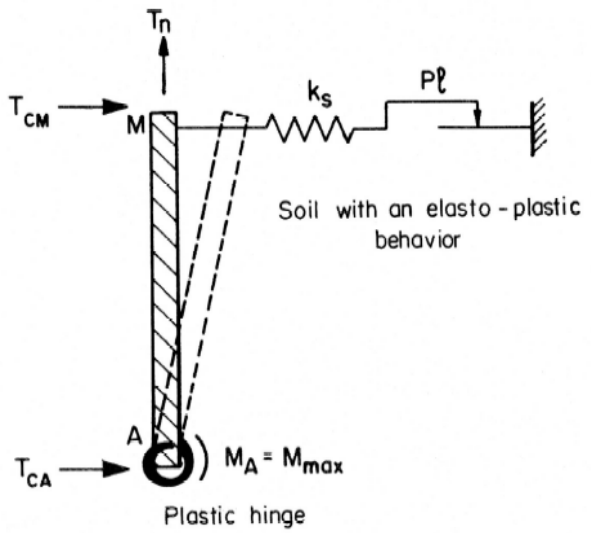

Figure 29: Schematic diagram of the plastic hinge for displacements after plastification at point A

For displacements greater than those given by eq. (54), the moment at point A is assumed to be constant (plastic hinge) and one can consider the diagram represented in Figure 29:

- Rigid bar AM;
- Elasto-plastic soil;
- Plastic hinge at point A;
- Inclusion infinitely long beyond point A.

The system equilibrium equations allow one to determine the relationship between the additional shear force ΔT_c and the additional displacement Δ_{yM} beyond plastification of the inclusion at point A:

$$\Delta T_c = \frac{\pi}{16}.\frac{\pi+8}{\pi+6}.E_s.L_0.\Delta y_M \approx 0{,}24.E_s.L_0.\Delta y_M \quad (55)$$

One thus obtains:

$$T_{cl2} = T_{cp} + \Delta T_c \text{ et } y_M = y_{Mp} + \Delta y_M \quad (56)$$

Soil plastification at point M occurs when:

$$p_M = k_s.y_M = p_l \text{ or: } y_M = \frac{p_l.B}{E_s} \quad (57)$$

From eq. (53), (54), (55), (56) and (57) the expression becomes:

$$T_{cl2} = 1{,}62.\frac{M_{\max}}{L_0} + 0{,}24.p_l.B.L_0 \quad (58)$$

Admitting approximation (41a) the expression becomes:

$$T_{cl2} = 1{,}62.\frac{M_{\max 0}}{L_0}.\left(1 - \frac{T_n^{\,2}}{R_n^{\,2}}\right) + 0{,}24.p_l.B.L_0 \quad (59)$$

This criterion is of the parabolic type with a downward concavity in the (T_n, T_c) diagram (Figure 30).

The evolution of $T_c(y)$ at point M is presented on Figure 31a.

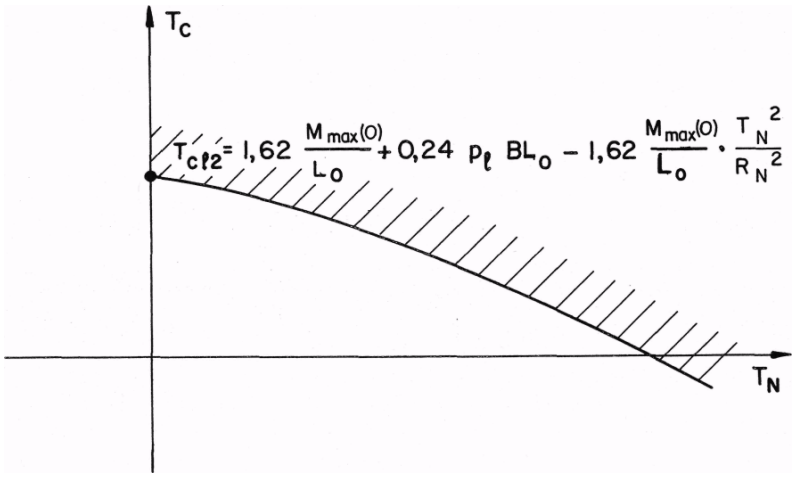

Figure 30: Stability domain of the bar at point A and of the soil taking into account the maximum moment of plastification of the bar and the soil-inclusion normal interaction at point M (criterion T_{cl2})

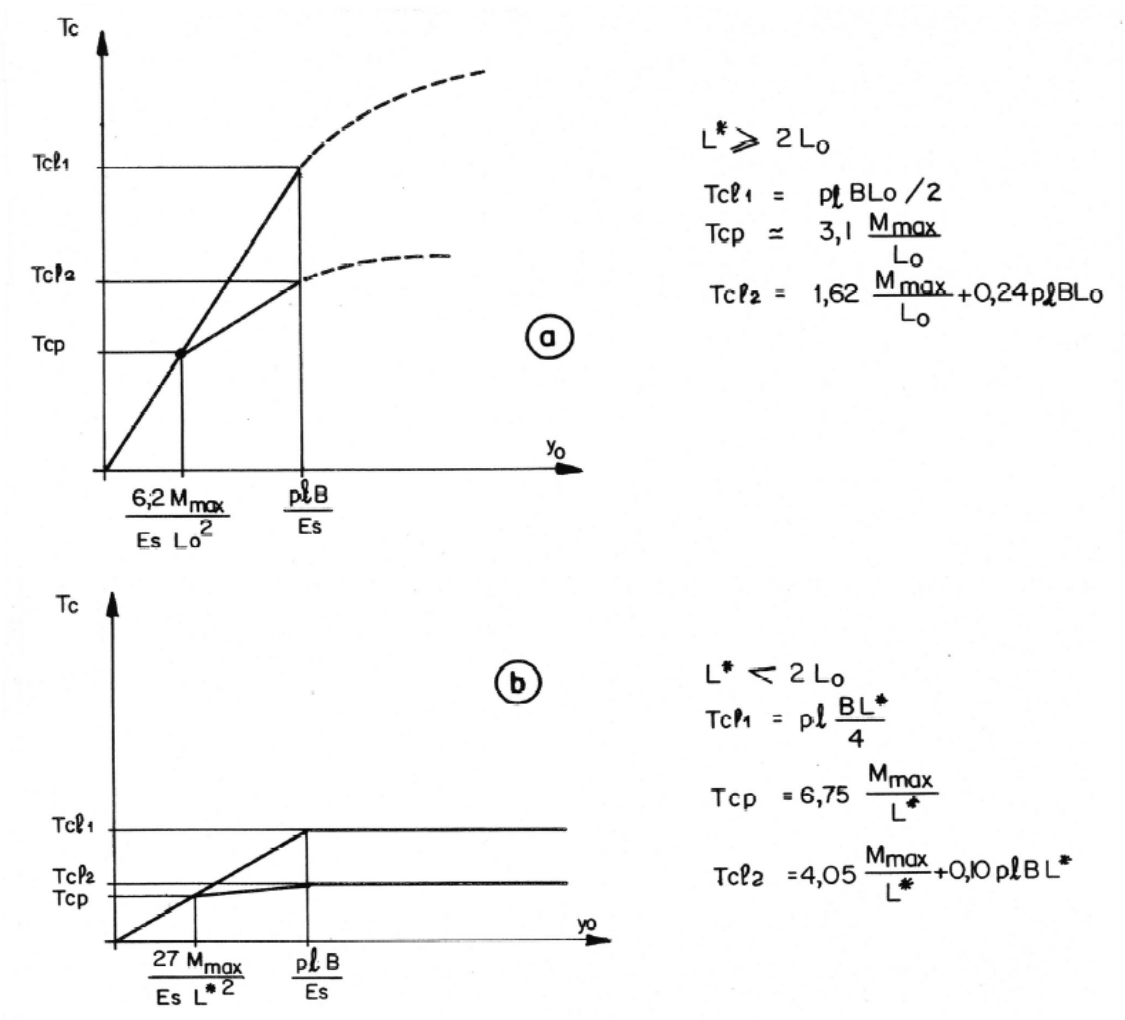

Figure 31: Development of the shear force at point M as a function of the lateral displacement of this point, the relative soil-inclusion flexibility, and the minimal "free length" of the inclusion

4.2.2.4. Solution of the problem for L* < 2.L0

In the case of an infinitely rigid inclusion (negligible deformations), the equilibrium solution can be written:

$$T_c = \frac{1}{4}.E_s.L^*.y_M \tag{60}$$

$$M_{\max} = \frac{4}{27}.T_c.L^* \tag{61}$$

or $$M_{\max} = \frac{1}{27}.E_s.L^{*2}.y_M$$

The point of maximum moment is at a distance L*/3 from the failure surface.

a) Criterion T_{cl1} ($M_{max} \geq p_l.B.L^{*2}/27$)

The plastification at point M is initiated when:

$$T_{cl1} = p_l.B.\frac{L^*}{4} \tag{62}$$

This value is less than that given by eq. (52) for an infinitely long inclusion.

b) Criterion T_{cl2} ($M_{max} < p_l.B.L^{*2}/27$)

The plastification at point A ($M = M_{max}$) occurs when:

$$y_{Mp} = 27.\frac{M_{\max}}{E_s.L^{*2}} \text{ and } T_{cp} = 6{,}75.\frac{M_{\max}}{L^*} \tag{63}$$

Note: for $L^* = 2.L_0$, one obtains: $T_{cp} = 3{,}37.\frac{M_{\max}}{L_0}$

When comparing this value to eq. (53), the difference is 9%.

The introduction of a plastic hinge (as for chapter 4.2.2.3) leads to the following expression for the law relating to the increase in the shear force:

$$\Delta T = 0{,}10.E_s.L^*.\Delta y_M \tag{64}$$

Soil plastification at point M occurs when:

$$\Delta y_M = \frac{p_l.B}{E_s} - y_{Mp} \tag{65}$$

which results in the following expression for the limit shear:

$$T_{cl2} = 4{,}05.\frac{M_{\max 0}}{L^*}.\left(1 - \frac{T_n^{\,2}}{R_n^{\,2}}\right) + 0{,}10.p_l.B.L^* \tag{66}$$

The results obtained from these two solutions differ by less than 25% when considering the limit case where $L^* = 2.L_0$.

The development of $T_c(y)$ at point M is illustrated on Figure 31b. Table 1 summarises these solutions.

Bending resistance of the inclusion (M_{max})	Minimal length available on one side of the failure surface	
	"long" inclusion $L^* > 2.L_0$	"short" inclusion $L^* < 2.L_0$
HIGH (rigid)	$M_{max} > 0{,}16.p_l.B.L_0^2$ $T_{cl1} = p_l.B.L_0/2$	$M_{max} > p_l.B.L^{*2}/27$ $T_{cl1} = p_l.B.L^*/4$
LOW (flexible)	$M_{max} < 0{,}16.p_l.B.L_0^2$ $T_{cl2} = 0{,}24.p_l.B.L_0 + 1{,}62.M_{max}/L_0$	$M_{max} < p_l.B.L^{*2}/27$ $T_{cl2} = 0{,}10.p_l.B.L^* + 4{,}05.M_{max}/L^*$

Note: the values of M_{max} and p_l used in the above relationships are the values given in the data by the user, factored by the appropriate 'partial safety factors (Table 3).

Table 1: Available shear force in the inclusion (T_{cl1}, T_{cl2})

4.3. COMBINATION OF THE FAILURE CRITERIA: APPLICATION OF THE PRINCIPLE OF MAXIMUM PLASTIC WORK

The combination of failure criteria relative to the inclusions leads to the stability domain illustrated on Figure 32a.

The vector T (T_n,T_c) must be located within the "internal envelope" of the stability domain satisfying the set of criteria. The form of the "internal envelope" obviously depends on the relative position of the curves.

The following comments can be made:

- The criterion for the lateral friction interaction can be situated arbitrarily with respect to the ellipse corresponding to the inclusion's internal stability at point M. Reducing the adherence length (L_a) beyond the failure surface, or the limit adherence (f_{lim}) causes a decrease in the value of T_{nl} which consequently limits the ellipse.
- The soil-inclusion interaction criterion relative to the normal force at point M (T_{cl1} and T_{cl2}) is almost always less than R_c for reinforcement in retaining structures, especially for inclusions used to "nail" unstable slopes. This criterion therefore generally limits the contribution of the inclusions.

Consequently, the stability domain generally has the shape shown on Figure 32a.

To define the point on the boundary of the domain at which the point representing (T_n, T_c) is located, reference is made to the principle of maximum plastic work. One can find a presentation of this principle by Mandel *(*Propnetes mecaniques des materiaux, 1978*)*.

At the point of intersection between the failure surface and the inclusion (point M), the relative displacement δ at failure between the two parts of the inclusion is assumed parallel to the failure surface (Figure 32b). If T is the force mobilised at failure and T^* is an arbitrary permissible force situated inside the stability domain, the principle of maximum work implies that:

$$\left(\vec{T} - \overrightarrow{T^*}\right).\vec{\delta} \geq 0 \qquad (67)$$

By placing the values δ(δ_n, δ_c) and T(T_n,T_c) in the same axis system, application of this principle results in the consideration that the point of contact between the envelope of the stability domain and the tangent perpendicular to the δ direction can be taken as an extremity of T (Figure 32a).

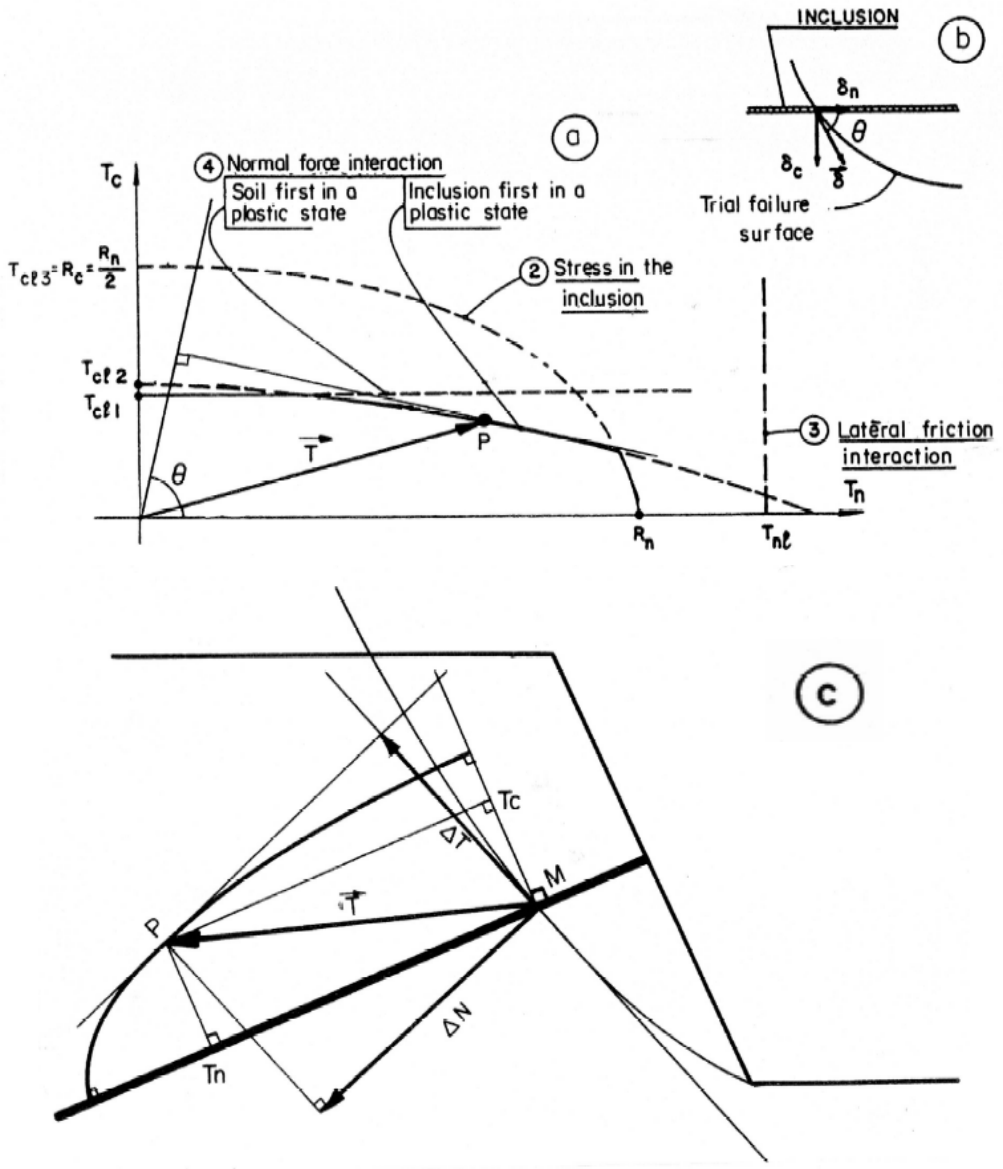

Figure 32: Stability domain resulting from all individual criteria of stability

Note: In the case of a circular failure surface (Figure 32c), the stabilising moment of the inclusion is maximum with respect to the circle centre when the force projection $T(T_n,T_c)$ is maximum in the direction of the tangent to point M. This results on an intuitive basis, in the general rule presented hereafter.

Application of the principle of maximum work assumes that:

- the different flow criteria are of the type perfectly plastic and consequently, each component T_n or T_c at point M retains the value that it possessed when it attained one or another of the criteria or during a possible unloading in the case of strain softening beyond the peak load. This hypothesis does not consequently allow a fragile failure of the system.
- the δ direction is determined with respect to the inclusion's position at the moment of failure. One can refer to section 5.3 for additional comments relative to taking into account the deformations before failure.

In practice, considering the angle between the inclusion and the failure surface θ, it appears that:

- for a small θ angle (orientation of the inclusion near to that of the failure surface), the inclusion works essentially in tension;
- for θ near $\pi/2$ (inclusion perpendicular to the failure surface), the inclusion works primarily in shear;
- the stability domain is generally very flat; the tension is therefore mobilised very rapidly and attains a value near the maximum value in pure tension as soon as θdiffers slightly from $\pi/2$*;*
- introducing the shear forces can be penalising in the case of frictional soils because it results in the loss of normal force, which thereby reduces the soil resistance (section 5). On the other hand, not taking into account the shear forces ignores a possible failure mechanism of the inclusion and the surrounding soil.

These observations are consistent with common sense and observations made on actual structures. Introduction of a safety factor for the inclusions will be discussed in chapter 5.6.3.

5 INTRODUCING REINFORCEMENTS IN TALREN

5.1. GENERAL

The inclusion effect on each slice "affected" is taken into account by applying the components normal (ΔN) and tangent (ΔT) to the failure surface at the base of the slice, along its axis. These components are determined from T_n and T_c, mobilised in accordance with the principle of maximum work.

In order to more accurately take into account the inclusions, TALREN allows their effect to be redistributed within a certain zone along the failure surface (Figure 33). This approach allows one to reduce the transition effect between soils with highly different natures.

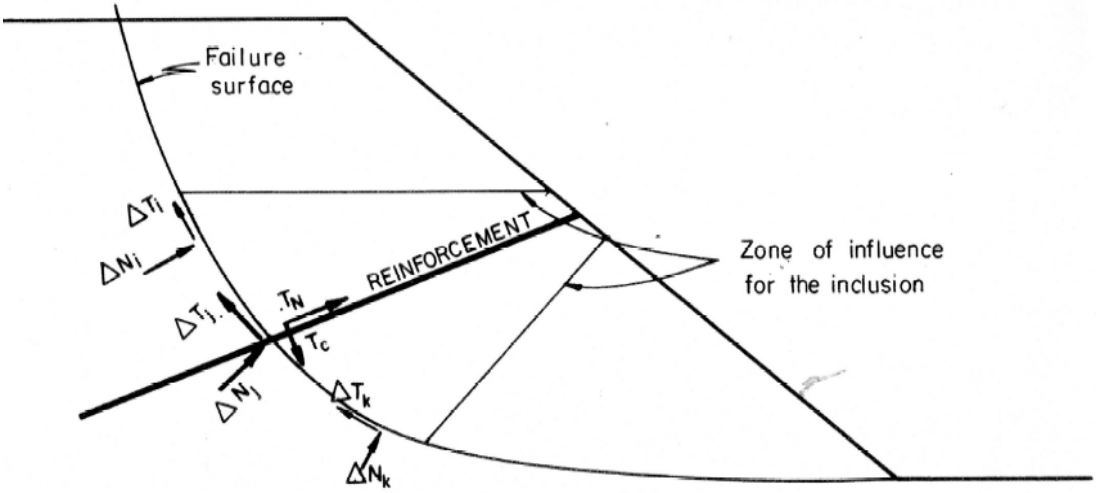

Figure 33: Possible diffusion of the effect of an inclusion on a certain part of the failure surface

As a result, the general approach used by the program consists of the following steps:

- calculation of the safety factor for the unreinforced soil: $\Gamma_{0;}$
- calculation of the components ΔN and ΔT for each reinforcement, weighted by partial safety factors Γ_{qs}, Γ_{acier}, $\Gamma_{pl;}$
- determination of the distribution of forces (ΔN_i, ΔT_i) equivalent to (ΔN, ΔT);
- calculation of the reinforced soil safety factor Γ.

5.2. RULES FOR SIMULATION OF THE DIFFERENT INCLUSION TYPES

Simulation of the various inclusion types is made by adopting the hypotheses presented in Table 2. The listed parameters are those actually taken into account by TALREN. The safety factor for these parameters is introduced by the user during data generation (section 5.6.3).

	Resistance of the inclusion		Soil-inclusion interaction	
	Normal force	Shear force	Pull-out	Normal reaction
	R_n	R_c	T_{nl}	T_{cl}
Soil nails	T_G	$T_G/2$	$F_{lim}.L_a$	$\min(T_{cl1},T_{cl2})$
Ground anchors	T_G	0	T_{lim}	0
Reinforcing strips	Specific rules	0	Specific rules	0
Nail-piles (slope stability)	0	R_c	Voir 5.3.4	
Stone columns	Soil homogenisation: refer to section 5.3.5			

Table 2: Parameters taken into account at failure

The various parameters have the following significations:

f_{lim} : limit soil-nail adherence per unit length of the inclusion;

L_a : adherence length (Cf. section 4.2.2);

T_G : tensile strength (elastic limit for steel nails);

T_{lim} : pull-out resistance of the grouted length (refer to specifications TA 86 for prestressed anchors);

R_c : shear strength of the inclusion;

T_{cl} : $\inf(T_{cl1}, T_{cl2})$: flow criterion for the soil-inclusion normal interaction;

Specific rules: this concerns reinforcement with strips.

5.3. RULES SPECIFIC TO THE DIFFERENT INCLUSION TYPES

Hereafter, we will deal with the rules specific to each type of inclusion. The rule pertaining to the force distribution is common to all inclusion types and will be presented in section 5.4)

5.3.1. Soil nails

Only the steel is taken into account in the determination of R_n, R_c et M_{max} (involved in determining T_{cl2})

Conversely, the soil-nail interaction (T_{nl}, T_{cl}) depends on the borehole diameter B (grouted nail) or the equivalent diameter B for driven nails, which is defined as:

$$B = \frac{Périmètre\ de\ contact}{\pi}$$

The value of f_{lim} used in determining T_{nl} (Table 2), can be introduced in one of two forms:

f_{lim} = given value (determined from experience or actual tests)

$f_{lim} = \pi.B.q_s$

with qs: limit interface friction per unit area (obtained from CLOUTERRE, TA 86, Fascicule *62* or other specific design charts, or from experience).

This value is given for each soil layer to allow treatment of heterogeneous soils.

The adherence length (L_a) taken into account is the length of the nail extending beyond the failure surface (Figure 34). This gives:

$$T_{nl} = \int L_a . f_{\lim} . dl \qquad (68)$$

Although there is no theoretical justification, the compressive strength of the inclusions in not explicitly introduced in TALREN (refer to the section pertaining to θ_{cr}, presented hereafter). The normal interaction criterion T_{cl2} is determined as a function of the inclusion length:

$L^* = \min(L_1, L_2)$ (Figure 22) to choose the appropriate formula (59) or (66).

With regards to this criterion the present version of TALREN assumes that the entire inclusion is located in the soil (assumed homogeneous) encountered at its intersection with the failure surface. For highly heterogeneous soils, this can introduce a discontinuity in the results obtained for two neighboring failure surfaces, one intersecting the inclusion within a stiff soil and the other within a soft soil (Figure 34). It may therefore be necessary to predetermine the maximum value of T_{cl2} from a calculation of an elastically supported beam in a stratified medium and to impose the maximum shear resistance in the TALREN calculation (section 5.3.1.3).

(T_{cl1}, T_{cl2})calculated for an inclusion completely included in a soft soil

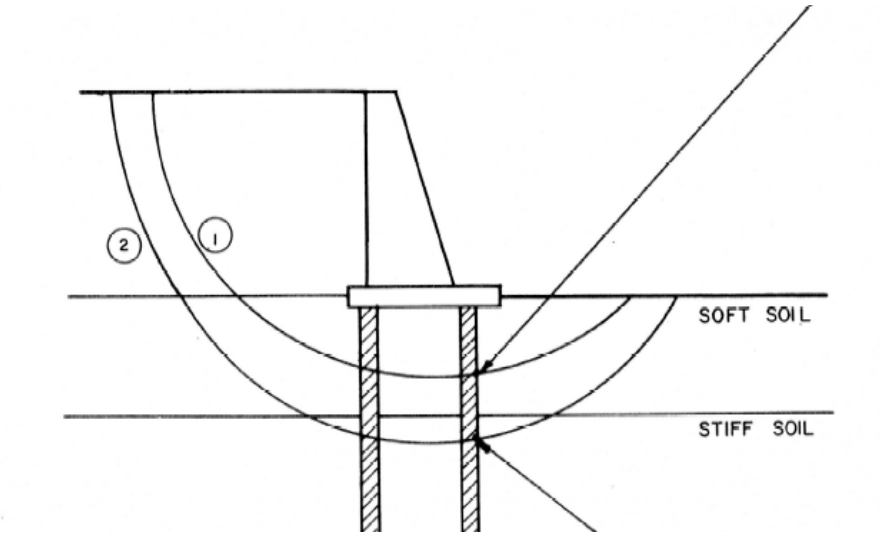

(T_{cl1}, T_{cl2}) calculated for an inclusion completely included in a stiff soil

Figure 34: Possible discontinuity of the results in case of soil heterogeneity

5.3.1.1. Choice of the couple (T_n, T_c)

Some modifications are made concerning the strict application of the principle of maximum work relating to the choice of the couple (T_n, T_c), in order to take into account the following observations:

a) In reality, the nail rotation in the vicinity of the failure surface can be large (Figure 35a).

- for an infinitely long inclusion, with or without a plastic hinge and having a transfer length L_0, the deformation can be defined by the following expression:

$$\frac{p_l.B}{E_s.L_0} < \tan\theta_{rot} < 1{,}5.\frac{p_l.B}{E_s.L_0} \qquad (68a)$$

- For an infinitely rigid inclusion, with or without a plastic hinge and having a length $L^* < 2.L_0$, this expression becomes:

$$1{,}5.\frac{p_l.B}{E_s.L^*} < \tan\theta_{rot} < 3{,}6.\frac{p_l.B}{E_s.L^*} \qquad (68b)$$

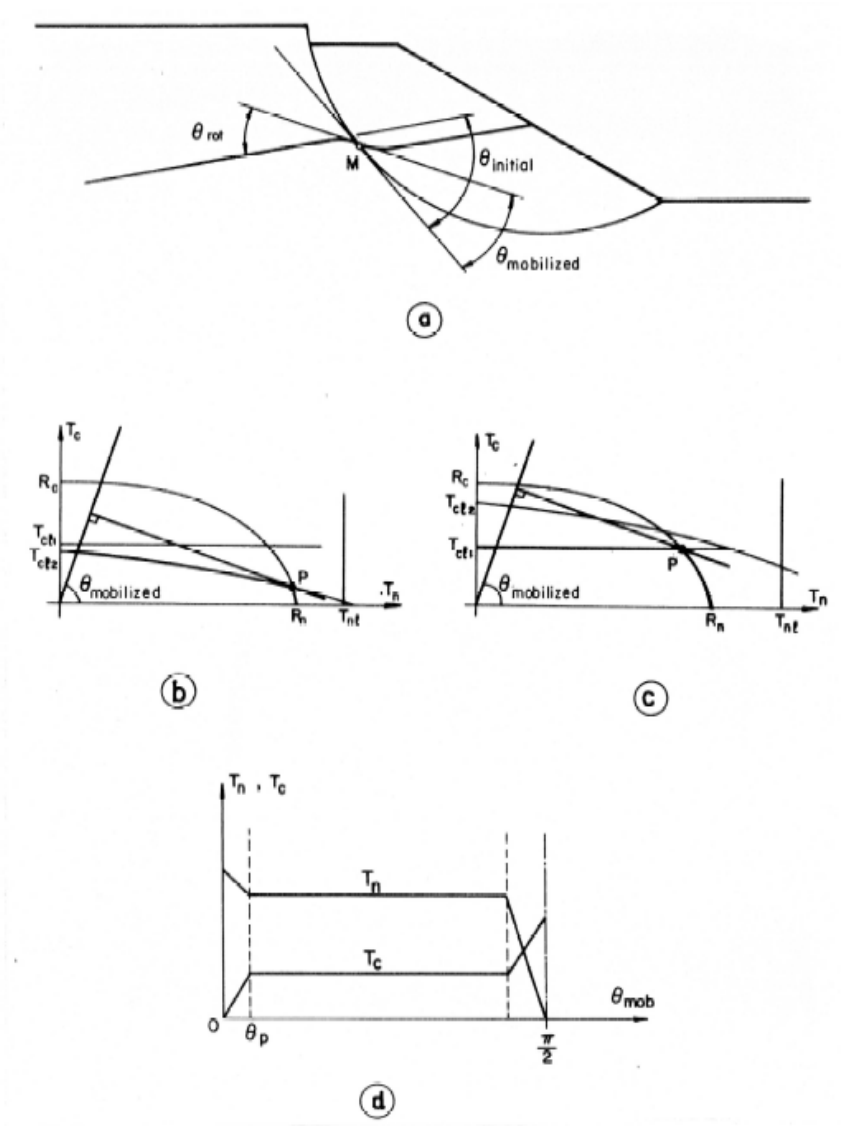

Figure 35: Consequence of the rotation induced by the deformation of the inclusion, on the application of the principle of maximum work

If one adopts the simple simultaion relating to the pressuremeter characteristics, p_l and E_M the expression becomes: $E_s \approx 2.E_M$ (E_M = pressuremeter modulus) with $E_M \approx 10.p_l$ or $E_s \approx 20.p_l$

Therefore:

$$\frac{p_l.B}{E_s.L_0} \approx \frac{B}{20.L_0} \tag{69}$$

or:

$$\frac{p_l.B}{E_s.L^*} \approx \frac{B}{20.L^*} \tag{69a}$$

This confirms the fact that the shorter (L^* small) or more flexible (L_0 small) the nail is, the more it will deform prior to plastification.

For nails with a small inertia (L_0 small), in medium quality soil (p_l between 0.5 and 2 MPa), the rotation θ_{rot} of the inclusion can easily attain 2° to 3° before plastification. Thus, the "mobilised" θ angle, determined from the principle of maximum work, can be significantly smaller than the theoretical θ angle, corresponding to the initial position of the inclusion within the soil.

b) The shape of the stability domain is generally such that a small difference with respect to θ = 90°, leads to the almost total mobilisation of the tension (Fig. 36). This situation occurs systematically when $\theta_{initial} \leq \pi/2$ and when the inclusion is flexible.

c) The case of inclusions liable to work in compression ($\theta_{initial} > \pi/2$) is more complex (Figure 36). In TALREN, the "at failure" calculations do not explicitly take into account the behavior of the mass before failure (except locally for the definition of the soil-inclusion normal pressure limit equilibrium criteria T_{cl1} and T_{cl2}). It is therefore assumed that displacements prior to failure result in a θ value near $\pi/2$ and consequently, the inclusions works in pure shear (Figure 36b), with:

$$T_c = \min(R_c, T_{cl1}, T_{cl2}) \tag{70}$$

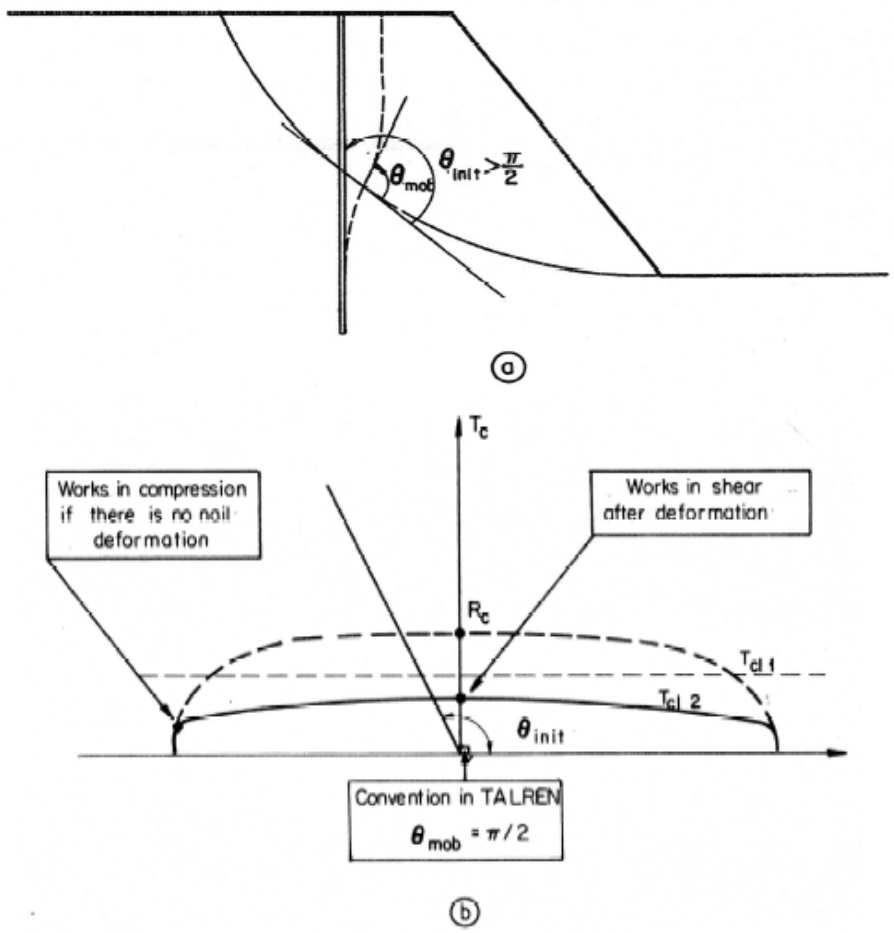

Figure 36: Particular case of compression work brought to the case of pure shearing

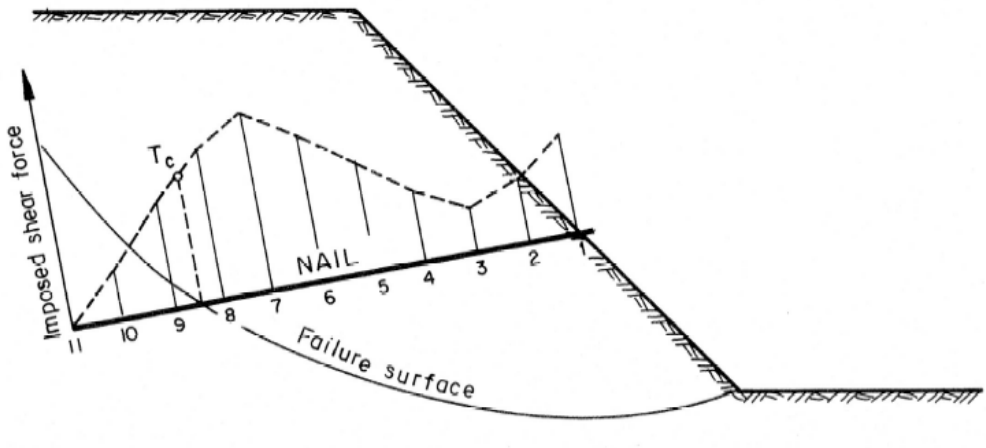

Figure 36b: Imposed shear force along the nail

5.3.1.2. Practical rule

The position of point P in the (T_n, T_c) stability diagram is extremely sensitive to the value of the angle θ. This sensitivity can lead to a radically different manner for taking into account the inclusion for two failure surfaces which are very close, when the deformation of the inclusion has a tendency to orient the inclusion in such a way that they work primarily in tension. To take this into account, TALREN refers to the critical θ_{cr} angle, defined by the user and corresponding to the rules shown on Figure 37, notably:

$$\text{Works in pure tension: } \theta_{initial} \le \theta_{cr} \text{ , or } T_c = 0 \text{ and } T_n = \min(T_{nl}, R_n) \quad (71)$$

$$\text{Works in combined tension-shear: } \theta_{cr} \le \theta_{initial} \le \pi/2 - \theta_{cr} \text{ , or } T_c \ne 0 \text{ and } T_n \ne 0 \quad (71a)$$

defined by point P, which is situated in the upper right quadrant of the stability domain (Figure 38)

$$\text{Works in pure shear: } \theta_{initial} \ge \pi/2 - \theta_{cr} \text{ , or } T_c = \min(R_c, T_{cl1}, T_{cl2}) \text{ and } T_n = 0 \quad (71b)$$

The value of θ_{cr} is left to the choice of the user. Since it expresses the effect of the inclusion's deformability, its value is reduced in proportion to the increase in the inclusion's rigidity. Because of the lack of a more elaborate rule, it is recommended that one adopts $\theta_{cr} \le 5°$ for classical inclusions.

5.3.1.3. Possible options

To allow a comparison with other calculation methods, TALREN gives the user the possibility of specifying certain properties rather than determining them from the principle of maximum work.

These possibilities include:

a) imposing a shear value T_c and determining the value of the normal force T_n:

The imposed shear T_c can be given a constant value along the entire length of the nail or can be interpolated by the program from the 11 values imposed at equal distances between the two extremities of the nail (Figure 36b).

$$T_n = \min(T_{nl}, R_n) \quad (72)$$

In this case, the normal force T_n is calculated similarly to nails working in pure tension.

b) imposing zero normal force and calculating the shear force

$$T_n = 0 \text{ with } T_c = \min(R_c, T_{cl1}, T_{cl2}) \quad (73)$$

The shear force T_c for nails working in pure shear or coupled tension-shear is only taken into account when the nail length beyond the failure surface (L^*) is greater than the value imposed by the user.

This option can be used in the case of pile-soil nails stabilising a slope in a stratified medium.

An additional option allows the user to directly introduce the reinforcement effect, in the form of the values $\Delta\sigma$ and $\Delta\tau$ at the points discretising the failure surface. This option is useful in incorporating, if desired, the results of Finite Element calculations.

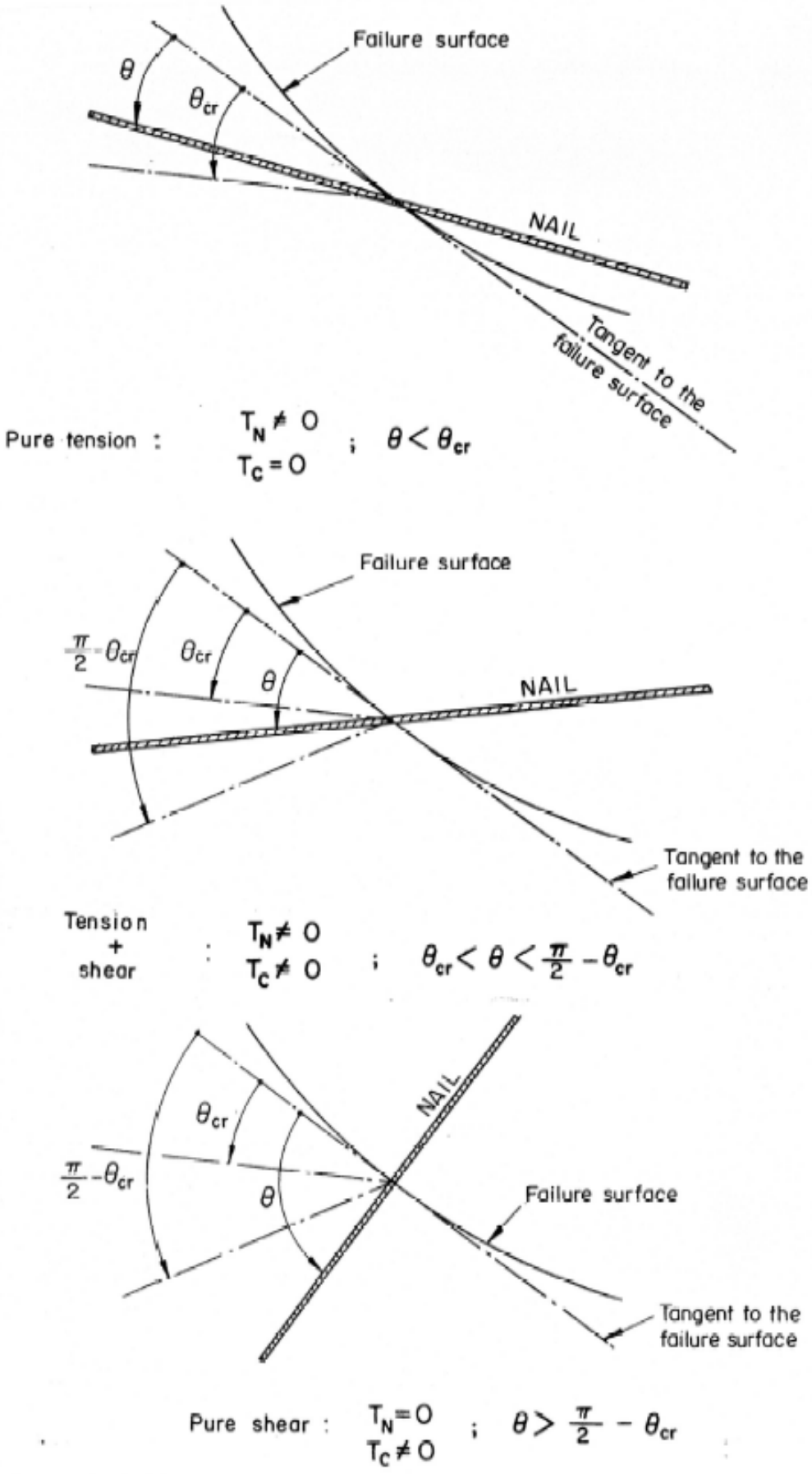

Figure 37: Practical rules for mobilisation of the traction and shear in TALREN

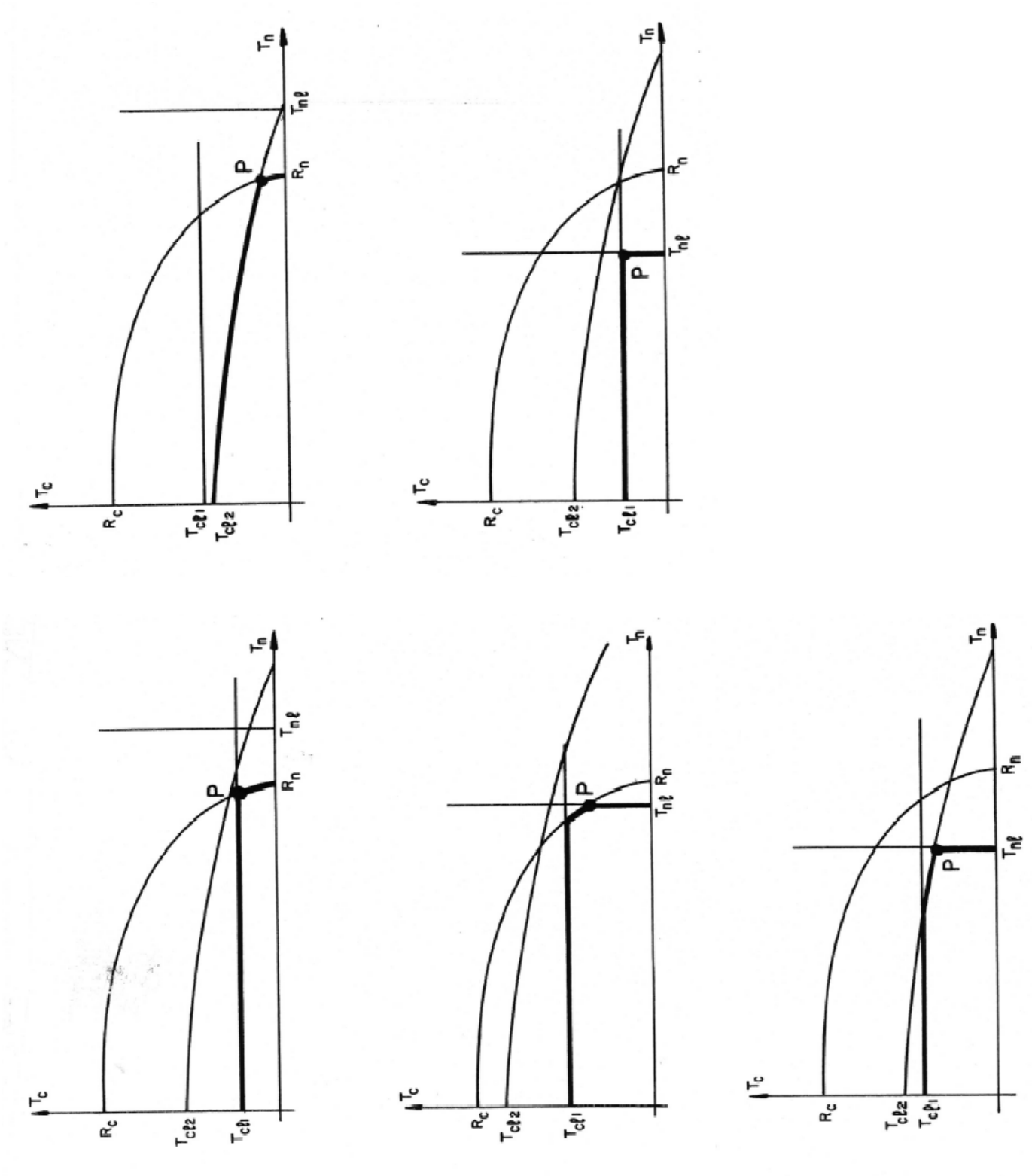

Figure 38: Choice of the position of point P(T_n/T_c) in TALREN

5.3.2. Prestressed anchors

Conforming to the specifications TA 86, a prestressed anchor can only work in pure tension. Its value is equal to:

$$T_n = \min(T_{nl}, R_n) \tag{74}$$

where: T_{nl} (pull-out resistance) and R_n (pure tensile strength of the steel) are given by the operator.

Two options are provided to the user for determining the pull-out resistance:

- Non proportional: T_{nl} = fully mobilised or zero: in accordance with the specifications TA 86, a prestressed anchor is only taken into consideration in the equilibrium if its fictitious anchoring point (FAP), assumed to be situated at the midpoint of the grouted length, is outside the failure surface (Figure 39). This rule introduces a completely artificial discontinuity between two adjacent failure surfaces, depending if the FAP is inside or outside the failure surface.
- Proportional: T_{nl} determined as a function of the grouted length beyond the failure surface (l_s) (Figure 39b), with:

$$T_{nl} = (R_{grout} . l_u) / l_{grout} \tag{74b}$$

where R_{grout} is the pull-out resistance corresponding to the entire grouted length

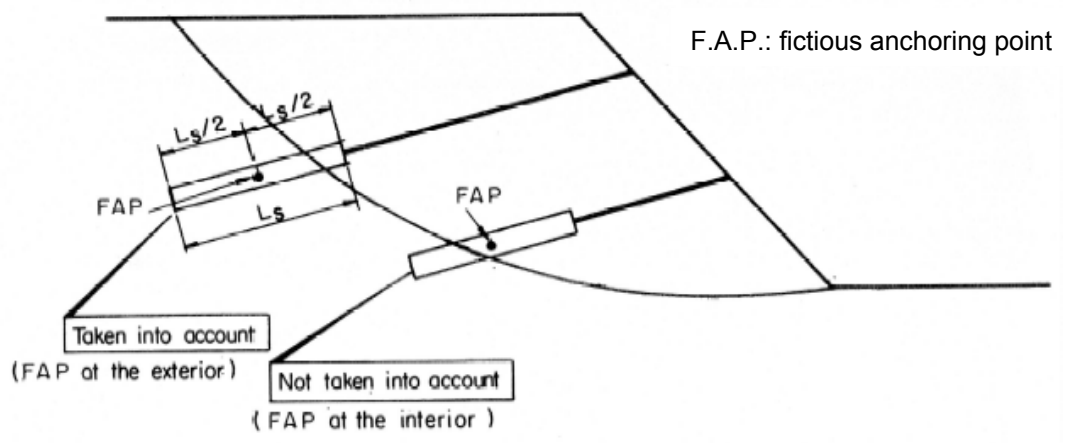

Figure 39: Situations considered by TALREN for prestressed anchors: non proportional option

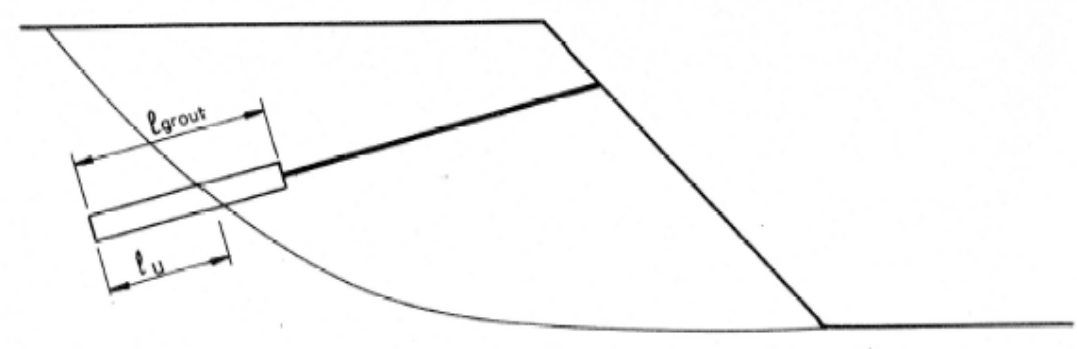

Figure 39b: Situations considered by TALREN for prestressed anchors: proportional option

5.3.3. Reinforcing strips

In accordance with the current specifications, reinforcing strips and fabrics work only in pure tension. The soil-strip limit tensile strength T_{nl} is determined from the following parameters, defined in the data:

- inclusion width: B;
- apparent soil-inclusion friction coefficient (μ^*), conforming to the specifications for each type of strips (Figure 40). This parameter is a function of the vertical stress σ_v exerted on the inclusion.

One gets:

$$T_{nl} = \int_0^{l_a} 2.B.\sigma_v.\mu^*.dl \qquad (75)$$

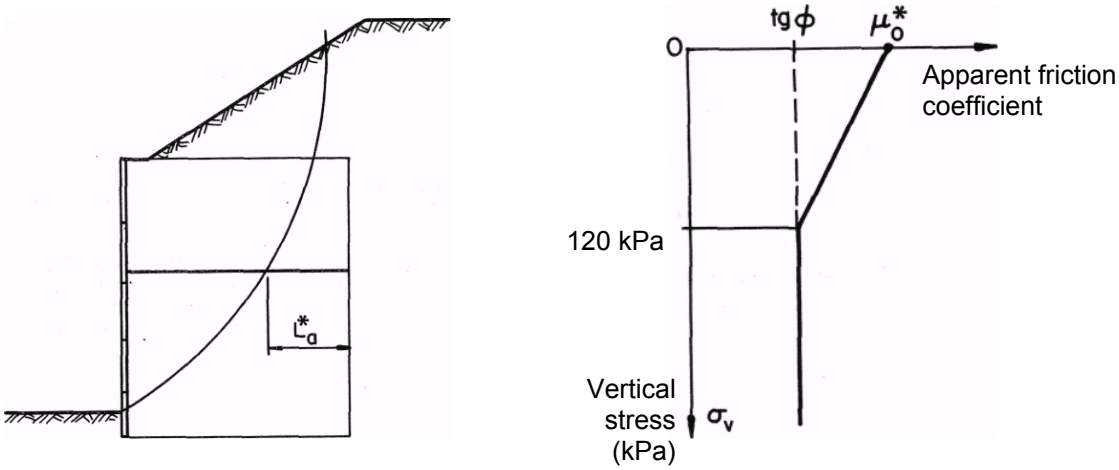

Figure 40: Criteria relative to the reinforcing strips

5.3.4. Pile-nails

The heading pile-nails groups the inclusions destined to stabilise unstable slopes (Figure 41). These inclusions work primarily in shear since they possess a high bending inertia and are oriented in such a way that: $\theta > \pi/2$

Conforming to the rules presented in section 5.3.1, these types of inclusions are characterised by the following:

$T_n = 0$ avec $T_c = \min(R_c, T_{cl1}, T_{cl2})$ ou T_c = valeur imposée par l'opérateur (76)

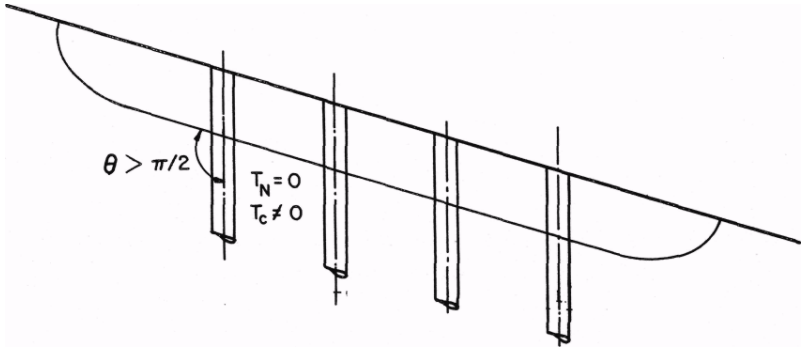

Figure 41: Slope stabilisation with pile-nails

5.3.5. Stone columns

Stone columns require a special treatment method because the deformability of this type of inclusion causes a redistribution of the stresses between the reinforced soil and the columns, which is not taken into account in an "at failure" calculation.

Rather than introducing each column as an individual inclusion, the soil is homogenised (c_{eq}, ϕ_{eq}) in accordance with the following rules:

$$c_{eq} = (1-a).c_{sol} + a.c_{col}$$
$$\tan\phi_{eq} = (1-m).\tan\phi_{sol} + m.\tan\phi_{col} \qquad (77)$$

m: is the load ratio

a: is the ratio of the column area (A_{col}) to its tributary area ($A_{sol} + A_{col}$)

$$a = \frac{A_{col}}{A_{col} + A_{sol}}$$

The coefficient m depends on the factor of stress concentration on the columns n (Figure 42), which depends on the relative soil-column deformability. The following simple rule is often applied:

$$m = \frac{a.n}{1 + a.(n-1)} \qquad (78)$$

with $n = \frac{E_{col}}{E_{sol}}$

with:

E_{col} : deformation modulus of the stone column

E_{sol} : deformation modulus of the soil

However, in the case of soft soils (low modulus), this ratio n can reach high values (> 10), whereas experience shows that, for structures, it rather ranges from 4 to 6 on the long term. The choice of the values for n must therefore result from the operator's experience and is under his responsibility.

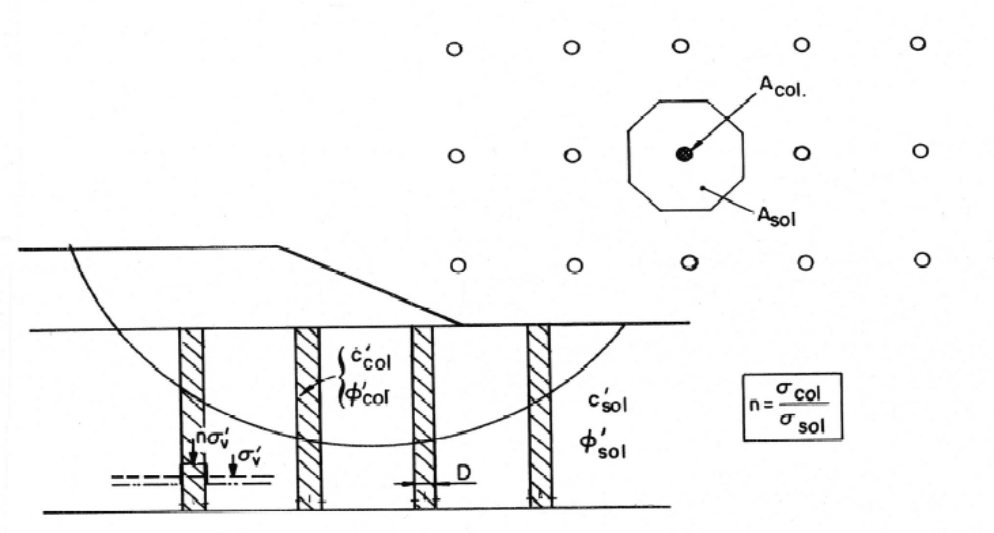

Figure 42: Stone columns

5.4. DIFFUSION OF THE INCLUSION EFFECT

In order to limit the possible effect of the soil's heterogeneity on the method used to take into account the forces generated in the inclusions, it is possible in TALREN to diffuse the effect of each reinforcement. This is done in accordance with the following rules (Figure 43).

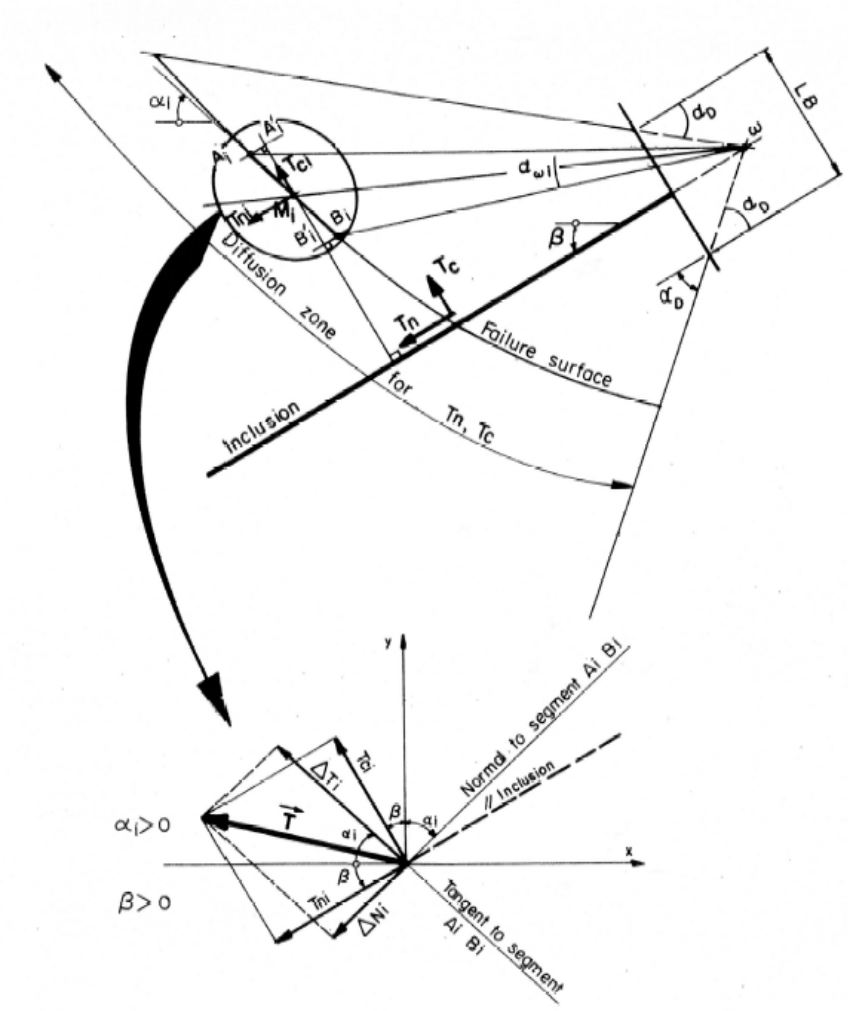

Figure 43: Diffusion of the inclusion effect

The zone of influence for each inclusion is defined by a "diffusion base" with width LB at the head of the reinforcement (slope facing) and a diffusion angle α_D defining the spreading of the zone over which the inclusion effect will be diffused.

The force components T_n, T_c of the inclusions are distributed between the segments discretising the failure surface, which lie within the diffusion zone (giving $[T_{ni},T_{ci}]$). These forces are defined as:

$$T_{ni} = \rho_i . T_n \text{ and } T_{ci} = \rho_i . T_c \qquad (79)$$

T_{ni} and T_{ci} are the components along the axes parallel to T_n and T_c.

The value of ρ_i is determined by the simple relationship:

$$\rho_i = \frac{\left(\frac{\overline{A'_i B'_i}}{\overline{wM_i}}\right)}{\sum_i \left(\frac{\overline{A'_i B'_i}}{\overline{wM_i}}\right)} \qquad (80)$$

A'_i and B'_i are the projections of A_i and B_i defined on Figure 43.

This relationship is equivalent to the assumption that ρ_i is approximately proportional to the angle α_{wi} which defines the arc length A_iB_i along the failure surface.

If the angle α_D is zero, then:

$$\rho_i = \frac{\overline{A'_i B'_i}}{\sum_i \overline{A'_i B'_i}} \qquad (80')$$

Note: This equation satisfies the equilibrium of the force components:

$$\Sigma T_{ni} = T_n$$
$$\Sigma T_{ci} = T_c$$

but does not satisfy the equilibrium of the moments.

For each segment i along the failure surface, an addition of the forces T_{ni}, T_{ci}, generated by each inclusion is made.

Some corrections are made for a given inclusion to take into account special geometrical conditions between the segments of the failure surface, the slope and the diffusion zone.

It is always possible to suppress the diffusion of the inclusion effect by defining $L_B = 0$ and $\alpha_D = 0$.

The resultant force [T_{ni}, T_{ci}] on a segment of the failure surface, in the reference system defined by the normal to the considered segment, can be expressed by the components:

$$\Delta N_i = T_{ni}.\sin(\alpha_i + \beta) - T_{ci}.\cos(\alpha_i + \beta)$$
$$\Delta T_i = T_{ni}.\cos(\alpha_i + \beta) + T_{ci}.\sin(\alpha_i + \beta) \qquad (81)$$

(α_i and β are considered positive as shown on Figure 43).

5.5. SIMULATION OF LOADS BY FICTITIOUS INCLUSIONS

A load Q (Figure 44) can be simulated by a fictitious anchor for which one considers a very large pull-out resistance and strength:

$$R_n = |Q| \qquad T_{nl} = +\infty \tag{82}$$

The degree of spreading of the diffusion zone is left to the judgment of the user, who must keep in mind that the model is two-dimensional and that certain corrections should be anticipated when the load to be simulated is punctual.

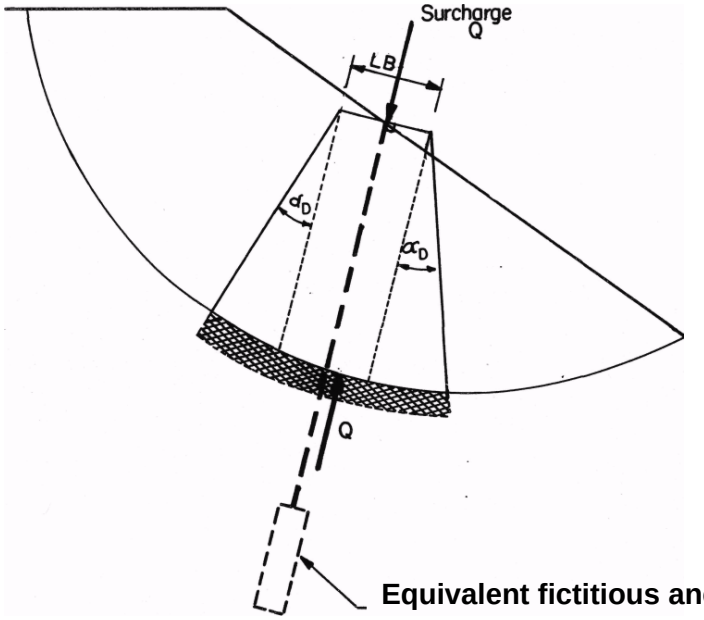

Figure 44: Simulation of a load by an equivalent fictitious inclusion

5.6. INTRODUCING REINFORCEMENTS IN THE EQUATIONS TO DETERMINE Γ

5.6.1. Fellenius and Bishop methods

The values of ΔN_i and ΔT_i are introduced in the Bishop and Fellenius methods by the relationship:

$$\Gamma = \frac{\sum_{i=1}^{n}\left(T_{i\max} + \Delta N_i \cdot \frac{\tan\phi_i}{\Gamma_{\phi i}}\right)}{\Gamma_{s3}\cdot\sum_{i=1}^{n}\left(T_i - \Delta T_i\right)} \tag{83}$$

Important remark concerning the Bishop method

In the Bishop method, T_{imax} involves the coefficient $\Gamma.\Gamma_{S3}$ in the expression $m(\alpha)$ (eq. 15).

In the absence of reinforcement, there is no ambiguity in the signification of Γ calculated from eq. (14) or (17). One can easily show that for this case, there is an equivalence between the Bishop method and the "wedge" method when the considered failure surface is planar (case of a circle with an infinite radius). To simplify the development, this safety factor will be denoted "Γ_{sol} " corresponding to the unreinforced soil.

When reinforcements are introduced into the problem, it is naturally logical to try to conserve the equivalence between the two methods (Bishop and Wedge). The equation corresponding to the Wedge method will be developed later (eq. 90). To accomplish this, it is necessary to conserve in the expression for m(α), the value Γ_{sol} soil calculated from the equilibrium of the unreinforced slope. Otherwise, one will systematically obtain:

$$\Gamma_{BisRd} = \Gamma_{Bishop\ reinforced} > \Gamma_{reinforced\ wedge}$$

Taking this fact into account, eq. (83) can be written:

$$\Gamma_{BisR} = \frac{\sum_{i=1}^{n}\left(\frac{\frac{c_i}{\Gamma_{ci}} + \left(\Gamma_{s1}.\gamma_i.h_i - u_i\right).\frac{\tan\phi_i}{\Gamma_{\phi i}}}{1+\frac{\tan\alpha_i.\tan\phi_i}{\Gamma_{Bish\ sol}.\Gamma_{s3}.\Gamma_{\phi i}}}.\frac{b_i}{\cos\alpha_i} + \Delta N_i.\frac{\tan\phi_i}{\Gamma_{\phi i}}\right)}{\Gamma_{s3}.\sum_{i=1}^{n}\left(\Gamma_{s1}.\gamma_i.h_i.b_i.\sin\alpha_i - \Delta T_i\right)}$$

in which $F_{Bish\ sol}$ is calculated beforehand by eq. (17).

Note: For a nonlinear shear strength curve (section 3.4.2), an iterative process is performed to determine:

$$T_{i\max} + \Delta N_i.\tan\phi'^{*}_i = c'^{*}_i.\frac{b_i}{\cos\alpha_i} + \left(N_i + \Delta N_i\right).\tan\phi'^{*}_i$$

5.6.2. Perturbation method

In the Perturbation method and considering the adopted sign convention, the introduction of reinforcement is made by introducing the forces ΔN_i and ΔT_i generated by the set of inclusions, and by replacing σ by $\sigma + \Delta\sigma_{renf}$ in eq. (19) to (21), with:

$$\Delta\sigma_{renf}(x_i) = +\frac{\Delta N_i}{L_i} \qquad (84)$$

where L_i is the length at the base of slice i (note: ΔN_i has a positive value when the reinforcement is in tension)

The only parameters in eq. (25) which change in regards to the set of parameters calculated for the soil alone are H5, V5 and 05, which become:

$$\begin{aligned} H_{5\,renf} &= H_{5\,sol} - \sum\left(\Delta N_i.\sin\alpha_i + \Delta T_i.\cos\alpha_i\right) \\ V_{5\,renf} &= V_{5\,sol} - \sum\left(\Delta N_i.\cos\alpha_i - \Delta T_i.\sin\alpha_i\right) \\ O_{5\,renf} &= O_{5\,sol} - \sum\left(\Delta N_i.\cos\alpha_i - \Delta T_i.\sin\alpha_i\right).x_i + \sum\left(\Delta N_i.\sin\alpha_i + \Delta T_i.\cos\alpha_i\right).y_i \end{aligned} \qquad (85)$$

x_i and y_i are the point coordinates of the failure surface on which ΔN_i and ΔT_i are applied.

In all relationships which depend on σ_{Fel}, the value of this expression is replaced by:

$$\sigma_{FelR} = \sigma_{Fel\ sol} + \Delta\sigma_{renf} \quad \text{où} \quad \sigma_{Fel\ sol} \text{ est donné par (9).} \qquad (86)$$

5.6.3. "Calculation with yield design calculation method

Chapter under construction.

The yield design calculation method is under the process of being validated and is therefore not yet available in TALREN 4.

6 TAKING INTO ACCOUNT THE SAFETY FACTORS

6.1. PRINCIPLE OF THE SEMI-PROBABILISTIC METHOD (U.L.S CALCULATION)

In the present version of TALREN, the safety is introduced in the following manner (Table 3):

Factored parameters	Comments
• Additional safety factor Γ	Γ is calculated by TALREN and should be ≥ 1 for equilibrium
• Coefficient relating to the calculation method Γ_{s3}	Γ_{s3} is imposed by the user
• Soils $\gamma^* = \gamma . \Gamma_{s1}$	Γ_{s1} is imposed by the user for each soil
$c^* = c/\Gamma_c$	Γ_c is imposed by the user for each soil
$\tan\phi^* = \tan\phi/\Gamma_\phi$	Γ_ϕ is imposed by the user for each soil
$P_l^* = p_l/\Gamma_{pl}$ (= p_f)	Γ_{pl} is imposed by the user for each soil
• Adherence $q_s^* = q_s/\Gamma_{qs}$	Γ_{qs} is imposed by the user for nails, anchors and strips
• Loads (distributed, linear and additional moments) $Q^* = Q . \Gamma_Q$	Γ_Q is imposed by the user for each load
• Inclusions: $R_N = T_G/\Gamma_{mR}$	T_G is the tensile or compressive yield strength
$R_C = R_N/2$	Γ_{mR} is imposed by the user for each type of reinforcement (nails, anchors, strips, struts)
$M^*_{max} = M_{max}/\Gamma_{mR}$	M_{max} maximum moment in the inclusion
with: $\Gamma_{mR} = \Gamma_{aclo}$ or Γ_{atir} or Γ_{abu} or Γ_{aTA}	

Table 3: Partial safety factors in TALREN

The semi-probabilistic method corresponds to the principles applied in Clouterre recommendations, in the French Standards or in Eurocode 7, but each of these documents recommends different values for the partial safety factors.

The following sections give a few extracts of different reference documents (recommendations and standards).

Table 12 of section 6.8 summarises the different partial safety factor sets predefined in Talren 4, and completes them with a few suggestions (which do not have normative value), for the anchors in the case of Clouterre 1991 for example.

6.2. APPLICATION OF CLOUTERRE RECOMMENDATIONS

Table 4 gives the values of the load factors proposed by Clouterre 1991 recommendations.

In the case of Q loads including permanent and variable loads, it will be necessary to make a composition of the weighting coefficient Γ_Q.

Example: an industrial building brings to the soil a destabilising total load Q_t = 500 kPa that can be decomposed into a permanent load Q_{perm} = 200 kPa and a variable load Q_{var} = 300 kPa. One shall adopt the weighting coefficient Γ_Q equal to:

$$\Gamma_Q = \frac{1{,}2.Q_{perm} + 1{,}33.Q_{\text{var}}}{Q_t} = 1{,}28$$

		Weighting coefficients of the actions	
Nature of the loads	TALREN Notation	Fundamental combination	Accidental combination
1) Permanent			
On G (destab.)	Γ_{s1}	1,05	1
On G (stab.)	Γ'_{s1}	0,95	1
On Q (destab.)		1,2	1
On Q (stab.)		0,90	1
2) Variable			
On Q (destab.)	Γ_Q	1,33	1
3) Accidental			
On Q (destab.)	Γ_Q	-	1
Calculation method	Γ_{s3}	1,125	1

Table 4: Load factors, Clouterre 1991

Table 5 gives the values of the partial safety factors applied to the material strength properties, proposed by "Clouterre recommendations 1991".

		Partial safety factors			
		Fundamental combination		Accidental combination	
Charactersitics	TALREN notation	Standard	Sensitive	Standard	Sensitive
1) Soils					
Friction (tanϕ')	Γ_{ϕ}	1,2	1,3	1,1	1,2
Effective cohesion c'	$\Gamma_{c'}$	1,5	1,65	1,4	1,5
Undrained coh. c_u	Γ_{cu}	1,3	1,4	1,2	1,3
2) Reinforcements					
Steel nails (σ_e)	Γ_{aclou}	1,15	1,15	1,0	1,0
3) Soil/reinforcement interaction					
qs for nails					
• q_s from charts	$\Gamma_{qscl\ ab}$	1,8	1,9	1,6	1,7
• q_s from tests	$\Gamma_{qscl\ es}$	1,4	1,5	1,3	1,4
Limit pressure p_l	Γ_{pl}	1,9	2,0	1,0	1,1

Table 5: Partial safety factors on the strength properties, Clouterre 1991

6.3. APPLICATION OF FRENCH STANDARDS

6.3.1. French standard XP P 94-240: "Soutènement et talus en sol en place renforcé par des clous" (Retaining walls and slopes reinforced with nails)

The tables below are an extract of the standard.

It is however necessary to refer to the standard for more complete information: it includes additional information (for example, the definition of the categories 1, 2a and 2b).

		Load factors	
Nature of the actions	TALREN notation	Fundamental combination	Accidental combination
Soil weight			
Destabilising	Γ_{s1}	1,05	1
Stabilising	Γ'_{s1}	0,95	1
Other permanent actions			
Destabilising		1,2	1
Stabilising		0,90	1
Variable loads			
Q	Γ_Q	1,33	1
Accidental loads			
F_A	Γ_Q	-	1
Action of anchors			
F_T stabilising		0,9	1
F_T destabilising		1,2	1
With F_T: blocking tension			
Calculation method	Γ_{s3}	1	1

Table 6: Load factors, French Standard XP P 94-240

		Partial safety factors			
		Fundamental combination		Accidental combination	
Characteristics	TALREN notation	Category 1-2a	Category 2b	Category 1-2a	Category 2b
Soils					
Friction (tanϕ')	Γ_{ϕ}	1,35	1,45	1,1	1,2
Effective cohesion c'	$\Gamma_{c'}$	1,7	1,85	1,4	1,5
Undrained coh. c_u	Γ_{cu}	1,45	1,6	1,2	1,3
Passive steel					
Yield stress σ_e		1,15	1,15	1,0	1,0
Soil/nail interaction					
• q_s from charts (structures in category 1 only)	$\Gamma_{qscl\ ab}$	1,8		1,6	
• q_s from tests	$\Gamma_{qscl\ es}$	1,4	1,5	1,3	1,4
Limit pressure p_l	Γ_{pl}	1,9	2,0	1,0	1,1

Table 7: Partial safety factors on the strength properties, French Standard XP P 94-240

6.3.2. French standard XP P 94-220-0: "Ouvrages en sols rapportés renforcés par armatures ou nappes peu extensibles et souples"

The tables below are an extract of the standard.

It is however necessary to refer directly to the standard for more complete information: it includes additional comments, as well as a definition of the standard and sensible structure categories.

		Load factors	
Nature of the actions	TALREN notation	Fundamental combination	Accidental combination
Proper weight of the soil			
Destabilising	Γ_{s1}	1,05	1
Stabilising	Γ'_{s1}	0,95	1
Loads			
Q	Γ_{Q}	1,33	0
On the method	Γ_{s3}	1,125	1

Table 8: Load factors, French Standard XP P 94-220-0

		Partial safety factors			
		Fundamental combination		Accidental combination	
Characteristics	TALREN notation	Standard	Sensitive	Standard	Sensitive
Soils					
Friction (tanϕ') of the reinforced backfill	Γ_{ϕ}	1	1	1	1
Friction (tanϕ')	Γ_{ϕ}	1,2	1,3	1,1	1,2
Effective cohesion c'	$\Gamma_{c'}$	1,5	1,65	1,4	1,5
Undrained cohesion c_u	Γ_{cu}	1,3	1,4	1,2	1,3
Traction resistance of the reinforcement in standard section	Γ_{aba}	1,5	1,65	1,5	1,65
Resistance due to the soil/reinforcement interaction	Γ_{qsba}	1,2	1,3	1,2	1,3

Table 9: Partial safety factors on the strength properties, French Standard XP P 94-220-0

6.4. APPLICATION OF EUROCODE 7

The national appendices to Eurocode 7 have not been completed yet, so we could not include partial safety factor sets corresponding to Eurocode 7 in TALREN 4.

However, the user can, of course, create his own factor sets, to define a set of factors compatible with EC7 recommendations, for example.

6.5. TRADITIONAL CALCULATION

6.5.1. Comparing the semi-probabilistic method (ULS) to traditional calculation

Traditional formulation of the global safety factor according to Fellenius (87):

$$F_{Fel} = \frac{\sum_{i=1}^{n}\left(\left[c_i + \left(\gamma_i.h_i.\cos^2\alpha_i - u_i + \frac{dU_i}{dx_i}.\sin\alpha_i.\cos\alpha_i\right).\tan\phi_i\right].\frac{b_i}{\cos\alpha_i} + \Delta N_i.\tan\phi_i\right)}{\sum_{i=1}^{n}\left(\gamma_i.h_i.b_i.\sin\alpha_i - \Delta T_i\right) + \sum\frac{M_{ext}}{R}} \tag{87}$$

ULS formulation according to Fellenius (88):

$$F_{Fel} = \frac{\sum_{i=1}^{n}\left(\left[\frac{c_i}{\Gamma_{ci}} + \left(\Gamma_{s1}.\gamma_i.h_i.\cos^2\alpha_i - u_i + \frac{dU_i}{dx_i}.\sin\alpha_i.\cos\alpha_i\right).\frac{\tan\phi_i}{\Gamma_{\phi i}}\right].\frac{b_i}{\cos\alpha_i} + \Delta N_i.\frac{\tan\phi_i}{\Gamma_{\phi i}}\right)}{\Gamma_{s3}.\left[\sum_{i=1}^{n}\left(\Gamma_{s1}.\gamma_i.h_i.b_i.\sin\alpha_i - \Delta T_i\right) + \sum\frac{M_{ext}}{R}\right]} \tag{88}$$

Traditional formulation of the global safety factor according to Bishop (89):

$$F_{Bish} = \frac{\sum_{i=1}^{n}\left(\frac{c_i + \left(\gamma_i.h_i - u_i\right).\tan\phi_i}{1 + \frac{\tan\alpha_i.\tan\phi_i}{F_{Bish\ sol}}}.\frac{b_i}{\cos\alpha_i} + \Delta N_i.\tan\phi_i\right)}{\sum_{i=1}^{n}\left(\gamma_i.h_i.b_i.\sin\alpha_i - \Delta T_i\right) + \sum\frac{M_{ext}}{R}} \tag{89}$$

ULS formulation according to Bishop (90):

$$F_{Bish} = \frac{\sum_{i=1}^{n}\left(\frac{\frac{c_i}{\Gamma_{ci}} + \left(\Gamma_{s1}.\gamma_i.h_i - u_i\right).\frac{\tan\phi_i}{\Gamma_{\phi i}}}{1 + \frac{\tan\alpha_i.\tan\phi_i}{\Gamma_{Bish\ sol}.\Gamma_{s3}.\Gamma_{\phi i}}}.\frac{b_i}{\cos\alpha_i} + \Delta N_i.\frac{\tan\phi_i}{\Gamma_{\phi i}}\right)}{\Gamma_{s3}.\left[\sum_{i=1}^{n}\left(\Gamma_{s1}.\gamma_i.h_i.b_i.\sin\alpha_i - \Delta T_i\right) + \sum\frac{M_{ext}}{R}\right]} \tag{90}$$

with, for the traditional calculation:

$$\Delta N_i \ et \ \Delta T_i = \left(\frac{TR}{F_R}, \frac{p_l}{F_{pl}}, \frac{q_s}{F_{qs}} \right)$$

with for the ULS calculation

$$\Delta N_i \ et \ \Delta T_i = \left(\frac{TR}{\Gamma_{mR}}, \frac{p_l}{\Gamma_{pl}}, \frac{q_s}{\Gamma_{qs}} \right)$$

To extend these formulations to loads, which was not done here because it would have made the formulations heavier, one just has to replace:

- For distributed loads:
  in (87) and (89) $\gamma_i.h_i$ par $\gamma_i.h_i + q_i$
  in (88) and (90) $\Gamma_{s1}.\gamma_i.h_i$ par $\Gamma_{s1}.\gamma_i.h_i + \Gamma_Q.qi$
- For linear loads:
  in (87) and (89) ΔN_i and ΔT_i $\Delta N_i + \Delta N_{Qi}$ and $\Delta T_i + \Delta T_{Qi}$
  in (88) and (90) ΔN_i and ΔT_i $\Delta N_i + \Gamma_Q.\Delta N_{Qi}$ and $\Delta T_i + \Gamma_Q.\Delta T_{Qi}$
- For additional moments:
  in (87) and (89) $\Sigma M_{ext}/R$ $(\Sigma M_{ext} + \Sigma M_{add})/R$
  in (88) and (90) $\Sigma M_{ext}/R$ $(\Sigma M_{ext} + \Gamma_Q.\Sigma M_{add})/R$

By moving Γ_{Fel} and Γ_{Bish} to the right-hand side of the equalities, dividing eq. (88) and (90) by $\Gamma_{s3}.\Gamma_{s1}$, and comparing eq. (87) with (88) or eq. (89) with (90), one obtains for the same soil unit weight, the schematic relationships shown in Table 10:

Schematic comparison of the safety factors			
		Global	ULS calculation
For shear strength characteristics			
Internal friction	ϕ	F_{glob}	$\Gamma.\Gamma_{s3}.\Gamma_{\phi}$
Cohesion	c' or c_u	F_{glob}	$\Gamma.\Gamma_{s3}.\Gamma_c.\Gamma_{s1}$
For loads			
Loads	Q	1	Γ_Q/Γ_{s1}
For reinforcements			
Steel or concrete	σ_e ou f_{cj}	FR	$\Gamma_{mR}.\Gamma_{s1}$
For the soil/reinforcement interaction			
Limit pressure	p_l	F_{pl}	$\Gamma_{pl}.\Gamma_{s1}$
Friction	q_s	F_{qs}	$\Gamma_{qs}.\Gamma_{s1}$

(F_{glob} = F_{Fel} or F_{Bish})

Note: these relationships are approximative, in particular for cases involving a water table whose effects are not factored in the ULS method.

Table 10: Safety factors to be considered in order to allow a comparison between the traditional method (global safety factor) and ULS calculation (partial safety factors)

This comparative study can be extended to the perturbation method for which we find the same correspondences between the safety factors.

6.5.2. Traditional calculation with the ULS calculation version

From Table 10, we can establish the list of partial safety factors to be taken into account in TALREN ULS calculation to perform a traditional calculation (global safety factor):

		Coefficients
1) Soils		
Internal friction	$\tan\phi'$	$\Gamma_\phi = 1$
Cohesion	c' ou c_u	$\Gamma_c = 1$
Unitl weight	γ	$\Gamma_{s1} = 1$
2) Loads		
Loads	Q	$\Gamma_Q = 1$
3) Reinforcements		
Steel and concrete	σ_e or f_{cj}	$\Gamma_{mR} \neq 1$
4) Soil/reinforcement interaction		
Limite pressure	p_l	$\Gamma_{pl} \neq 1$
Friction	q_s	$\Gamma_{qs} \neq 1$

Table 11: Coefficients to be taken into account in TALREN to perform a traditional type of calculation with the ULS version of calculation

With:

σ_e : steel yield stress

f_{cj} : limit stress in the concrete

To define Γ_{mR}, it is necessary to consider the factors that can limit the mechanical strength of the reinforcements (for example the non-buckling condition for struts).

For this type of calculation, we look for a Γ_{min} coefficient (minimal coefficient for all calculated failure surfaces) equal to F_{glob} (traditional global safety factor on $\tan\phi$ and c).

One can also take Γ_ϕ and Γ_c equal to F_{glob}, and research $\Gamma_{min} = 1$.

6.6. SPECIFIC STRUCTURES

6.6.1. Reinforced soil structure using strips or fabrics

The analysis method used to determine the internal stability of soil structures reinforced by strips or fabrics (example: Reinforced Earth) is very different from the stability calculations performed using a slice method. This leads to an over-design coefficient Γ relatively low by applying CLOUTERRE recommended factors (example: in the case of a current structure 10 m high, one obtains $\Gamma \approx 0{,}8$).

Consequently, one could decompose the stability analysis of such structures in two verifications:

- Internal stability of which the verification method is given in the recommendations specific to the concerned structures;
- External stability for failure surfaces passing below the base of the reinforced soil wall facing.

6.6.2. Other reinforcements

For the other types of reinforcements (micropiles, piles, walls, sheetpiling, struts, ...), there are no rules nor recommendations relating to the stability analysis using the limit equilibrium method. The existing french documents (D.T.U., SETRA rules, etc) do not refer to this type of calculation.

It is therefore difficult to give partial safety factor values. It seems convenient to establish correlations with applicable documents for other applications.

Example: in the case of a micropile working in compression, the allowable loads are calculated from limit lateral friction value affected by a Fqs coefficient (variable according to the applicable documents and the types of structures). Applying the load factor provided by "CLOUTERRE 1991 Recommendations" or the french standard XP P 94-240, it seems logical to take the value $\Gamma_{qs} = F_{qs} / \Gamma_{s1}$.

6.6.3. Reinforced structure with a steep backslope

Retaining structures having a large backslope whose angle is close to the internal friction angle of the soil (case of retaining structures constructed on a sloped embankment), do not generally improve the safety factor for large radius failure surfaces.

One approach consists in analysing the slope stability for the slip surfaces in which the horizontal distance between the toe of the retaining structure and the upper or lower emergence point of the failure surface is limited to 3H, where H is the height of the excavation in the vicinity of the structure.

A second approach is provided by TALREN, which allows the user to apply different partial safety factors for the soil properties (refer to french standard NF P 94-220 - §9.3.3 relating to structures constructed on slopes). This approach consists in applying the usual safety factors to the soils located within the reinforced zone. Outside the reinforced zone, the partial safety factor applied to soil properties is equal to the safety factor of the original slope before construction of the retaining structure. The design of the retaining structure will thereby ensure that its construction will not affect the stability for large failure surfaces.

6.7. PARTICULAR CASE OF THE CALCULATION WITH YIELD DESIGN CALCULATION METHOD

Chapter under construction.

The yield design calculation method is in the process of being validated end is therefore not yet available in TALREN 4.

6.8. SUMMARY TABLE OF PARTIAL SAFETY FACTORS

PARTIAL SAFETY FACTORS IN TALREN 4

Name	Γmin	Γs1	Γ's1	Γphi	Γc'	Γcu	ΓQ	Γqsna ab	Γqsna es	Γqsan ab	Γqsan es	Γqsstrip	Γpl	Γanail	Γaanc	Γastrip	Γbu	Γs3
Traditional method / Temporary	1.3	1	1	1	1	1	1	1.8	1.5	1.8	1.5		2	1.3	1.3			1
Traditional method / Permanent	1.5	1	1	1	1	1	1	2	1.5	2	1.5		2	1.5	1.5			1
Clouterre Fundamental / Standard	1	1.05	0.95	1.2	1.5	1.3	1.33	1.8	1.4	1.8	1.4		1.9	1.15	1.15			1.125
Clouterre Fundamental / Sensitive	1	1.05	0.95	1.3	1.65	1.4	1.33	1.9	1.5	1.9	1.5		2	1.15	1.15			1.125
Clouterre Accidental / Standard	1	1	1	1.1	1.4	1.2	1	1.6	1.3	1.6	1.3		1	1	1			1
Clouterre Accidental / Sensitive	1	1	1	1.2	1.5	1.3	1	1.7	1.4	1.7	1.4		1.1	1	1			1
French standard XP P 94-240 Fund. 1-2a	1	1.05	0.95	1.35	1.7	1.45	1.33	1.8	1.4	1.8	1.4		1.9	1.15	1.15			1
French standard XP P 94-240 Fund. 2b	1	1.05	0.95	1.45	1.85	1.6	1.33	-	1.5	-	1.5		2	1.15	1.15			1
French standard XP P 94-240 Acc. 1-2a	1	1	1	1.1	1.4	1.2	1	1.6	1.3	1.6	1.3		1	1	1			1
French standard XP P 94-240 Acc. 2b	1	1	1	1.2	1.5	1.3	1	-	1.4	-	1.4		1.1	1	1			1
French standard XP P 94-220 Fund/stand.	1	1.05	0.95	1.2*	1.5	1.3	1.33					1.2				1.5		1.125
French standard XP P 94-220 Fund/sens.	1	1.05	0.95	1.3*	1.65	1.4	1.33					1.3				1.65		1.125
French standard XP P 94-220 Acc./stand.	1	1	1	1.1*	1.4	1.2						1.2				1.5		1
French standard XP P 94-220 Acc./sens.	1	1	1	1.2*	1.5	1.3						1.3				1.65		1
EC7 - Approach 1	1	National appendices of EC7 not available yet																
EC7 - Approch 2	1																	
EC7 - Approach 3	1																	
ROSA 2000 Fundamental standard	1	Not provided in present version																
ROSA 2000 Fundamental sensitive	1																	
ROSA 2000 Accidental standard	1																	
ROSA 2000 Accidental sensitive	1																	

*: except in reinforced backfill : = 1

Sets and values provided with TALREN 4

Sets or values proposed here, but not mentionned in the standards or recommendations. These proposed values have no normative or contractual meaning, and the Talren 4 user alone is responsible for using them.

Table 12: Summary table for partial safety factors

7 COMPATIBILITY OF THE OPTIONS WITH THE CALCULATION METHODS

In the 3 following tables is described the compatibility between data and calculation methods for circular failure surfaces (Table 13), polygonal failure surfaces (Table 14) and logarithmic spirals (Table 15).

Note: the yield design calculation method associated with logarithmic spirals is not yet available in Talren 4.

		Calculation methods			
Option	**Type of data**	**Fellenius**	**Bishop**	**Perturb.**	**Yield design**
Hydraulic	Pore pressures	●❍*	●❍*	●	●
	External ground water	●❍*	●❍*	●	●
Soil	Linear shear strength curve	●	●	●	●
	Non-linear shear strength curve	●	●	●	●
	Anisotropic cohesion	●	●	●	●
Seismic	Seismic accelerations	●	●	●	●
Loads	Distributed and vertical	●	●	●	●
	Distributed and inclined	❍	❍	❍	●
	Linear without diffusion	●	●	●	●
	Linear with diffusion	●	●	●	●
	Additional moments	●	●	●	●
Reinforcements	Soil nails	●	●	●	●
	Prestressed anchors	●	●	●	●
	Reinforcing strips	●	●	●	●
	Struts	●	●	●	●

●: Method compatible with the option
○: Method incompatible with the option
○*: Method incompatible with the option when the vertical extension of a circular failure surface or the vertical portion of a non-circular failure surface intersects the water table

Table 13: Compatibility between data and calculation methods
Case of circular failure surfaces

		Calculation methods			
Option	**Type of data**	**Fellenius**	**Bishop**	**Perturb.**	**Yield design**
Hydraulic	Pore pressures	●❍*	●❍*	●	●
	External ground water	❍	❍	●	●
Soil	Linear shear strength curve	●	●	●	●
	Non-linear shear strength curve	●	●	●	●
	Anisotropic cohesion	●	●	●	●
Seismic	Seismic accelerations	❍	❍	●	●
Loads	Distributed and vertical	●	●	●	●
	Distributed and inclined	❍	❍	❍	●
	Linear without diffusion	❍	❍	●	●
	Linear with diffusion	●	●	●	●
	Additional momments	❍	❍	●	●
Reinforcements	Soil nails	●	●	●	●
	Prestressed anchors	●	●	●	●
	Reinforcing strips	●	●	●	●
	Struts	●	●	●	●

●: Method compatible with the option
○: Method incompatible with the option
○*: Method incompatible with the option when the vertical extension of a circular failure surface or the vertical portion of a non-circular failure surface intersects the water table

Table 14: Compatibility between data and calculation methods
Case of polygonal failure surfaces

Note: in the case of polygonal failure surfaces really plane, it is not possible to use the Perturbations calculation method (the system of equations has no solution).

In this case, one must either use another calculation method, or approach the plane surface with a circular surface.

		Calculation methods
Option	**Type of data**	**Yield design**
Hydraulic	Pore pressures	●
	External ground water	●
Soil	Linear shear strength curve	●
	Non-linear shear strength curve	●
	Anisotropic cohesion	●
Seismic	Seismic accelerations	●
Loads	Distributed and vertical	●
	Distributed and inclined	●
	Linear without diffusion	●
	Linear with diffusion	●
	Additional momments	●
Reinforcements	Soil nails	●
	Prestressed anchors	●
	Reinforcing strips	●
	Struts	●

●: Method compatible with the option
○: Method incompatible with the option
○*: Method incompatible with the option when the vertical extension of a circular failure surface or the vertical portion of a non-circular failure surface intersects the water table

Table 15: Compatibility between data and calculation methods
Case of logarithmic spirals

APPENDICES

APPENDIX 1: PARAMETERS TAKEN INTO ACCOUNT IN THE SOIL INCLUSION NORMAL INTERACTION

A1.1 REACTION LAW

The law of soil-inclusion normal reaction can be written: $EI.\frac{d^4y}{dz^4} + k_s.y.B = 0$

Where the notations shown on Figure 45 are taken from Bourges and Frank (1979). The variable k_s is the sub grade reaction coefficient defined by $p = k_s.y$.

The general solution of the equation for a homogeneous soil (k_s = constant) can be written:

$$y = e^x.(a_1.\cos x + a_2.\sin x) + e^{-x}.(b_1.\cos x + b_2.\sin x)$$

where:

x : z/L_0

L_0 : $(4.EI / E_s)^{1/4}$ (transfer length)

E_s : $k_s.B$ (reaction modulus per unit length of the inclusion)

EI : bending stiffness of the inclusion

For an "infinitely long" inclusion ($L > 3.L_0$) not subjected to a moment at its head (symmetrical loading on the two sides of the failure surface), the solution is:

$$y = \frac{2.T_0}{E_s.L_0}.e^{-x}.\cos x \qquad \text{and} \qquad M = -T_0.L_0.e^{-x}.\sin x$$

The values determined at the origin (x = 0) are: $y_0 = \frac{2.T_0}{E_s.L_0}$, $M_0 = 0$ and $p_0 = \frac{2.T_0}{B.L_0}$

For an "infinitely rigid" inclusion ($L<L_0$), the expression becomes: $y = y_0.(1 - 3x/2)$, avec

x = z/L $\qquad y_0 = 4.T_0/(E_s.L) \qquad p_0 = 4.T_0/(B.L)$

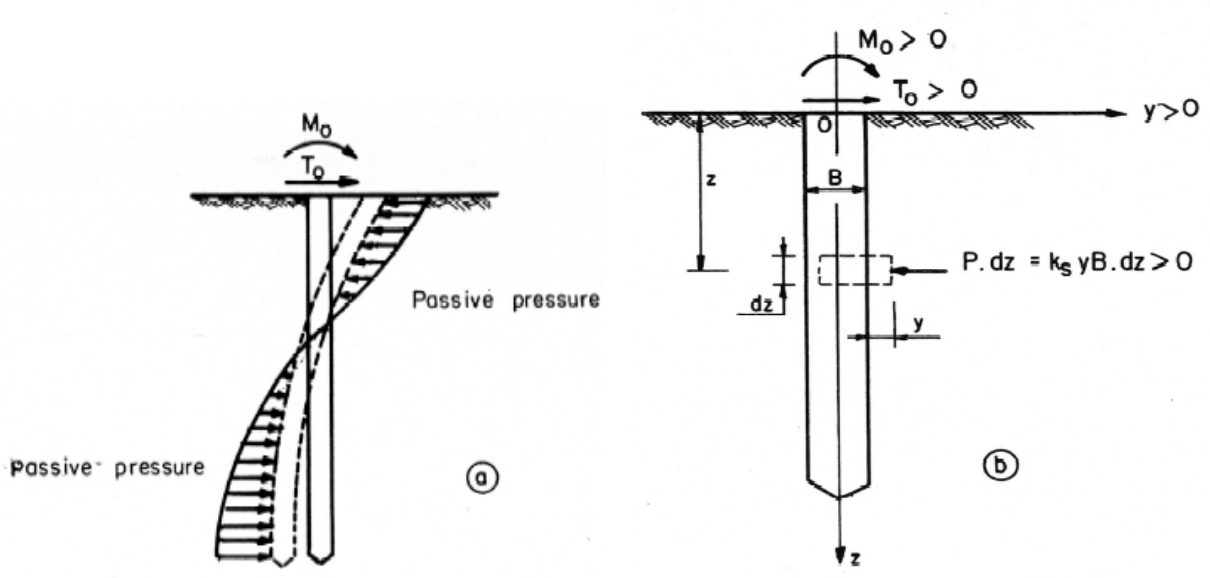

Figure 45: Conventions for the normal soil-inclusion interaction

A1.2 REACTION MODULUS: E_s

The value of E_s is determined from the rules pertaining to the Menard pressuremeter. For a small diameter inclusion (B < 0.60 m), which is generally the case, E_s is obtained from:

$$\frac{E_s}{E_M} = \frac{1}{\left(\frac{2}{9}.2{,}65^{\alpha} + \frac{\alpha}{6}\right)}$$

where:

E_M : pressuremeter modulus

α : rheological coefficient

E_s : k_s.B

Figure 46 shows that within the common range of α (1/3 < α < 2/3), the value of E_s/E_M is between 2 and 3, which can be considered small with respect to the imprecision involved in determining E_M.

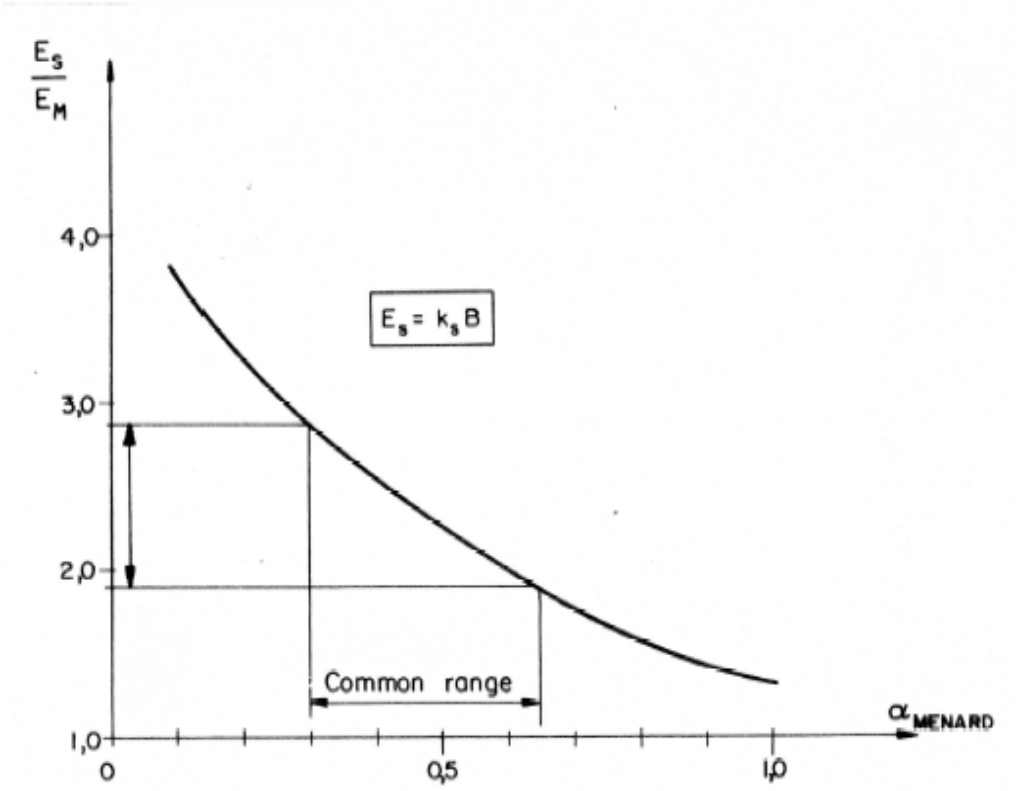

Figure 46: Evolution of the E_s/E_M ratio as a function of the rheological coefficient α (Ménard rules)

A1.3 RIGIDITY OF THE INCLUSION

The grout is not taken into account in the bending stiffness of the inclusion. It is assumed that only the steel provides the bending resistance, except in the case of large diameter inclusions of the type "pile-nails", constructed according to the specifications for reinforced concrete.

One is reminded on Figure 47 of the inertia of various geometries, remembering that when the geometry is not symmetrical about the centre of rotation, one must first consider the smallest inertia value (except when the position of the inclusion with respect to its loading direction is controlled during placement).

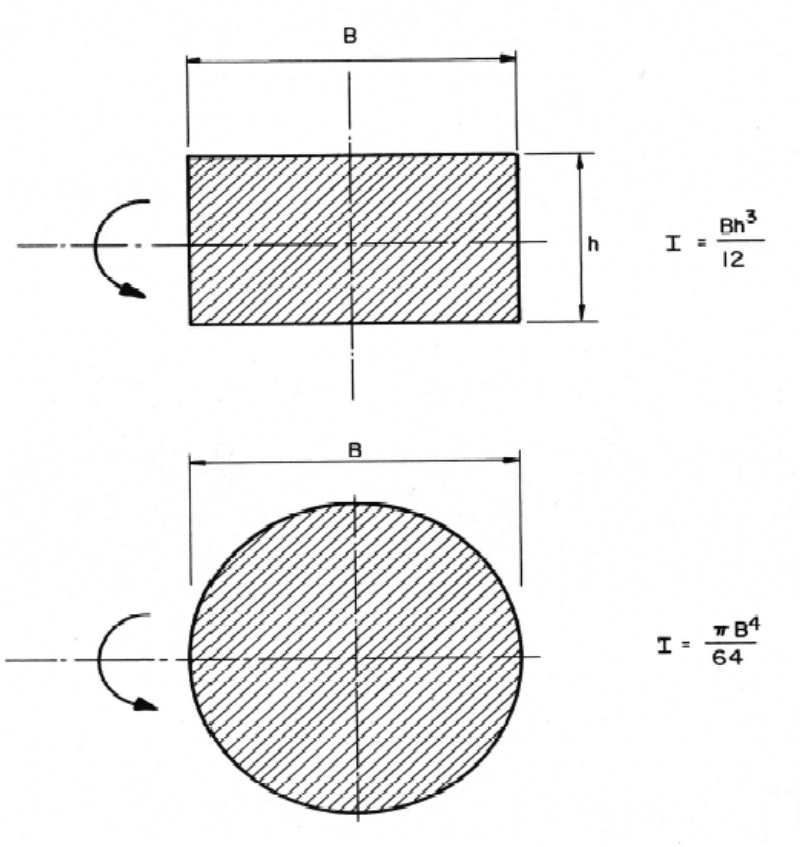

Figure 47: Inertia moments of typical sections

A1.4 TRANSFER LENGTH L_0

To provide an indication, the common transfer lengths for three types of inclusions are presented on Figure 48. The transfer length seldom exceeds 0.4 m. When the inclusions extend more than 0.8 m beyond the potential failure surface, they can be considered as "infinitely long".

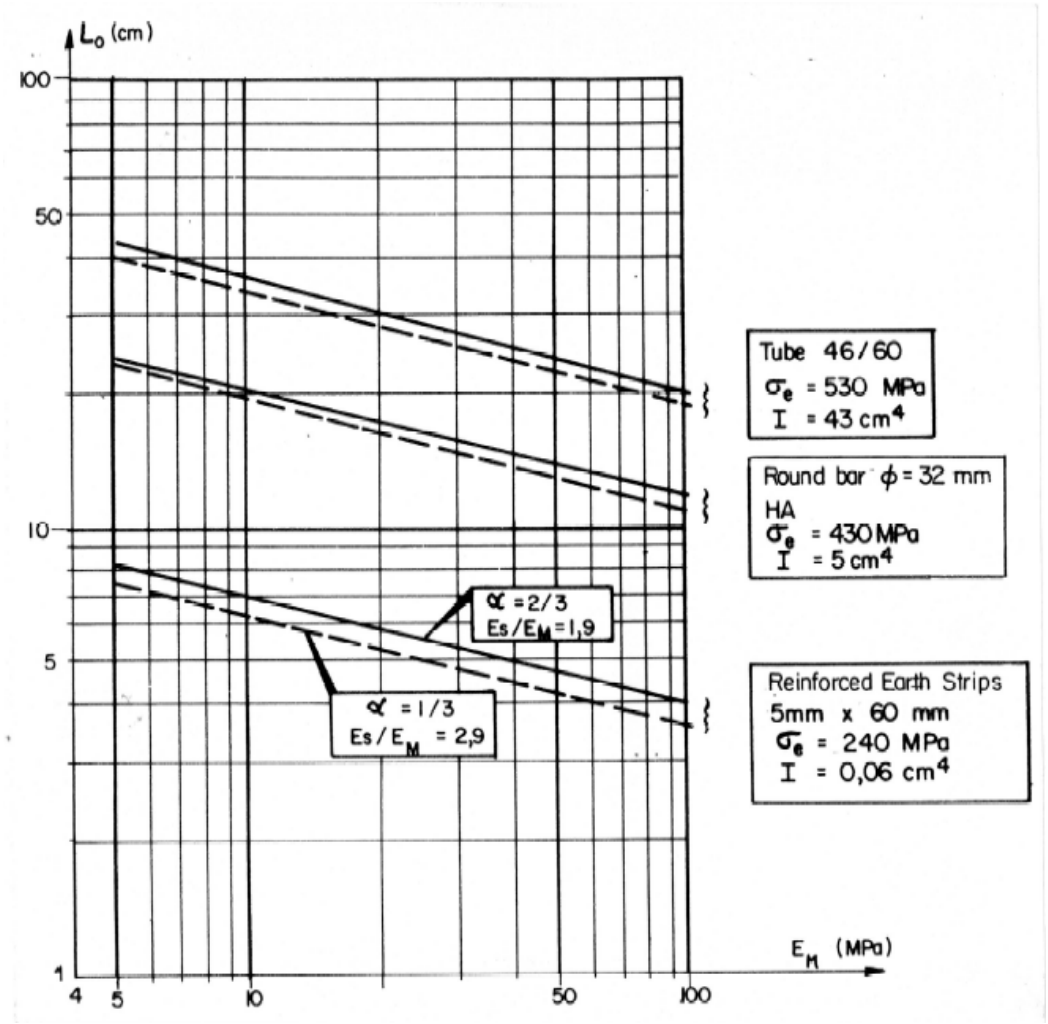

Figure 48: Transfer lengths for various inclusions

A1.5 PLASTIFICATION MOMENT $M_{max}(T_n)$: Criterion T_{cl2}

The moment at the instant of complete plastification by combined bending depends on the form of the reinforcement's cross-section and is given by the following expressions (considering *k* = shear resistance of the steel). One should note that $M_{max}(0)$ is the maximum allowable moment in simple bending (T_n=0).

a) Section rectangulaire B.h (Figure 49a)

Tension $T_n = 2.k.B.(h_1 - h_2)$

Pure tensile resistance $R_n = 2.k.B.h$

Moment / O $M_{\max} = 2.k.B.h_1.h_2$

$$M_{\max}(T_n) = \frac{k.B.h^2}{2}.\left(1 - \frac{T_n{}^2}{R_n{}^2}\right) \qquad M_{\max}(0) = \frac{k.B.h^2}{2}$$

$$M_{\max}(T_n) = M_{\max}(0).\left(1 - \frac{T_n{}^2}{R_n{}^2}\right)$$

b) Circular section ϕ = B (Figure 49b)

Pure tensile resistance $R_n = 2.k.\pi.B^2 / 4$

Tension $T_n = k.B^2.\dfrac{[2.\theta_0 + \sin(2.\theta_0]}{4}$

Moment $M_{\max}(T_n) = \dfrac{k.B^3}{3}.\cos^3\theta_0 = M_{\max}(0).\cos^3\theta_0$

with: $\dfrac{T_n}{R_n} = \dfrac{1}{\pi}.[2.\theta_0 + \sin(2.\theta_0)]$

Figure 50 indicates that the value of Mmax(Tn) does not vary by more than 18% from $M_{\max}(T_n) = M_{\max}(0).\left(1 - \dfrac{T_n{}^2}{R_n{}^2}\right)$ independent of the distribution of the plasticised zones in tension and compression.

Taking this remark into account and considering the analogy with a rectangular section, one can retain for a circular section, the expression:

$$M_{\max}(T_n) = M_{\max}(0).\left(1 - \frac{T_n{}^2}{R_n{}^2}\right)$$

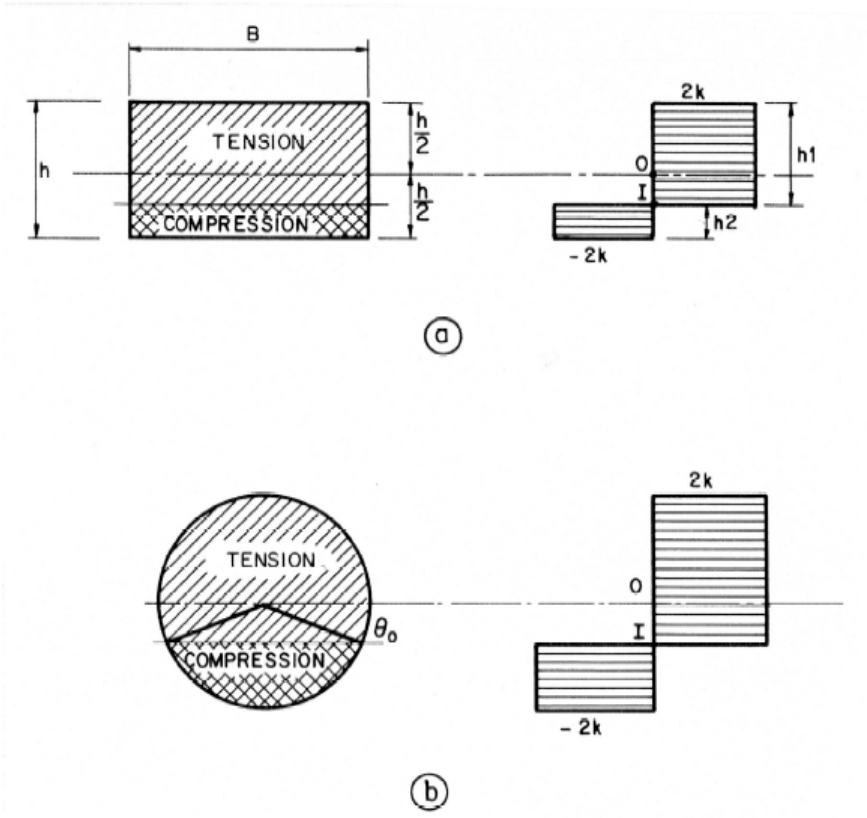

Figure 49: Diagram of complete plastification by combined bending

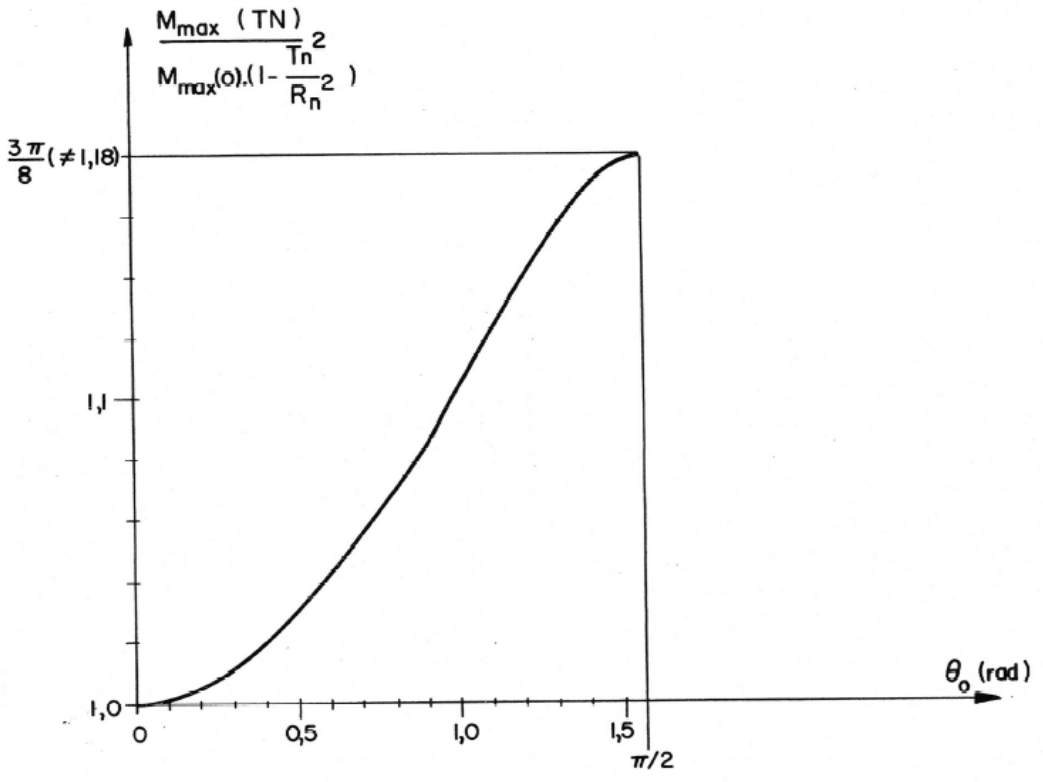

Figure 50: Approximation of M_{max} for a circular section

c) Tubular section

A tubular section can be simulated by the difference between two concentric circular sections. The approximation is therefore the same as that given above.

A1.6 EXAMPLES OF THE STABILITY DOMAIN FOR THE NORMAL INTERACTION

As an example, Figure 51 presents the normal interaction stability domains for three different types of inclusions, previously discussed in section 4, and assumed to be "long" ($L^* \geq 2.L_0$).

Except for reinforcing strips, which are only employed within a limited geotechnical context (selected soil types), the inclusions are assumed to be placed in two types of soils:

- relatively deformable soil: p_l = 1,5 MPa E_M = 15 MPa α = 1/3
- very stiff soil (or soft rock): p_l = 10,0 MPa E_M = 100 MPa α = 2/3

The round bar and the tube are assumed to be placed within a borehole ϕ = 100 mm. The grout is not considered in the evaluation of $M_{max.}$

It appears that for inclusions with a small inertia, the available shear resistance is small. Considering the application of the principle of maximum plastic work results in most cases in the choice of point P as the point representing the force couple (T_n, T_c). The value of the shear force at this point does not exceed 10% of the pure tensile strength for a stiff soil and 2% for a deformable soil, in all the cases studied.

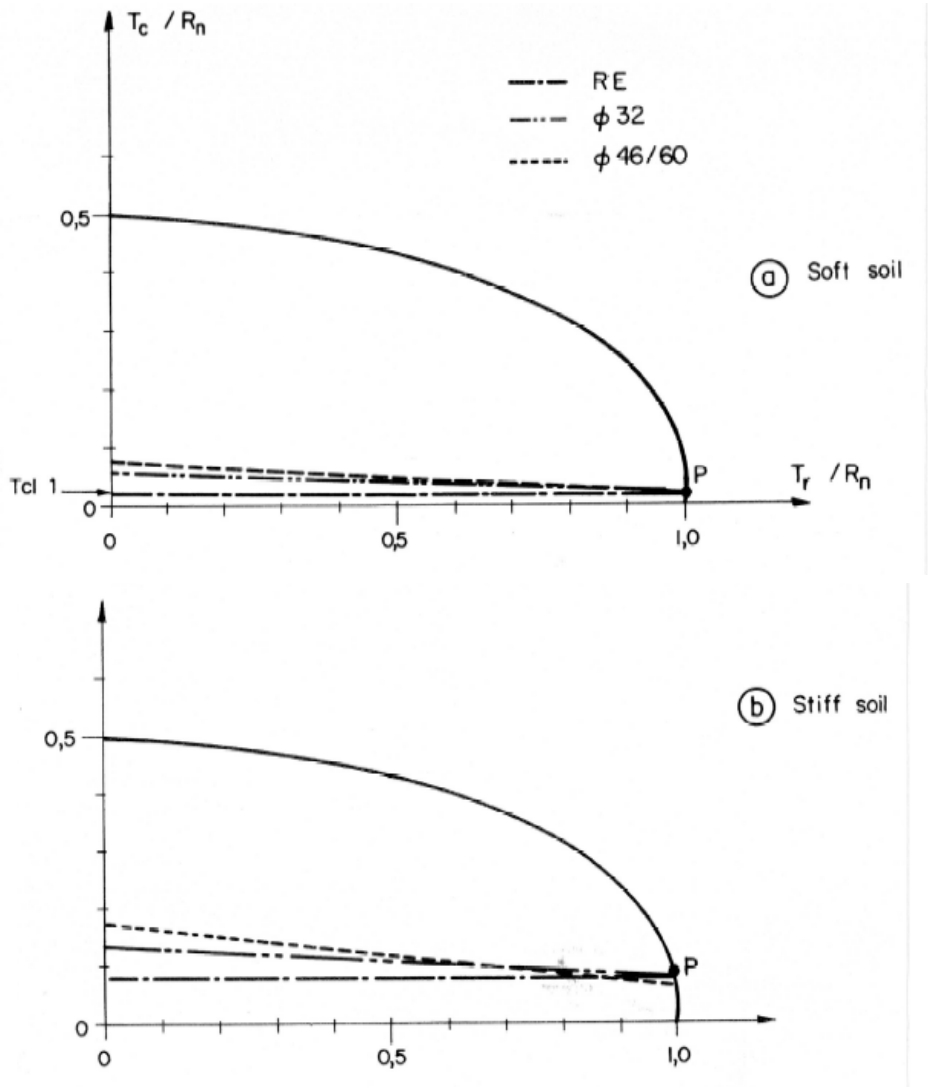

Figure 51: Relative positions of the failure criteria for two types of soils and three types of inclusions

BIBLIOGRAPHY

BLONDEAU F. — Application de l'Informatique à la Mécanique des Sols, Bulletin de Liaison des L.P.C., n° spécial S (1972)

BLONDEAU F. — Réflexions sur la prise en compte de la sécurité en matière d'ouvrages en terre avec inclusions et soutènements – TERRASOL – Avril 1996

BOURGES F.
FRANK R. — Fondations profondes – Cours de mécanique des sols de l'ENPC. Techniques de l'Ingénieur, Chapitre C 248 (1989)

BLONDEAU F.
CHRISTIANSEN M.
GUILLOUX A.
SCHLOSSER F. — TALREN: Méthode de calcul des ouvrages en sol renforcé. Colloque International: Renforcement en place des sols et des roches – ENPC Paris 1984.

GUILLOUX A. — Evaluation du frottement latéral sol-inclusion dans le clouage des sols. Colloque International: Renforcement en place des sols et des roches – ENPC Paris 1984.

RAULIN P.
ROUQUES G.
TOUBOL A. — Calcul de la stabilité des pentes en rupture non-circulaire. Rapport de recherche des LPC n° 36 - 1974

MANDEL — Propriétés mécaniques des matériaux (Eyrolles, 1978)

SALENCON J. — Calcul à la rupture et analyse limite, Presses de l'ENPC, 1983

Standards and recommendations

Standard XP P 94-240 (Août 1998)	Renforcement des sols: Soutènement et talus en sol en place renforcé par des clous. Justification du dimensionnement
Standard NF P 94-220-0 (Juin 1998)	Renforcement des sols: Ouvrages en sols rapportés renforcés par armatures ou nappes peu extensibles et souples. Partie 0: Justification du dimensionnement
EC 7	Eurocode 7: Projet définitif prEN 1997-1, janvier 2004, version française
MUR 73	Ouvrages de soutènement – SETRA (1973)
TA 86 / TA 95	Tirants d'ancrage – Eyrolles
Terre Armée	Recommandations et règles de l'art LCPC-SETRA 1979
CLOUTERRE 91 / CLOUTERRE 2	Recommandations Clouterre 1991 et Clouterre 2
FASCICULE 62	Règles techniques de conception et de calcul des fondations des ouvrages de Génie Civil (septembre 1992)